

POZZOLANIC REACTIVITY TEST OF SUPPLEMENTARY CEMENTITIOUS MATERIALS

Journal:	ACI Structural and Materials Journals
Manuscript ID	M-2021-207.R1
Journal Name:	ACI Materials Journal
Date Submitted by the Author:	n/a
Complete List of Authors:	Choudhary, Antara Bharadwaj, Keshav; Oregon State University, School of Civil and Construction Engineering; Ghantous, Rita; Oregon State University Isgor, O. Burkan; Oregon State University, School of Civil and Construction Engineering Weiss, Jason; Oregon State University, Civil Engineering
Keywords:	Pozzolanic reaction, Reactivity, Fly ash, Silica fume, Calcined clay, SCM, Thermodynamic modeling, GEMS

SCHOLARONE™ Manuscripts

POZZOLANIC REACTIVITY TEST OF SUPPLEMENTARY CEMENTITIOUS MATERIALS

Antara Choudhary, Keshav Bharadwaj, Rita Maria Ghantous, O. Burkan Isgor*, and W. Jason Weiss

*Corresponding author, burkan.isgor@oregonstate.edu

ABSTRACT

The reactions of supplementary cementitious materials (SCMs) in concrete can be pozzolanic, hydraulic, or a combination of both. This paper focuses on the pozzolanic reactivity test (PRT) for SCMs that are blends of reactive aluminous and siliceous phases. The PRT quantifies reactivity by measuring heat release (Q) and calcium hydroxide (CH) consumption, which are interpreted using thermodynamic modeling. The robustness of PRT is examined by experimentally varying CH-to-SCM ratio, solution-to-solid ratio, sulfate content, alkali type (Na vs. K), and alkali content. The paper also assesses similarities and differences between the PRT and the R3 test (ASTM C1897). It was found that sulfates, which are used in the R3 test, did not impact the siliceous reactions; however, they led to the preferential reaction with aluminous phases to form monosulfo-aluminates and ettringite. A generalized relationship for the degree of reactivity is proposed as a function of Q and CH consumption.

Keywords: Pozzolanic reaction, reactivity, fly ash, silica fume, calcined clay, supplementary cementitious materials, thermodynamic modeling, GEMS

BIOGRAPHICAL SKETCH OF AUTHORS

ACI member **Antara Choudhary** is a Ph.D. Student at Oregon State University. Her research interests include the reaction chemistry of supplementary materials and fillers, cement hydration, and durability of concrete.

ACI member **Keshav Bharadwaj** is a Ph.D. Student at Oregon State University. His research interests include thermodynamic modeling, reactivity and transport in cementitious systems, and predicting the properties of concrete using thermodynamic/kinetic modeling approaches.

ACI member **Rita Maria Ghantous**, is a Research Associate in the School of Civil and Construction Engineering at Oregon State University. She is a member of ACI Committee 130. Her research interests include carbonation, durability, and sustainability of concrete and cementitious materials.

O. Burkan Isgor, FACI, is a professor in the School of Civil and Construction Engineering at Oregon State University. He is the chair of ACI Committee 222. His research interests include corrosion of steel in concrete, service-life modeling, and thermodynamic modeling.

Jason Weiss, FACI, is the Edwards Distinguished Professor of Engineering in the School of Civil and Construction Engineering at Oregon State University. He is Editor in Chief of the ACI Materials Journal and a Member of the ACI Board.

INTRODUCTION

Supplementary cementitious materials (SCM) have been widely used to partially replace Ordinary Portland Cement (OPC) in modern concrete (1, 2). Common SCMs include coal ashes (e.g., fly ash), ground granulated blast-furnace slag, silica fume, metakaolin, pumice, ground glass, calcined clay, or rice husk ash (3-7). These SCMs typically contain a combination of reactive and nonreactive silica, alumina, and calcium, and they can undergo both pozzolanic and hydraulic reactions depending on their chemical compositions (8-14). Hydraulic reactions of calcium-rich phases in the presence of reactive silica can produce calcium silicate hydrate (C-S-H) and calcium hydroxide (CH) in addition to those produced by the reactions of OPC clinker and water. The silica and alumina phases of the SCM typically react pozzolanically with CH in the system (15-18). Pozzolanic reactions are considered secondary reactions as their occurrence depends on the availability of CH produced by the hydraulic reactions (19). SCMs like silica fume, Class F fly ash, and calcined clay mainly react pozzolanically with CH in the presence of adequate moisture to produce stable cementing compounds (20). SCMs like slag are primarily hydraulic (21-23). Pozzolanic reactions make SCMs highly beneficial in concrete through two primary mechanisms. First, the partial replacement of OPC with SCM leads to a lower OPC clinker content in the mixture (dilution), which reduces the carbon dioxide (CO₂) footprint of the concrete (13, 14, 24, 25). Second, pozzolanic reactions produce more C-S-H, making the concrete stronger and more durable (26-28). While dilution is directly related to SCM's replacement level in the mixture, several other factors such as chemical composition and reactivity of SCMs affect pozzolanic reactions. Traditionally, the reactivity of SCMs in OPC-based mixtures is quantified through the strength activity index (SAI) as defined by ASTM C311 (29). Several specifications use SAI as a criterion for allowing SCM to be used in concrete. For example, ASTM C618 (30) specifies that fly ashes need to satisfy a minimum SAI for use in concrete. Similarly, ASTM C 989 (6) specifies SAI requirements for using slag in concrete. However, it is widely accepted that SAI is a poor indicator of pozzolanic (or chemical) reactivity because non-reactive SCMs have been shown to pass the SAI criteria of published specifications (31, 32).

To address some of the issues with strength testing, several test methods have been developed to assess the pozzolanic reactivity of SCMs. The lime reactivity test (IS 1727-1967) (33) has practical issues due to long test duration and reproducibility (32, 34). The Frattini test (EN 196-5) (35, 36), the reactive silica test (EN 196-2 (37) and EN 197-1(38)), and the modified Chapelle test (NF P18-513) (39-41) have all been proposed to address this challenge. More recently, the R3 test method is developed, initially by Snellings and Scrivener (42) and later standardized in ASTM C1897-20 (43), as a more rapid test for assessing pozzolanic reactivity of SCMs. The R3 method determines the reaction potential of an SCM by mixing it with CH in a medium that contains sulfates, carbonates, and alkali and measuring the heat of reaction (Q) or the non-evaporable water of the reacted paste. This test is accelerated by maintaining the temperature of the paste at 40°C.

In parallel with the R3 test, another test, dubbed as the Pozzolanic Reactivity Test (PRT), was developed (44). The PRT method determines the reaction potential of an SCM by mixing it with CH in an alkaline solution. The Q and CH consumption are measured at 50°C for ten days and the ultimate heat of reaction (Q_{∞}) is determined. The results of this test, Q_{∞} and CH consumption, are superimposed on plots of predetermined degrees of reaction of pure SiO₂ and Al₂O₃ systems to estimate the maximum degree of reactivity (DOR*) of the SCM (45-47). The DOR* of an SCM is the theoretical maximum mass fraction of the SCM that can react. A series of papers have demonstrated the use of the PRT (45, 48-52) with refined predictions of DOR* (53, 54), especially when calcium oxide (CaO) is present in the SCM (45, 50). The PRT provides a quantifiable DOR*,

which has been shown to be related to the glass (amorphous) content in the SCM (45, 55). The DOR* can also be used as an input in thermodynamic modeling. Recent work has used these models to make successful predictions of several parameters of OPC+SCM pastes and concrete, such as the porosity, compressive strength, formation factor, CH content, calcium oxychloride formation potential, and time to freeze-thaw damage (25, 28, 47, 48, 53, 54, 56-65).

The R3 test and PRT methods are similar conceptually; however, the two methods differ practically in a few distinct areas. First, the tests are performed at different temperatures: the R3 test is performed at 40°C and the PRT is at 50°C, and this difference is not expected to cause major differences in the way the two methods assess pozzolanic reactivity. The testing temperature used is mainly dependent on user preference. Higher temperatures (40°C or 50°C) generally result in a faster test, however, they might also lead to reactions that do not typically occur at room temperature (19). This is a distinction that can be investigated; however, it is not in the scope of the study presented in this paper. The second area in which the tests differ is in the use of sulfate or carbonate. Unlike the PRT test (where no sulfate or carbonate is added for the test), the R3 test uses added potassium sulfate (4.8 g SO₃/100 g SCM) and calcium carbonate (50 g CaCO₃/100 g SCM) in the simulated solution. This fundamental difference between the two tests on the results of the reactivity tests is investigated in this paper. The third difference is in the liquid-to-powder ratio (ratio of the mass of alkaline pore solution added to the mass of SCM+CH in the test) with the R3 method using a ratio of 1.2 and the PRT using 0.9. Finally, the pore solution pH (alkali loading) is also different between the two test methods, with the R3 test using K₂O=1.96 g / 1 L= 0.07 M (corresponding to a pH of 12.85) and the PRT using KOH=0.5 M (corresponding to a pH of 13.7).

In this paper, the differences between the R3 and PRT tests are studied experimentally and using thermodynamic calculations. The robustness of the PRT is examined by experimentally varying several test parameters: the CH-to-SCM ratio, the liquid-to-powder ratio, sulfate and carbonate contents, alkali cation type (NaOH vs. KOH), and alkalinity of the pore solution (pH of pore solution).

RESEARCH SIGNIFICANCE

This paper aims to provide insight into the robustness of the PRT, which quantifies the maximum degree of reactivity (DOR*) of an SCM. The quantification of DOR* is important because it is needed as an input for thermodynamic models. The robustness of the PRT is assessed by studying the impact of varying testing parameters such as the SCM:CH mass ratio, liquid-to-powder mass ratio, pore solution alkalinity, and the chemical composition of the test mixture. This work provides recommendations on the testing of pozzolanic reactivity and is a step toward developing performance specifications for SCMs.

EXPERIMENTAL INVESTIGATION

The PRT consists of preparing a paste by combining one-part SCM by mass, three parts CH, and 0.5 M KOH solution. The method has a solution-to-dry powder ratio of 0.9. After weighing the constituent materials, the paste is thoroughly mixed according to the procedure outlined in previous work (50). In the standard procedure, 40 g of SCM is mixed with 120 g of CH and 144 g of 0.5 M KOH solution. The heat of reaction is measured after mixing for 240-hours (10-days) at a temperature of 50°C using an isothermal calorimeter. The extent of the pozzolanic reaction is determined by measuring the amount of CH consumed by the SCM reaction after ten days at 50°C.

The CH consumed is measured using a thermogravimetric analyzer. The details on the approach are provided in previous works (45, 58).

Table 1 describes the experimental test matrix. The varied test parameters are shown in the first column and include the CH:SCM mass ratio, liquid-to-powder mass ratio, sulfate content (as gypsum), carbonate content (as calcium carbonate), alkali content, and alkali pore solution cation type. The sulfate levels are representative of and exceed the typical sulfate levels in concrete systems (66). Note that the "baseline case" (listed in the last column) includes the test parameters used for the PRT test (CH:SCM=3:1, liquid-to-powder ratio=0.9, etc.). The table provides the ranges over which the test parameters are varied. These ranges cover and extend beyond the differences between the R3 test and the PRT test parameter values.

Three SCMs are tested: silica fume (SF: 95.9% siliceous), class F fly ash (FA: 51.9% siliceous and 21.7% aluminous), and calcined clay (CC: 54.2% siliceous and 37.5% aluminous). The chemical composition of these SCMs is listed in Table 2.

THERMODYNAMIC MODELING

Thermodynamic modeling is a tool that can be used to determine the reaction products of cementitious mixtures at equilibrium (67-69). It can be used to calculate the mass and volume fractions of solid and gaseous phases and concentrations of ionic species by minimizing the system's Gibbs free energy. In this work, GEMS3K v3.5 (70, 71) and the Cemdata 18 (67) database were used to simulate reactions that take place in different examined variations of the PRT test as per Table 1. Specifically, it is used to calculate the amount of reaction products, as well as Q_{∞} and CH consumed during the reactions. Thermodynamic modeling also provides the theoretical amorphous silica and alumina lines that are used to quantify DOR* (45, 58). These theoretical

lines for pure SiO_2 and pure Al_2O_3 , which are typically used to quantify the reactivity of fly ashes, are shown in Figure 1. These lines indicate the Q_∞ and CH consumption pairs when pure silica and pure alumina are allowed to undergo pozzolanic reactions at different reactivities ranging from 0 to 100%. It should be noted that these theoretical lines are customized based on the composition of the SCM that is tested. In thermodynamic calculations presented in this work, some phases are blocked from forming based on evidence in the literature that they do not form in the time scales and temperature of the PRT test. The blocked phases include C_3AH_6 (72, 73), Gibbsite (67), and some monosulfate phases (C_4AH_{13} , C_4AH_{19} , and C_4AsH_{12} (45)). The SiO₂ and Al₂O₃ lines are refined from previous work (45) to include the pore solution's enthalpy while calculating the heat released.

RESULTS AND DISCUSSION

Typical results from experiments and simulation

The experimental results obtained from the PRT conducted following the experimental matrix described in Table 1 are discussed in this section. Figure 2 shows the Q_{∞} and CH consumed results obtained from thermodynamic simulations of the pozzolanic reactions of SF, FA, and CC as compared to the experimental results. The values of Q_{∞} and CH consumed for all the tests performed are also provided in Table A-1 and Table A-2 of the appendix. The majority of the modeled values lie within \pm 20% of the experimental values, indicating a good agreement between the model and the experiment. The next few subsections will examine the variation of each test parameter in detail and provide a discussion of the results.

Influence of varying CH:SCM ratio on the results of the PRT

Figure 3 (a) shows experimental results of the PRT along with results from the thermodynamic calculations for cases where the CH:SCM is varied for different SCMs. As the CH:SCM increases, the Q_{∞} and CH consumed increase, but Q_{∞} /CH consumed decreases, suggesting a potential change in the reaction products. To better understand the changes that may be occurring, the phase assemblages are examined.

Figure 3 (b) shows a plot of phase assemblages at equilibrium for various CH:SCM mass ratio is varied for pure SiO₂. As CH is added to the pure silica system, the silica reacts with water and the CH to form C-S-H phases. At low CH:SiO₂ levels (CH:SiO₂ <0.61), a portion of the silica remains unreacted. A minimum of 61 g of CH is required for the complete reaction of 100 g SiO₂ (solid red line). As the CH:SiO₂ is increased from 0.61 to 1.98 (red dashed line), various forms of C-S-H with varying C/S form (Jennite-D, Jennite-H, Tobermorite-D, Tobermorite-H). As a result, the average C/S of the C-S-H increases from 0.7 (at a CH:SiO₂ of 0.61) to 1.7 (at a CH:SiO₂ of 1.98)). For CH:SiO₂ above 1.98, unreacted CH remains, and the total volume of C-S-H, as well as the proportions of the C-S-H variations, remain constant.

Figure 3 (c) shows a plot of the phase assemblages at equilibrium for the pure alumina system. As CH is added to the pure alumina system, the alumina reacts with water and the CH to form C-A-H phases (C₂AH_{7.5} forms in the PRT at 50°C). At low CH contents a portion of the alumina remains. A minimum of 144 g of CH is required for the complete reaction of 100 g Al₂O₃ (shown as the red dashed line). If the CH:Al₂O₃ is less than 1.44, unreacted alumina remains, and if the CH:Al₂O₃ is greater than 1.44, unreacted CH remains.

The thermodynamic calculations indicate that, for any SCM, the minimum CH:SCM required for complete hydration is 1.98:1. However, it is possible that kinetic effects and local physical

availability of CH at low CH:SCM mass ratios may dominate, and therefore, the CH:SCM of 3:1 is recommended for the PRT.

The experimental test results of FA (circles) and CC (stars) (Figure 3 (a)) indicate that CH is still present after the reactivity test (10 days at 50°C) for all CH:SCM ratios (3:1, 2:1, and 1:1). This is because the FA or CC are not comprised of pure reactive aluminate or silicate and they do not have a DOR* of 100%. On the other hand, at a CH:SCM=1:1, the tested SF (96% siliceous) appears to consume the entire available CH (all 100 g CH added is consumed), which is also predicted by thermodynamic modeling.

Influence of varying liquid-to-powder ratio on the results of the PRT

Figure 4 shows the experimental results of varying the liquid (0.5 M KOH solution) to powder (SCM+CH) mass ratio. The liquid-to-powder ratios tested are 0.75, 0.9, 1, 1.5, and 2 (shown in Table 1). Theoretically, a liquid-to-powder ratio of 0.75 provides sufficient water and CH for complete reaction of both aluminate and silicate phases in the SCM. However, achieving a workable mixture at that liquid-to-powder ratio can be challenging for highly reactive materials with a high surface area like SF. The variation in the results of CH consumed for SF and CC could be attributed to the physical dispersion and local availability of CH around the SCMs. As the liquid-to-powder ratio increases, the SCM dispersion improves, and the reaction would tend toward equilibrium. However, the slight variations in the experimental results on altering liquid-to-powder ratios, result in a relatively small variation in DOR* (DOR* varies from 71% to 79% for SF, 43% to 39% for FA, and 75% to 89% for CC).

Thermodynamic modeling predicts that a minimum of 24 g water is required for a complete reaction of 100 g SiO₂ and CH to form C-S-H (the C-S-H formed has a C/S of 0.72), and a minimum of 97 g of water required for complete reaction of 100 g Al₂O₃ to form C₂AH_{7.5}. If the

CH-to-SCM mass ratio is constant at 3:1, the minimum liquid-to-powder mass ratio required for complete hydration of either SiO₂ or Al₂O₃ is 0.24. Therefore, for all tested cases, the values of liquid-to-powder ratios (0.75 to 2.00) satisfy this minimum requirement.

Influence of sulfates addition on the results of the PRT

Figure 5 (a) shows the experimental results of the PRT when sulfates are present. The sulfates (added as gypsum, CaSO₄.2H₂O) in the SCM+CH+liquid mixture vary from 0 g/100 g_{SCM} (the PRT baseline case) to 30 g/100 g_{SCM} for the tested SCMs. The addition of sulfate has a negligible impact on the DOR* of the SF (the DOR* values are within 5% of each other). This is because the tested SF has little to no alumina which is known to react with sulfates (Table 2). For both the FA and CC systems, when the sulfate increased, the Q_{∞} and CH consumed increased (approximately linearly proportional to the mass of gypsum added). For fly ash, Q_{∞} increased by 0.8 J/g_{gypsum} added, and the CH consumed increased by 0.15 g/g_{gypsum} added. For CC, Q_{∞} increased by 0.6 J/g_{gypsum} added, and the CH consumed increased by 0.1 g/g_{gypsum} added. Also, it can be seen in Figure 5 (a) the experimental results show a similar trend as what is predicted using thermodynamic simulations.

Figure 5 (b) shows the phase assemblage of the equilibrium reaction of pure SiO_2 as sulfates are added. The CH: SCM mass ratio is kept at 3:1 and the liquid-to-powder mass ratio at 0.90. As the gypsum content increases from 0 g/100 g_{SCM} to 30 g/100 g_{SCM} , thermodynamic modeling predicts

that the siliceous reactions are unaffected, i.e., the same amount of C-S-H forms with the same C/S ratio (C/S = 1.7). The CH consumption and Q_{∞} remain unchanged as well.

Figure 5 (c) shows the phase assemblage of the equilibrium reaction of pure Al_2O_3 system as sulfates are added. The sulfates react with the alumina, CH, and water in the mixture preferentially to form mono-sulfate phases. Any excess alumina (left over after all sulfates have been consumed) reacts with the CH and water in the mixture to form C-A-H phases ($C_2AH_{7.5}$). The reaction of alumina that produces mono-sulfate generates more Q_∞ than the reaction that produces the C-A-H phase observed (approximately 3.25 J/g_{gypsum} added more Q_∞ is produced). The reaction of alumina that produces mono-sulfate, however, does not seem to consume more CH than the reaction that produces C-A-H. Therefore, the alumina reaction is impacted by the presence of sulfates, and when sulfates are present, Q_∞ increases (due to changes in the reaction products, i.e., the formation of mono-sulfates at the expense of C-A-H phases). However, the CH consumed by the alumina-containing SCMs (FA and CC) seems to increase proportionally with the added sulfates. This is possibly due to the preferential formation of AFm in these systems over $C_2AH_{7.5}$ (74, 75) The formation of AFm approximately consumes 73.5 g_{CH}/100 g_{alumina} more than formation of $C_2AH_{7.5}$.

Influence of calcium carbonates on the results of the PRT

Figure 6 (a) shows the experimental results of the PRT when calcium carbonates are present. The calcium carbonate in the SCM+CH+liquid mixture varies from 0 g/100 g_{SCM} (baseline case for the PRT) to 10 g/100 g_{SCM} for the tested SCMs. The addition of calcium carbonate has an insignificant impact on the reactivity of SF (the DOR* values are within 5% of each other). This is because the tested SF has little to no alumina (Table 2). For both the FA and CC systems, when the mass of calcium carbonate added was increased, Q_{∞} and the consumption of CH increased (approximately linearly proportional to the mass of calcium carbonate added). For fly ash, Q_{∞} increased by 1.6

 J/g_{CaCO3} added and the CH consumed decreased by 0.1 g/g_{CaCO3} added for the FA. For CC, Q_{∞} increased by 1.2 J/g_{CaCO3} added, and the CH consumed increased by 0.06 g/g_{CaCO3} added. The experimental results of Q_{∞} and CH consumed show a similar trend as the predictions from thermodynamic modeling, as shown in Figure 6 (a).

Figure 6 (b) shows the phase assemblage of the equilibrium reaction of pure SiO_2 as carbonates are added. The CH: SCM mass ratio is kept at 3:1 and liquid-to-powder mass ratio at 0.90. As the calcium carbonate content is increased from 0 g/100g_{SCM} to 10 g/100g_{SCM}, thermodynamic modeling predicts that the siliceous reactions are unaffected, i.e., the same amount of C-S-H forms with the same C/S ratio (C/S=1.7). The CH consumption and Q_{∞} remain unchanged as well.

Figure 6 (c) shows the phase assemblage of the equilibrium reaction of the pure Al_2O_3 system as carbonate is added. The carbonate reacts with the alumina, CH, and water in the mixture preferentially to form hemi-/mono-carbonate phases. Any excess alumina left over after all the carbonates have reacted reacts with the CH and water in the mixture to form C-A-H phases ($C_2AH_{7.5}$). The reaction of alumina that produces hemi-/mono-carbonates generates more heat than the reaction that produces the C-A-H phase observed (an increase of approximately 10.95 J/g_{CaCO3}). The reaction of alumina that produces hemi-/mono-carbonates also consumes more CH than the reaction that produces C-A-H (an increase of approximately 2.23 g/g_{CaCO3}). Therefore, the alumina reaction is impacted by the presence of carbonates, and when carbonates are present, the Q_{∞} and CH consumed increase (due to changes in the reaction products – formation of hemi-/mono-carbonates at the expense of C-A-H phases). This is also observed in the experimental results of FA and CC, which contain reactive alumina according to Table 2.

Influence of alkali cation on the results of the PRT

Figure 7 (a) shows the experimental results of PRT with two different alkali pore solutions (KOH and NaOH) for the tested SCMs. It can be seen that the alkali content and cations have almost no impact on the results. The calculated values of the DOR* for SF, FA and CC are within 7%, 8%, and 0.5% of each other, respectively.

Figure 7 (b) and Figure 7 (c) show the result of varying the alkali cation for the PRT for pure SiO₂ and pure Al₂O₃, respectively. As alkali cations in the pore solution are changed (from pure 0.5 M KOH to pure 0.5 M NaOH) for both systems, the only change observed is in the pure siliceous system (a roughly 1% decrease in C-S-H volume when NaOH is used instead of KOH), where the C-S-H may bind potassium differently than sodium. It appears that the type of cation does not Influence of pH on the results of the PRT

Figure 8(a) shows the experimental results of the PRT with different pore solution concentrations for the tested SCMs. Figure 8 (b) and Figure 8 (c) depict the modeled phase assemblage of equilibrium reaction of pure SiO₂ and pure Al₂O₃ for different pore solution concentrations of KOH.

As seen from Figure 8 (b), as the concentration of hydroxyl ions in the pore solution is increased from 0.25 M (pH of 12.7) to 2 M (pH of 15.2), the volume of C-S-H that forms changes slightly due to the different amount of alkali binding (approximately 2% change in volume over the pH range studied). The amount of CH that becomes soluble is affected by the amount of KOH in the solution. There is no noteworthy change in the Q_{∞} or CH consumed in the model. Similarly, from Figure 8(c), it can be seen that the change in the pore solution pH has a minimal impact on the

phase assemblage (about a 1% change in volume of C-A-H that forms), and there is no noteworthy change in the Q_{∞} or CH consumed.

Comparing the PRT with other reactivity tests

This section discusses the comparison of the PRT with the R3 test procedure. Similarities and differences are shown in Table 3 and Figure 9. As previously mentioned, the most important difference appears to be the addition of sulfates and calcium carbonates to the reactants in the R3 test. The addition of these materials results in a substantial difference for aluminous systems. For example, when sulfates are added, the alumina in the SCM reacts to form mono-sulfate phases rather than C-A-H phases, which leads to a higher Q_{∞} . When carbonates and sulfates are present, the reactive alumina first forms ettringite, and the remaining reactive alumina forms carboaluminate phases. When sulfates are added to siliceous systems the reactions are relatively unaffected and both tests are similar. Therefore, if sulfates or/and carbonates are added, the changes to the reaction products need to be accounted for while calculating the reactivity of the SCM.

Figure 9 shows the initial reactants and final reaction products in the PRT and R3 tests for the three SCMs tested. The first column for each system shows the volumes of initial reactants and the second column shows the volume of reacted products. First, it can be seen when looking at the SCMs in the PRT test that SF reacts pozzolanically to form C-S-H, and FA and CC react pozzolanically to form C-S-H and C-A-H (C₂AH_{7.5}). In the R3 test, the SF reacts to form C-S-H (similar to the PRT), but the FA and CC react to form ettringite and carboaluminates rather than C-A-H. For example, when 100 g of the tested CC is subjected to the PRT, 12 cm³/100 g_{SCM} of C₂AH_{7.5} forms, while in the R3 test, no C-A-H forms (12 cm³/100 g_{SCM}) of ettringite and 71 cm³/100 g_{SCM} of carboaluminate form instead). This change in the phase assemblage in the R3 test

(formation of ettringite and carboaluminates rather than C-A-H) leads to a higher measured Q_{∞} and CH consumed (see Table 3). The relative proportions of these three reactions can also change. It can also be seen that in the R3 test, for the compositions of the SCMs tested, all the sulfate is consumed (to form ettringite) but not all the carbonate is consumed.

It should be noted that in both the R3 and PRT tests, the volumes of C-S-H that form are within $0.2~\text{cm}^3/100~\text{g}_{\text{SCM}}$ of each other (the reaction of 100 g SF produces 122 cm 3 C-S-H, that of 100 g FA produces 31 cm 3 C-S-H, and that of 100 g CC produces 64 cm 3 C-S-H). This is because the formation of C-S-H only depends on the pozzolanic reaction of silica in the SCM, and is unaffected by the presence of sulfates and carbonates.

In summary, the R3 test adds sulfates and carbonates; however, even the addition of a constant amount of sulfate and carbonate can cause various phases (and various amounts of each phase) to form when SCMs of different composition (and different percentages of reactive phases) are tested. For example, if an SCM with very low alumina content is tested, ettringite + hemicarbonates + monocarbonates would form in the R3 test, while if an SCM with high alumina is tested, ettringite + monocarbonates would form (the phases that form can be determined from the carbonate-sulfate-alumina stability diagram in (76)). This difference in the phase assemblage would result in different amounts of heat release (or non-evaporable water) measured. Therefore, SCMs of similar reactivities but different alumina contents could result in very different Q_{∞} (or non-evaporable water) measurements. The PRT on the other hand does not add sulfates and carbonates, and consistent phases form as a result of the pozzolanic reaction (C-S-H from silica, and C-A-H from alumina). This makes the PRT a more robust tool to evaluate the reactivity of alumina containing SCMs such as fly ash, metakaolin (or calcined clays), natural pozzolans, etc. Additionally, the R3 test output can only be used as a qualitative comparison tool between two

SCMs (determine which SCM is more reactive or to distinguish pozzolanic materials from inert fillers), while the PRT has been extended to allow for calculation of an absolute numerical value of reactivity (DOR*) which is described in the following section.

Relationship between CH consumed, Qoo, pore solution composition and DOR*

The PRT measures the DOR* of an SCM. For experimental results that fall in between the theoretical reactivity of pure SiO₂ and pure Al₂O₃, the results can be interpolated to obtain DOR* using:

$$DOR^* = \frac{Q_{\infty} - c_1 \cdot CH_{consumed}}{c_2} \tag{1}$$

where Q_{∞} is the Q_{∞} measured using an isothermal calorimeter (IC) (in J/g_{SCM}), $CH_{consumed}$ is the CH consumed by 100 g SCM measured using a thermogravimetric analyzer (TGA) (in g/100 g_{SCM}), and c_1 is 0.373 and c_2 is 695 for the PRT.

For conditions other than the PRT, the c_1 and c_2 constants can be calculated from the theoretical Q_{∞} and CH consumed at complete reaction of SiO₂ and Al₂O₃ using equation (2) and (3), shown below:

$$c_{1} = \frac{Q_{\infty}^{SiO_{2}} - Q_{\infty}^{Al_{2}O_{3}}}{CH_{consumed}^{SiO_{2}} - CH_{consumed}^{Al_{2}O_{3}}}$$
(2)

$$c_{2} = \frac{Q_{\infty}^{Al_{2}O_{3}} \cdot CH_{consumed}^{SiO_{2}} - Q_{\infty}^{SiO_{2}} \cdot CH_{consumed}^{Al_{2}O_{3}}}{CH_{consumed}^{Si} - CH_{consumed}^{Al_{2}O_{3}}}$$
(3)

where $Q_{\infty}^{SiO_2}$ and $Q_{\infty}^{Al_2O_3}$ are the Q_{∞} when pure 100% reactive silica and alumina react with CH and water, respectively (for the PRT, these values are $Q_{\infty}^{SiO_2}=769$ J/g_{SCM} and $Q_{\infty}^{Al_2O_3}=749$ J/g_{SCM}), and, $CH_{consumed}^{SiO_2}$ and $CH_{consumed}^{Al_2O_3}$ are the CH consumed when pure 100% reactive silica

and alumina react with CH and water, respectively (for the PRT, these values are $CH_{consumed}^{SiO_2} = 198 \text{ g}/100 \text{ g}_{SCM}$ and $CH_{consumed}^{Al_2O_3} = 144 \text{ g}/100 \text{ g}_{SCM}$).

The values of c_1 and c_2 are only dependent on the test parameters and not on the SCM chemistry. For example, for the R3 test, the values are $c_1 = 9.70$ and, $c_2 = -1151$. If sulfates are added during the test (though not recommended), the values of c_1 and c_2 vary as a function of sulfate and carbonate addition as shown in Figure 10 (note that the figure shows independent addition of sulfate or carbonate, not both together; if both are present together such as in the R3 test, thermodynamic calculations need to be performed to calculate the values of c_1 and c_2).

CONCLUSION

This paper examined the influence of the testing parameters on the results of the PRT (pozzolanic reactivity test) for SCMs. Three pozzolanic materials were measured experimentally: silica fume (primarily siliceous), class F fly ash (22% aluminous and 52% siliceous), and calcined clay (38% aluminous and 54% siliceous). The influence of varying several test parameters (e.g., the CH to SCM ratio, water to CH+SCM ratio, sulfate addition, carbonate addition, alkali loading, and alkali species) was assessed.

A CH:SCM ratio of 3:1 is recommended for determining reactivity, which is consistent with what is currently used in both R3 test and PRT (43, 44). The minimum liquid-to-powder ratio for a complete reaction of any SCM is theoretically determined to be 0.25; however, experimentally, it is observed that a value above 0.9 is needed to enable the samples to be prepared for consistent results. Liquid-to-powder ratios beyond 0.9 do not impact the results.

The siliceous reactions are unaffected by the presence of sulfate or carbonate (the same volume of C-S-H forms with the same C/S); however, the aluminous reactions are affected by the addition of both sulfate and carbonate. The impact of sulfate and carbonate is not due to a change in the pozzolanic reaction of the aluminous material but rather due to the formation of alternative reaction products. When no sulfates or carbonates are present, C-A-H phases (C₂AH_{7.5}) form due to the pozzolanic reaction of the Al₂O₃ in the SCM. In the presence of sulfates, monosulfates and ettringite are preferentially formed instead of C-A-H phases. In the presence of carbonates, Al₂O₃ preferentially reacts to form carboaluminates rather than C-A-H phases. This change to the reaction products is accompanied by an increase in heat release and CH consumption. As such, the addition of sulfates or carbonates is not recommended for the measurement of pozzolanic reactivity. However, if sulfates or carbonates present in the system, their impact on DOR* can be considered mathematically.

Variations in the hydroxide composition (cation used, K vs. Na) have a negligible impact on the reactivity for the same equivalent alkali loading (the variation in the DOR* for SF, FA, and CC is under 6%). The change alkali loading (pH/molarity) does impact the kinetics of the experiment though the equilibrium reactions (and reactivity of the SCM) remain relatively unaffected. A generalized relationship is developed between the Q_{∞} , and the CH consumed to mathematically calculate the DOR* of a pozzolan using the results of the PRT for the typical PRT and R3 testing conditions. The PRT test is shown to be a test that primarily measures the pozzolanic reaction and quantifies the maximum reactivity for an SCM. The paper recommends using standardized PRT to measure SCM DOR* due to practical advantages.

ACKNOWLEDGMENTS

The authors gratefully acknowledge the financial support provided by ARPA-E (Advanced Research Projects Agency-Energy), CALTRANS (California Department of Transportation), and National Science Foundation (Grant No. NSF CMMI 1728358). The authors gratefully acknowledge support from the Edwards Distinguished Chair at Oregon State. The authors also acknowledge fruitful discussions with Prof. Barbara Lothenbach (EMPA, Switzerland). The authors also acknowledge Oliver Hudson Opdahl and Audrey Collins for their laboratory assistance.

REFERENCES

- 1. A Neville, Properties of Concrete, 3rd Edition, Pitman, London, UK. 1981.
- 2. S Mindess, F Young and D Darwin, Concrete, 2nd Edition, Prentice Hall, 2003, 644 pp.
- 3. P Barnes and J Bensted, Structure and performance of cements, CRC Press, 2002.
- 4. GS Barger, ER Hansen, MR Wood, T Neary, DJ Beech and D Jaquier, "Production and use of calcined natural pozzolans in concrete," Cement, concrete and aggregates, V. 23, No. 2, 2001, pp. 73-80.
- 5. B Uzal, L Turanli and PK Mehta, "High-volume natural pozzolan concrete for structural applications," ACI Materials Journal, V. 104, No. 5., 2007, pp. 535-538.
- 6. ASTM C989-18 "Standard Specification for Slag Cement for Use in Concrete and Mortars", ASTM International, West Conshohocken, 2018.
- 7. JM Aldred, TC Holland, DR Morgan, DM Roy, MA Bury, RD Hooton, J Olek, MJ Scali, RJ Detwiler and TM Jaber, "Guide for the use of silica fume in concrete," ACI Committee 234, Farmington Hills, MI, USA, V. 234, 2006.

- 8. B Lothenbach, K Scrivener and R Hooton, "Supplementary cementitious materials," Cement and concrete research, V. 41, No. 12, 2011, pp. 1244-1256.
- 9. MC Juenger and R Siddique, "Recent advances in understanding the role of supplementary cementitious materials in concrete," Cement and Concrete Research, V. 78, 2015, pp. 71-80.
- 10. R Khatri, V Sirivivatnanon and W Gross, "Effect of different supplementary cementitious materials on mechanical properties of high performance concrete," Cement and Concrete research, V. 25, No. 1, 1995, pp. 209-220.
- 11. MC Juenger, R Snellings and SA Bernal, "Supplementary cementitious materials: New sources, characterization, and performance insights," Cement and Concrete Research, V. 122. 2019, pp. 257-273.
- 12. JM Justice, Evaluation of metakaolins for use as supplementary cementitious materials, M. Sc. Thesis, Georgia Institute of Technology, Atlanta, GA, 2005, pp. 134.
- 13. V Papadakis and S Tsimas, "Supplementary cementing materials in concrete: Part I: efficiency and design," Cement and concrete research, V. 32, No. 10, 2002, pp. 1525-1532.
- 14. V Papadakis, S Antiohos and S Tsimas, "Supplementary cementing materials in concrete: Part II: A fundamental estimation of the efficiency factor," Cement and Concrete research, V. 32, No. 10, 2002, pp. 1533-1538.
- 15. M Ghrici, S Kenai and M Said-Mansour, "Mechanical properties and durability of mortar and concrete containing natural pozzolana and limestone blended cements," Cement and Concrete Composites, V. 29, No. 7, 2007, pp. 542-549.
- 16. K De Weerdt, H Justness, KO Kjellsen amd E Sellevold, "Fly ash-limestone ternary composite cements: synergetic effect at 28 days," Nordic Concrete Research, V. 42, No. 4, 2010, pp. 51-70.

- 17. M Ahmaruzzaman, "A review on the utilization of fly ash," Progress in energy and combustion science, V. 36, No. 3, 2010, pp. 327-363.
- 18. R Siddique, "Utilization of silica fume in concrete: Review of hardened properties," Resources, Conservation and Recycling, V. 55, No. 11, 2011, pp. 923-932.
- 19. F Deschner, B Lothenbach, F Winnefeld and J Neubauer, "Effect of temperature on the hydration of Portland cement blended with siliceous fly ash," Cement Concrete Research, V. 52, 2013, pp. 169-181.
- 20. K Vessalas, P Thomas, A Ray, J-P Guerbois, P Joyce and J Haggman, "Pozzolanic reactivity of the supplementary cementitious material pitchstone fines by thermogravimetric analysis," Journal of Thermal Analysis and Calorimetry, V. 97, No. 1, 2009, pp. 71-76.
- 21. M House, CD Bella, H Sun, G Zima, L Barcelo and W Weiss, "Influence of Slag Aggregate Production on Its Potential for Use in Internal Curing," Transportation Research Record: Journal of the Transportation Research Board, V. 2441, 2014, pp. 105-111.
- 22. G Menéndez, V Bonavetti and E Irassar, "Strength development of ternary blended cement with limestone filler and blast-furnace slag," Cement and Concrete Composites, V. 25, No. 1, 2003, pp. 61-67.
- 23. C Shi, "Steel slag—its production, processing, characteristics, and cementitious properties," Journal of materials in civil engineering, V. 16, No. 3, 2004, pp. 230-236.
- 24. PK Mehta and PJ Monteiro, "Concrete: microstructure, properties, and materials." McGraw-Hill Education, 2014, 684 pp.
- 25. I De la Varga, J Castro, D Bentz, F Zunino and J Weiss, "Evaluating the hydration of high volume fly ash mixtures using chemically inert fillers," Construction and Building Materials, V. 161, 2018, pp. 221-228.

- 26. M Thomas, "Optimizing the use of fly ash in concrete." Portland Cement Association Skokie, IL, 2007, 24 pp.
- 27. ASTM C1709 "Standard Guide for Evaluation of Alternative Supplementary Cementitious Materials (ASCM) for Use in Concrete," ASTM International, West Conshohocken, 2018.
- 28. P Suraneni, V Azad, O Isgor and W Weiss, "Concrete paving mixture compositions that minimize deicing salt damage," Transportation Research Record, V. 2629, 2017, pp. 24-32.
- 29. ASTM C311 "Standard Test Methods for Sampling and Testing Fly Ash or Natural Pozzolans for Use in Portland-Cement Concrete," ASTM International, West Conshohocken, 2018.
- 30. ASTM C618, "Standard Specification for Coal Fly Ash and Raw or Calcined Natural Pozzolan for Use in Concrete," ASTM International, West Conshohocken, 2019.
- 31. RT Thorstensen and P Fidjestol, "Inconsistencies in the pozzolanic strength activity index (SAI) for silica fume according to EN and ASTM," Materials and Structures, V. 48, No. 12, 2015, pp. 3979-3990.
- 32. DP Bentz, A Durán-Herrera and D Galvez-Moreno, "Comparison of ASTM C311 strength activity index testing versus testing based on constant volumetric proportions," Journal of ASTM International, V. 9, No. 1, 2011, pp. 1-7.
- 33. IS, "1727: Methods of test for pozzolanic materials," Book 1727: Methods of test for pozzolanic materials, Editor, ed.^eds., Bureau of Indian Standards New Delhi, City, 1967, pp.
- 34. W Butler, "A critical look at ASTM C 618 and C 311," Cement, Concrete and Aggregates, V. 4, No. 2, 1982, pp. 68-72.
- N Frattini, "Richerche sulla calce di idrolisi nelle paste di cimento," Ann di Chim Appl, V.39, 1949, pp. 616-620.

- 36. R Snellings and KL Scrivener, "Rapid screening tests for supplementary cementitious materials: past and future," Materials and Structures, V. 49, No. 8, 2016, pp. 3265-3279.
- 37. BS EN 196-2 "Methods of testing cement-Part 2: Chemical analysis of cement," British Standards Institution. 2005.
- 38. BS EN 197-1 "Cement-Part 1: Composition, specifications and conformity criteria for common cements," British Standards Institution. 2000.
- 39. E Ferraz, S Andrejkovičová, W Hajjaji, AL Velosa, AS Silva and F Rocha, "Pozzolanic activity of metakaolins by the French Standard of the modified Chapelle Test: A direct methodology," Acta Geodyn. Geomater, V. 12, No. 3, 2015, pp. 289-298.
- 40. M Raverdy, F Brivot, A Paillere and R Dron, "Appréciation de l'activité pouzzolanique de constituents secondaires," Proceedings of the 7th International Congress on the Chemistry of Cement, Vol. 3, 1980, pp. 36-41.
- 41. J Chapelle, "Attaque sulfo-calcique des laitiers et des pouzzolanes." Imprimerie Centrale de l'Ortois-Orras, 1958.
- 42. F Avet, R Snellings, AA Diaz, MB Haha and K Scrivener, "Development of a new rapid, relevant and reliable (R3) test method to evaluate the pozzolanic reactivity of calcined kaolinitic clays," Cement and Concrete Research, V. 85, 2016, pp. 1-11.
- 43. ASTM C1897 "Standard Test Methods for Measuring the Reactivity of Supplementary Cementitious Materials by Isothermal Calorimetry and Bound Water Measurements," ASTM International, West Conshohocken, 2020.
- 44. P Suraneni and J Weiss, "Examining the pozzolanicity of supplementary cementitious materials using isothermal calorimetry and thermogravimetric analysis," Cement and Concrete Composites, V. 83, Supplement C, 2017, pp. 273-278.

- 45. D Glosser, A Choudhary, OB Isgor and J Weiss, "Investigation of the Reactivity of Fly Ash and its Effect on Mixture Properties," ACI Materials Journal, V. 116, No. 4, 2019, pp. 193-200.
- 46. VJ Azad, P Suraneni, O Isgor and W Weiss, "Interpreting the pore structure of hydrating cement phases through a synergistic use of the Powers-Brownyard model, hydration kinetics, and thermodynamic calculations," Advances in Civil Engineering Materials, V. 6, No. 1, 2017, pp. 1-16.
- 47. OB Isgor and J Weiss, "A nearly self-sufficient framework for modelling reactive-transport processes in concrete," Materials and Structures, V. 52, No. 1, 2019, pp. 1-17.
- 48. DB Glosser, "Equilibrium and Non-equilibrium Thermodynamic Modeling of Cement Pastes Containing Supplementary Cementitious Materials," Ph. D. Thesis, Oregon State University, Corvallis, OR, 2020, 206 pp.
- 49. S Ramanathan, M Kasaniya, M Tuen, MD Thomas and P Suraneni, "Linking reactivity test outputs to properties of cementitious pastes made with supplementary cementitious materials," Cement and Concrete Composites, V. 114, 2020, pp. 103742.
- 50. P Suraneni, A Hajibabaee, S Ramanathan, Y Wang and J Weiss, "New insights from reactivity testing of supplementary cementitious materials," Cement and Concrete Composites, V. 103, 2019, pp. 331-338.
- 51. P Suraneni, T Fu, V Jafari Azad, OB Isgor and J Weiss, "Pozzolanicity of finely ground lightweight aggregates," Cement and Concrete Composites, V. 88, 2018, pp. 115-120.
- 52. P Suraneni, VJ Azad, OB Isgor and J Weiss, "Role of supplementary cementitious material type in the mitigation of calcium oxychloride formation in cementitious pastes," Journal of Materials in Civil Engineering, V. 30, No. 10, 2018, pp. 04018248.

- 53. K Bharadwaj, D Glosser, MK Moradllo, OB Isgor and J Weiss, "Toward the Prediction of Pore Volumes and Freeze-Thaw Performance of Concrete Using Thermodynamic Modelling," Cement Concrete Research, V. 124, 2019, pp. 105820.
- 54. D Glosser, VJ Azad, P Suraneni, B Isgor and J Weiss, "An extension of the Powers-Brownyard model to pastes containing SCM," ACI Materials Journal, V. 116, No. 5, 2019, pp. 205-216.
- 55. MK Moradllo, C-W Chung, MH Keys, A Choudhary, SR Reese and WJ Weiss, "Use of borosilicate glass powder in cementitious materials: Pozzolanic reactivity and neutron shielding properties," Cement and Concrete Composites, V. 112, 2020, pp. 103640.
- 56. K Bharadwaj, RM Ghantous, FN Sahan, BO Isgor and J Weiss, "Predicting Pore Volume, Compressive Strength, Pore Connectivity, and Formation Factor in Cementitious Pastes Containing Fly Ash," Cement and Concrete Composites, V. 122, 2021, pp. 104113.
- 59. K Bharadwaj, BO Isgor, JW Weiss, KST Chopperla, A Choudhary, G Vasudevan, D Glosser, JH Ideker, D Trejo., "A mixture proportioning approach for concrete with SCM based on performance constraints," ACI Materials Journal, Accepted, 2021.
- 58. B Isgor, J Ideker, D Trejo, J Weiss, K Bharadwaj, A Choudhary, KST Chopperla, D Glosser, G Vasudevan, "Development of a performance-based mixture proportioning procedure for concrete incorporating off-spec fly ash," Technical Report, Energy Power Research Institute (EPRI), 2020, 78 pp.
- 59. P Suraneni, VJ Azad, BO Isgor and WJ Weiss, "Calcium oxychloride formation in pastes containing supplementary cementitious materials: Thoughts on the role of cement and supplementary cementitious materials reactivity," RILEM Technical Letters, V. 1, 2016, pp. 24-30.

- 60. P Suraneni, VJ Azad, OB Isgor and WJ Weiss, "Use of fly ash to minimize deicing salt damage in concrete pavements," Transportation Research Record, V. 2629, No. 1, 2017, pp. 24-32.
- 61. D Glosser, A Choudhary, J Ideker, D Trejo, WJ Weiss and OB Isgor, "Thermodynamic Investigation of Cementitious Mixtures Incorporating Off-Spec Fly Ashes." 2019.
- 62. P Suraneni, VJ Azad, OB Isgor and WJ Weiss, "Deicing salts and durability of concrete pavements and joints," Concrete International, V. 38, No. 4, 2016, pp. 48-54.
- 63. HS Esmaeeli, Y Farnam, DP Bentz, PD Zavattieri and WJ Weiss, "Numerical simulation of the freeze-thaw behavior of mortar containing deicing salt solution," Materials and Structures, V. 50, No. 1, 2017, pp. 1-20.
- 64. P Suraneni, J Monical, E Unal, Y Farnam and W Weiss, "Calcium oxychloride formation potential in cementitious pastes exposed to blends of deicing salt," ACI Materials Journal, V. 114, No. 4, 2017, pp. 631-641.
- 65. SN Whatley, P Suraneni, VJ Azad, OB Isgor and J Weiss, "Mitigation of Calcium Oxychloride Formation in Cement Pastes Using Undensified Silica Fume," Journal of Materials in Civil Engineering, V. 29, No. 10, 2017, pp. 04017198.
- 66. BS 8110-1 "Structural use of concrete, part 1: Code of practice for design and construction", British Standards Institution, UK. 2007.
- 67. B Lothenbach, DA Kulik, T Matschei, M Balonis, L Baquerizo, B Dilnesa, GD Miron, and RJ Myers, "Cemdata 18: A chemical thermodynamic database for hydrated Portland cements and alkali-activated materials," Cement Concrete Research, V. 115, 2019, pp. 472-506.

- 68. B Lothenbach, T Matschei, G Möschner and FP Glasser, "Thermodynamic modelling of the effect of temperature on the hydration and porosity of Portland cement," Cement Concrete Research, V. 38, No. 1, 2008, pp. 1-18.
- 69. B Lothenbach and F Winnefeld, "Thermodynamic modelling of the hydration of Portland cement," Cement Concrete Research, V. 36, No. 2, 2006, pp. 209-226.
- 70. DA Kulik, "Improving the structural consistency of CSH solid solution thermodynamic models," Cement Concrete Research, V. 41, No. 5, 2011, pp. 477-495.
- 71. DA Kulik, T Wagner, SV Dmytrieva, G Kosakowski, FF Hingerl, KV Chudnenko and UR Berner, "GEM-Selektor geochemical modeling package: revised algorithm and GEMS3K numerical kernel for coupled simulation codes," Computational Geosciences, V. 17, No. 1, 2013, pp. 1-24.
- 72. V Antonovič, J Kerienė, R Boris and M Aleknevičius, "The effect of temperature on the formation of the hydrated calcium aluminate cement structure," Procedia engineering, V. 57, 2013, pp. 99-106.
- 73. HF Taylor, Cement chemistry, 2nd Edition, Thomas Telford, London, 1997, 459 pp.
- 74. P Garcés, EG Alcocel, S Chinchón, CG Andreu and J Alcaide, "Effect of curing temperature in some hydration characteristics of calcium aluminate cement compared with those of Portland cement," Cement Concrete Research, V. 27, No. 9, 1997, pp. 1343-1355.
- 75. C Gosselin, "Microstructural development of calcium aluminate cement based systems with and without supplementary cementitious materials," Ph. D. Thesis, EPFL, Lausanne, Switzerland, 2009.
- 76. T Matschei, B Lothenbach and F Glasser, "The AFm phase in Portland cement," Cement Concrete Research, V. 37, No. 2, 2007, pp. 118-130.

for peer perion only

TABLES AND FIGURES

List of Tables:

 Table 1: Experimental test matrix

Table 2: Chemical characterization of SCMs used

Table 3: Comparison of the PRT and R3 test methods

Table A-1: Values of $Q\infty$ and CH consumed as predicted using thermodynamic modelling and as measured from experiments when the test parameters of the PRT are varied

Table A-2: Values of $Q\infty$ and CH consumed as predicted using thermodynamic modelling and as measured from experiments when sulfates and carbonates are added in the PRT.

List of Figures:

Figure 1- Thermodynamically simulated lines of pozzolanic reactions of amorphous silica (SiO₂) and alumina (Al₂O₃)

Figure 2- Plot of experimentally measured and model-predicted values of (a) CH Consumed and (b) Q_{∞} for the PRT test.

Figure 3- Plot showing (a) the influence of CH to SCM ratio on the CH consumed and Q_{∞} in the reactivity test, (b) the phase assemblage when pure SiO₂ reacts with CH, and (c) the phase assemblage when pure Al₂O₃ reacts with CH. The values of Q_{∞} and CH consumed are also noted in Table A-1 of the appendix.

Figure 4- The influence of liquid to SCM+CH ratio on the CH consumed and Q_{∞} in the reactivity test. The values of Q_{∞} and CH consumed are also noted in Table A-1 of the appendix.

Figure 5- Plots showing (a) the influence of $[SO_4]^{2-}$ on the CH consumed and Q_{∞} in the reactivity test, (b) the phase assemblage and Q_{∞} when pure SiO_2 reacts with CH and sulfates are added, (c)

the phase assemblage and Q_{∞} when pure Al_2O_3 reacts with CH and sulfate is added. The values of Q_{∞} and CH consumed are also noted in Table A-2 of the appendix.

Figure 6- Plots showing (a) the influence of CaCO3 on the CH consumed and Q_{∞} in the reactivity test, (b) the phase assemblage and Q_{∞} when pure SiO₂ reacts with CH and carbonates are added, and (c) the phase assemblage and Q_{∞} when pure Al₂O₃ reacts with CH and carbonates are added. The values of Q_{∞} and CH consumed are also noted in Table A-2 of the appendix.

Figure 7- Plot showing (a) the influence of alkali cation on the CH consumed and Q_{∞} in the reactivity test, (b) phase assemblage and Q_{∞} when pure SiO₂ reacts and the alkali cation is varied, and (c) phase assemblage and Q_{∞} when pure Al₂O₃ reacts and the alkali cation is varied. The values of Q_{∞} and CH consumed are also noted in Table A-1 of the appendix.

Figure 8- Plot showing (a) the influence of pH of pore solution on the CH consumed and Q_{∞} in the reactivity test, (b) the phase assemblage and Q_{∞} when pure SiO₂ reacts, and the pH is varied, and (c) the phase assemblage and Q_{∞} when pure Al₂O₃ reacts and the pH is varied. The values of Q_{∞} and CH consumed are also noted in Table A-1 of the appendix.

Figure 9- Volumes of initial reactants and final products for the three SCMs studied in the PRT and R3 tests.

Figure 10- (a) Variation of c_1 and c_2 as a function of sulfate addition, and, (b) variation of c_1 and c_2 as a function of carbonate addition. Markers are at the locations of the sulfate/carbonate additions tested in the experiments (see Table 1).

Table 1: Experimental test matrix

Table 1. Experimental test matrix							
Varied test parameter	CH:SCM	Liquid: SCM	Sulfate (g/100 g SCM)	Calcium Carbonate (g/100 g SCM)	NaOH (M)	KOH (M)	Baseline
СН	3:1	0.90	0	0	0.00	0.50	٧
	2:1	0.90	0	0	0.00	0.50	
	1:1	0.90	0	0	0.00	0.50	
Liquid-to-SCM ratio	3:1	0.75	0	0	0.00	0.50	
	3:1	0.90	0	0	0.00	0.50	٧
	3:1	1.00	0	0	0.00	0.50	
	3:1	1.50	0	0	0.00	0.50	
	3:1	2.00	0	0	0.00	0.50	
Sulfate	3:1	0.90	0	0	0.00	0.50	٧
	3:1	0.90	5	0	0.00	0.50	
	3:1	0.90	10	0	0.00	0.50	
	3:1	0.90	20	0	0.00	0.50	
	3:1	0.90	30	0	0.00	0.50	
Calcium Carbonate	3:1	0.90	0	0	0.00	0.50	٧
	3:1	0.90	0	2	0.00	1.00	
	3:1	0.90	0	6	0.50	0.00	
	3:1	0.90	0	10	0.50	0.00	
Alkali/Molarity	3:1	0.90	0	0	0.00	0.25	
	3:1	0.90	0	0	0.00	0.50	٧
	3:1	0.90	0	0	0.00	1.00	
	3:1	0.90	0	0	0.00	2.00	
	3:1	0.90	0	0	0.50	0.00	

Table 2: Chemical characterization of SCMs used

%	Silica Fume (SF)	Fly Ash (FA)	Calcined Clay (CC)	
SiO ₂	95.88	51.86	53.22	
Al ₂ O ₃	0.69	21.70	36.90	
Fe ₂ O ₃	0.12	5.04	1.21	
CaO	0.70	8.61	0.57	
MgO	0.26	2.58	0.36	
SO ₃	0.15	0.78	0.06	
LOI	4.30	1.42	2.21	
Na ₂ O	0.16	2.58	0.15	
K ₂ O	0.49	1.45	0.68	
TiO ₂	0.01	1.19	1.87	
P ₂ O ₅	0.05	0.23	0.11	
ZnO	0.06	0.02	0.01	
Mn ₂ O ₃	0.04	0.03	0.01	
Cl	0.01	0.01	0.01	

Table 3: Comparison of the PRT and R3 test methods

Test Paramete	er	PRT	R3	
CH:SCM		3:1	3:1	
Liquid-to-powder ratio		0.9	1.2	
Pore Solution alka	alinity	0.5M KOH	0.07M KOH	
CaCO ₃ adde	d	None	$50g/100g_{SCM}$	
Sulfates added		None	10.547g K ₂ SO ₄ /100g _{SCM}	
Test Output		Value of ultimate pozzolanic	Bound Water,	
		reactivity (DOR*)	Heat of Reaction	
Theoretical Q∞ (J/gscm)	SF	646	648	
	FA	277	378	
	CC	519	778	
Theoretical CH	SF	162	162	
Consumed (g/100	FA	55	59	
gscm)	CC	148	153	

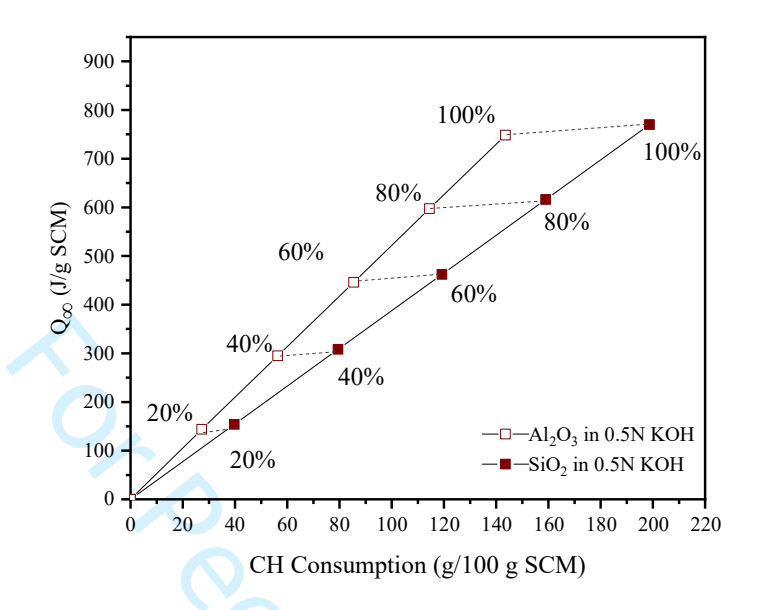


Figure 1- Thermodynamically simulated lines of pozzolanic reactions of amorphous silica (SiO₂) and alumina (Al₂O₃) at various degrees of reaction

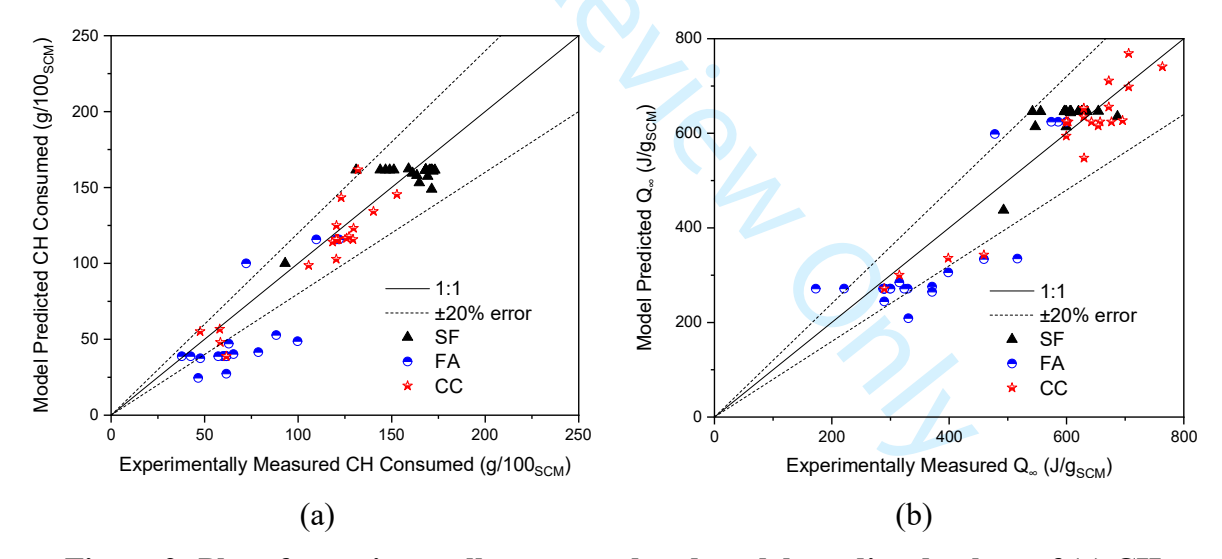
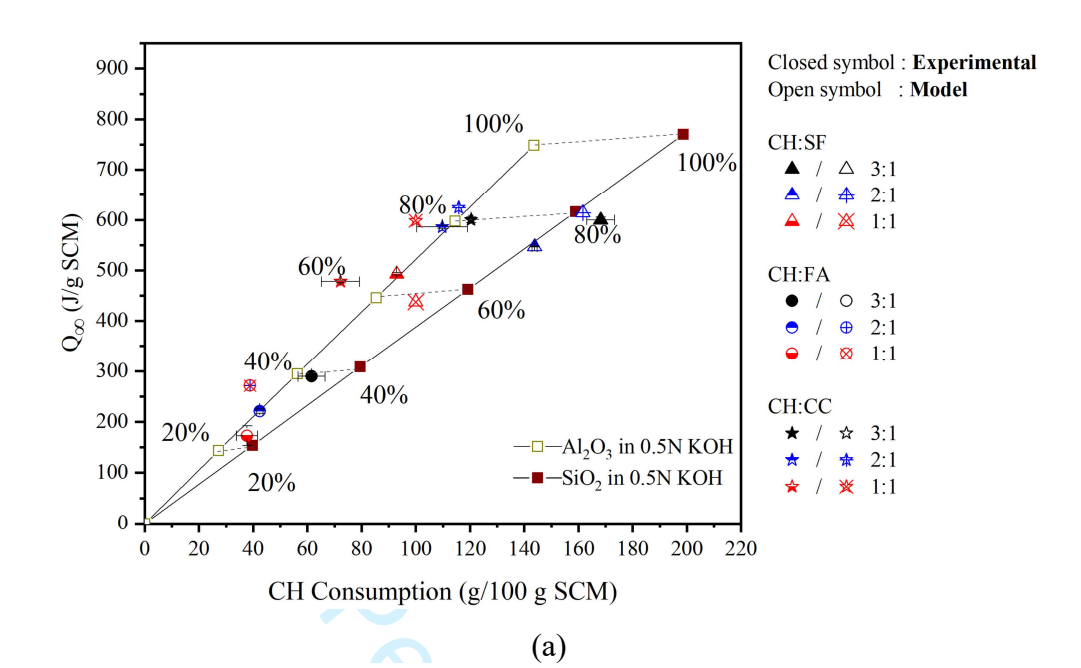
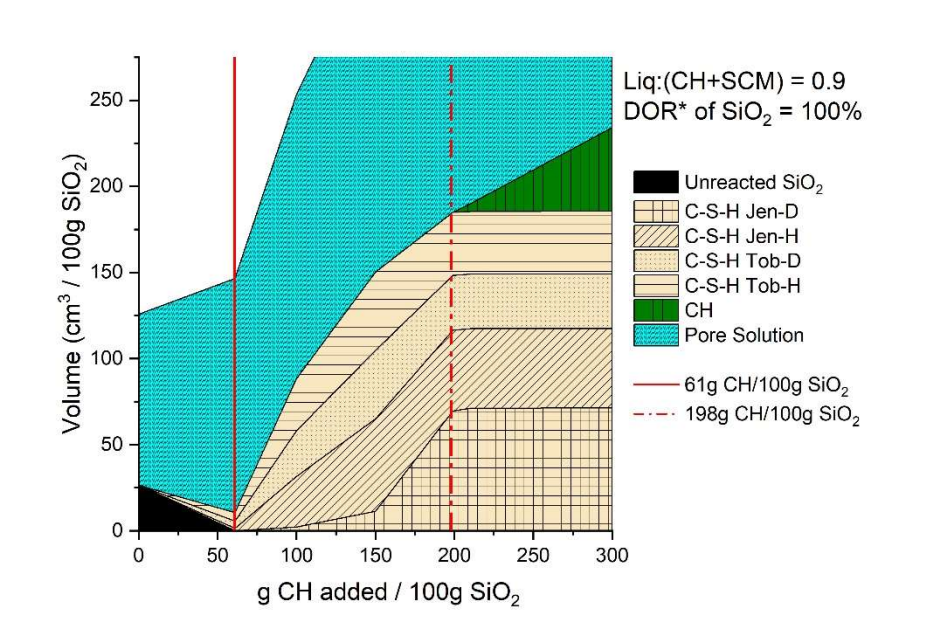


Figure 2- Plot of experimentally measured and model-predicted values of (a) CH Consumed and (b) Q_{∞} for the PRT test. The values of Q_{∞} and CH consumed are also noted in Table A-1 and Table A-2 of the appendix.





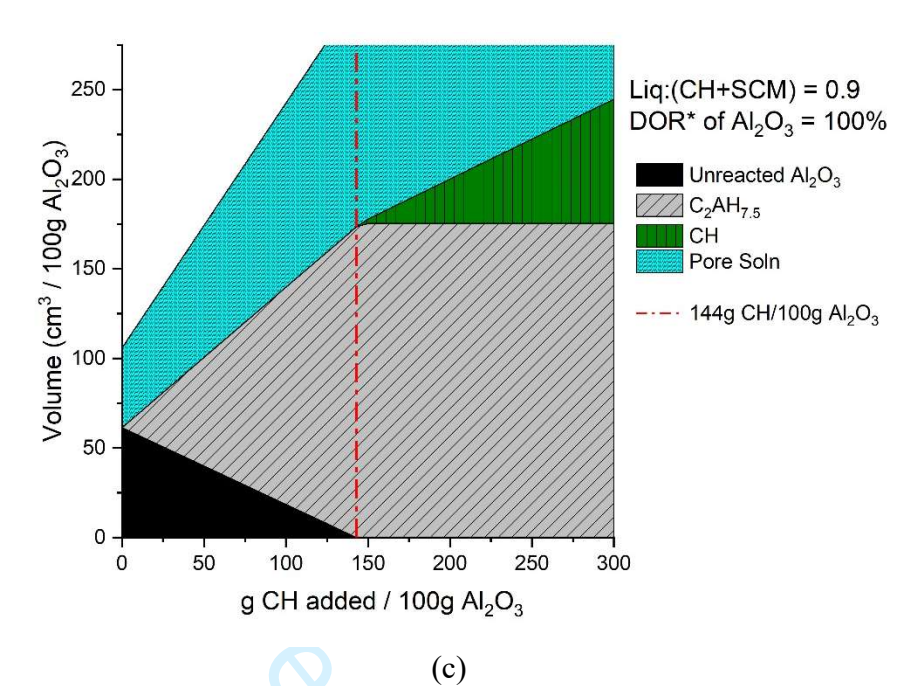


Figure 3- Plot showing (a) the influence of CH to SCM ratio on the CH consumed and Q_{∞} in the reactivity test, (b) the phase assemblage when pure SiO_2 reacts with CH, and (c) the phase assemblage when pure Al_2O_3 reacts with CH. Vertical lines represent the critical CH:SCM as described in the test. The values of Q_{∞} and CH consumed are also noted in Table A-1 of the appendix.

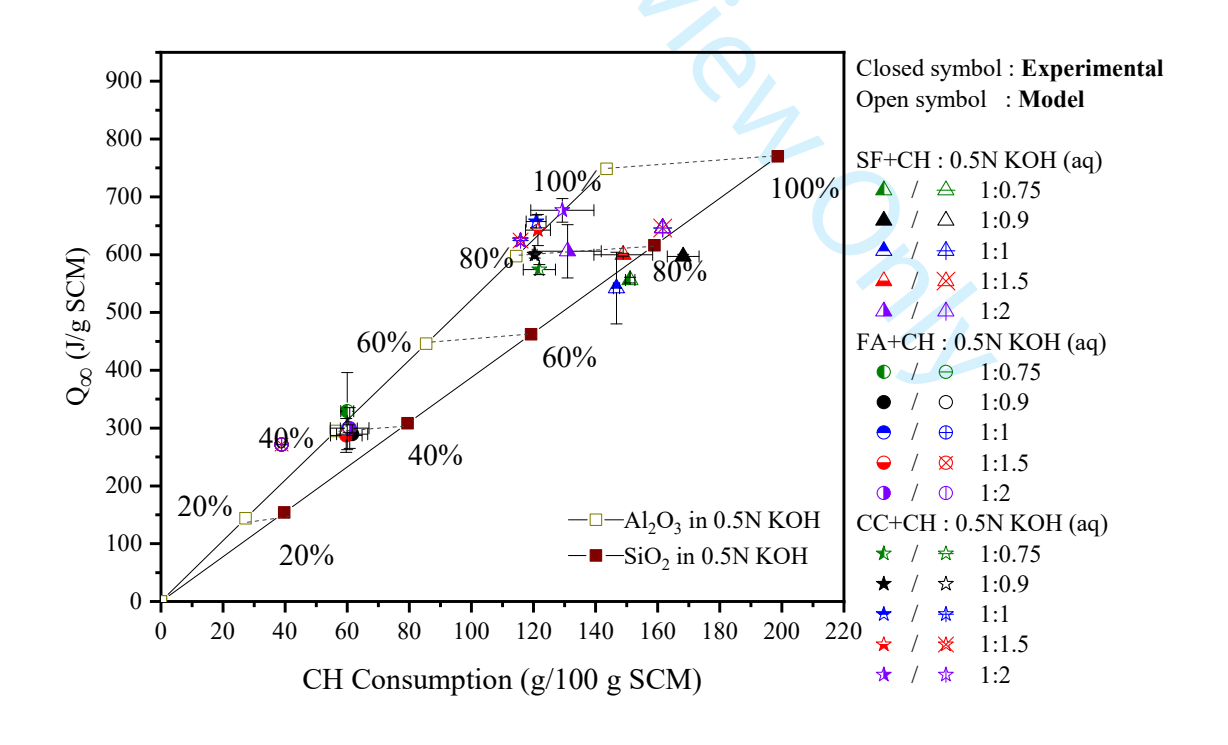
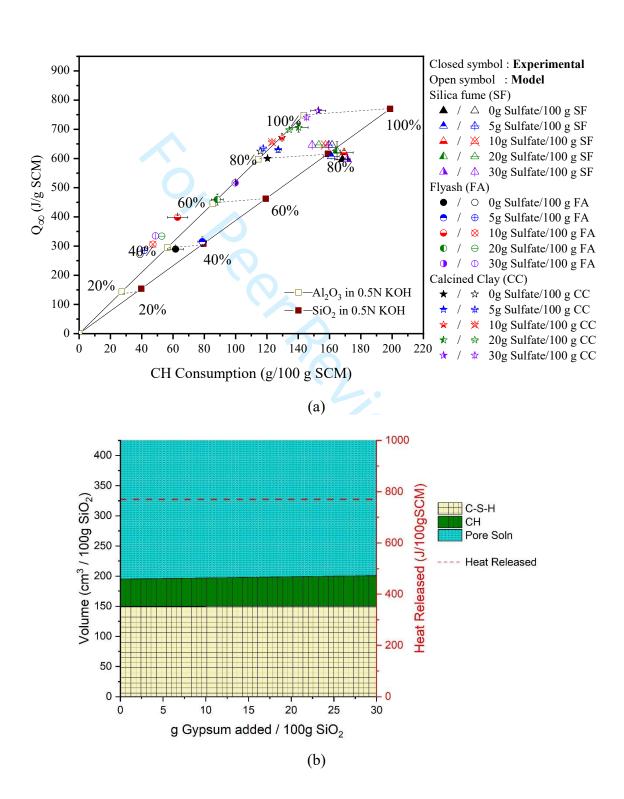


Figure 4- The influence of liquid to SCM+CH ratio on the CH consumed and Q_{∞} in the reactivity test. The values of Q_{∞} and CH consumed are also noted in Table A-1 of the appendix.



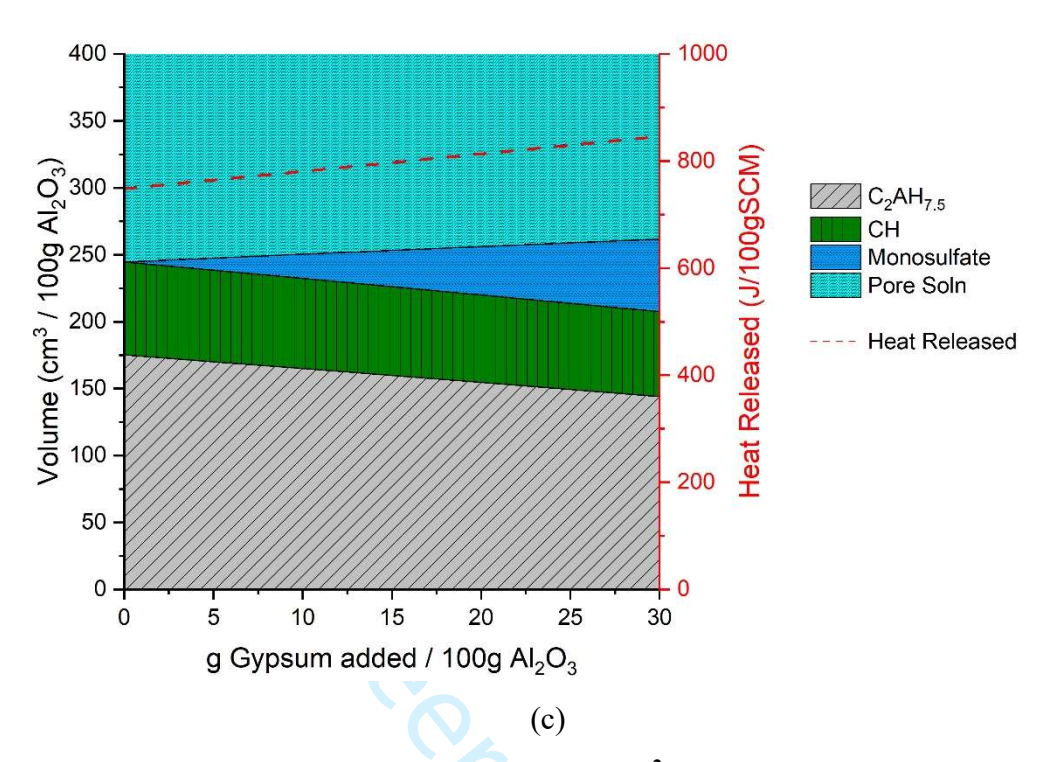
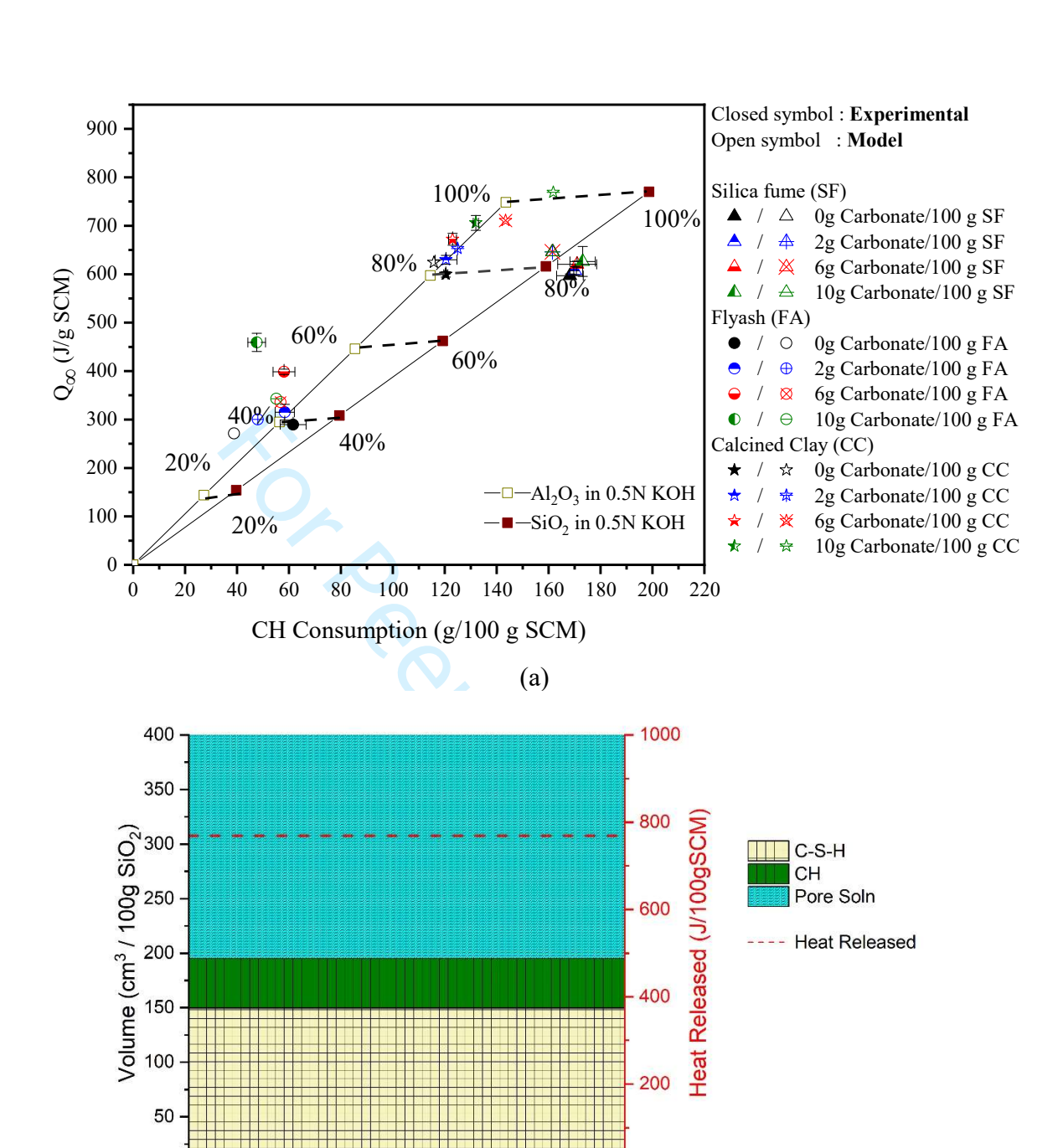


Figure 5- Plots showing (a) the influence of $[SO_4]^{2-}$ on the CH consumed and Q_∞ in the reactivity test, (b) the phase assemblage and Q_∞ when pure SiO_2 reacts with CH and sulfates are added, (c) the phase assemblage and Q_∞ when pure Al_2O_3 reacts with CH and sulfate is added. The values of Q_∞ and CH consumed are also noted in Table A-2 of the appendix.



(b)

g CaCO₃ added / 100g SiO₂

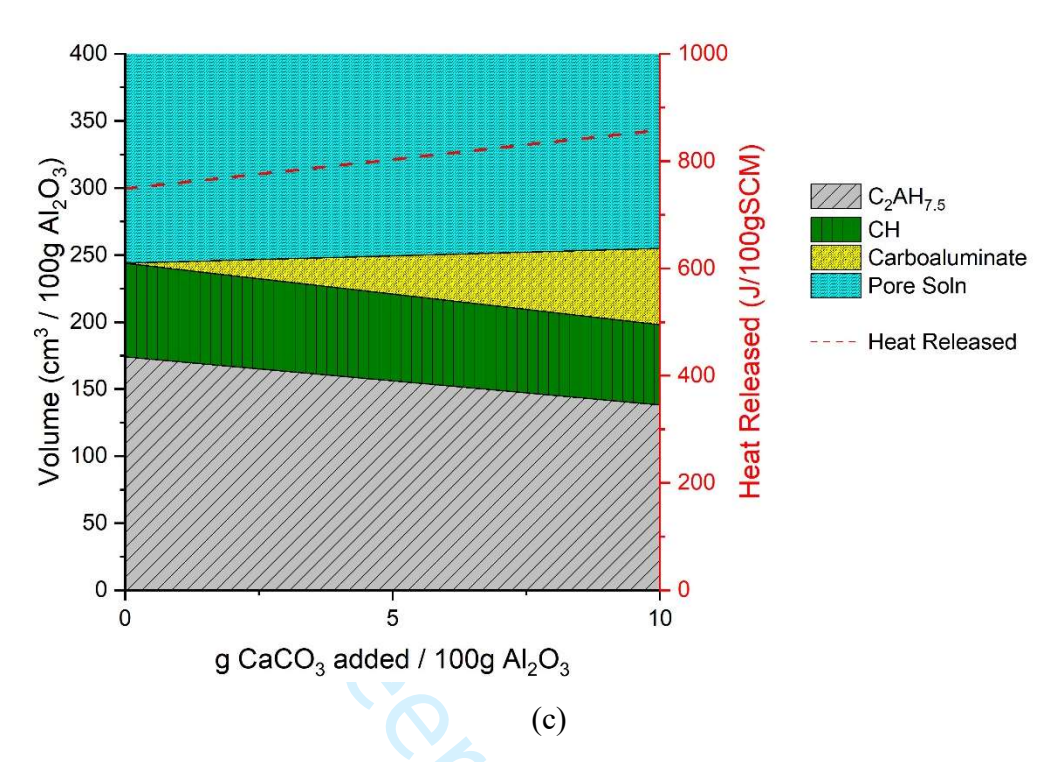
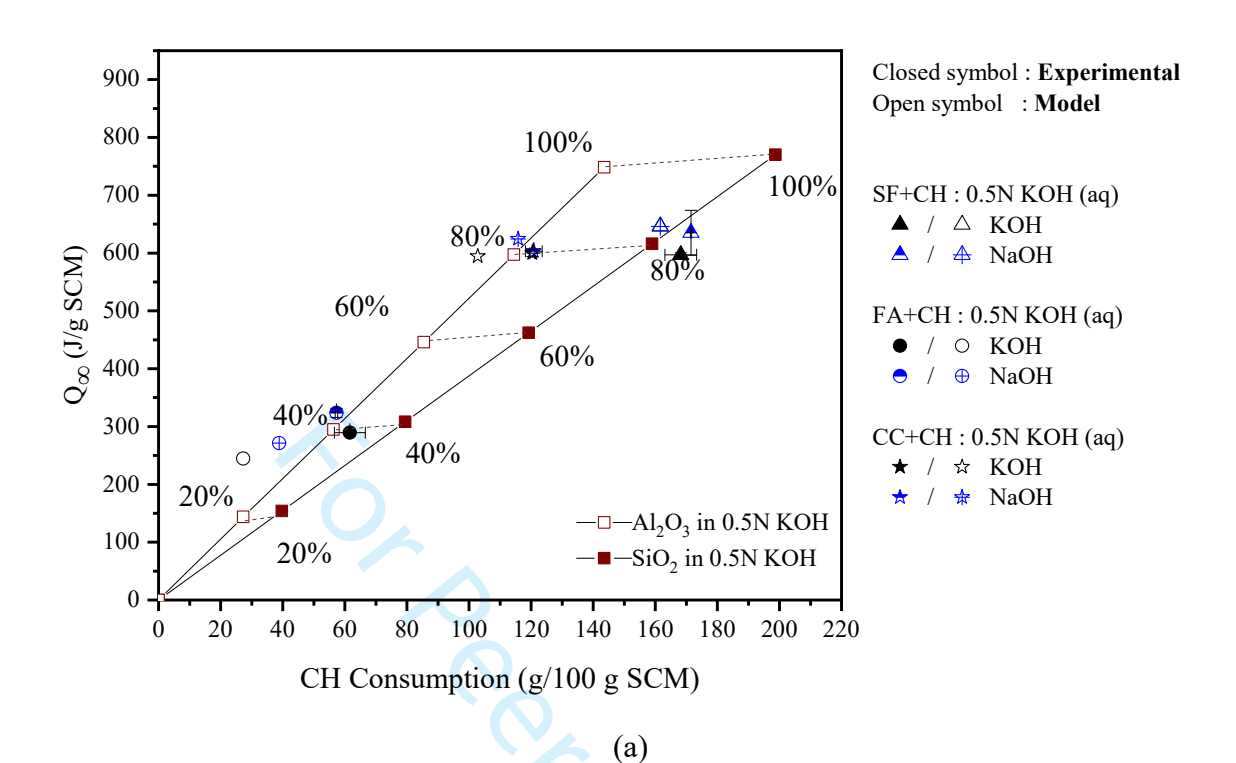
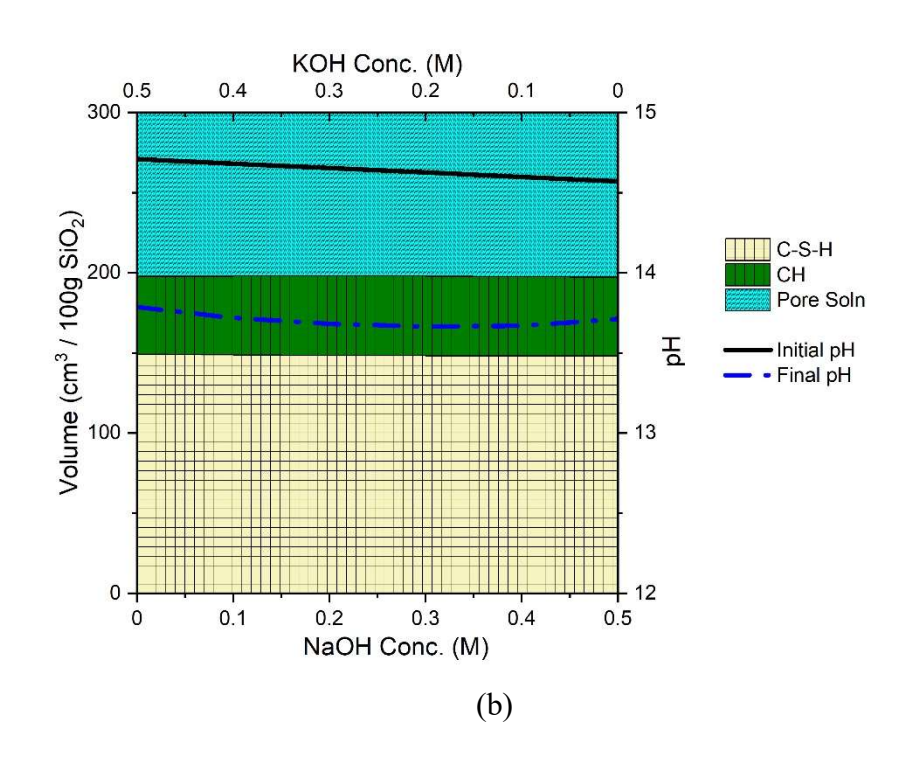


Figure 6- Plots showing (a) the influence of CaCO3 on the CH consumed and Q_{∞} in the reactivity test, (b) the phase assemblage and Q_{∞} when pure SiO2 reacts with CH and carbonates are added, and (c) the phase assemblage and Q_{∞} when pure Al₂O₃ reacts with CH and carbonates are added. The values of Q_{∞} and CH consumed are also noted in Table A-2 of the appendix.





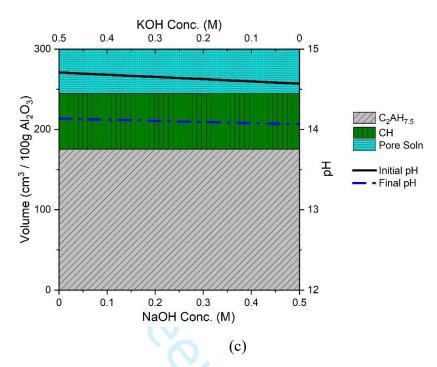
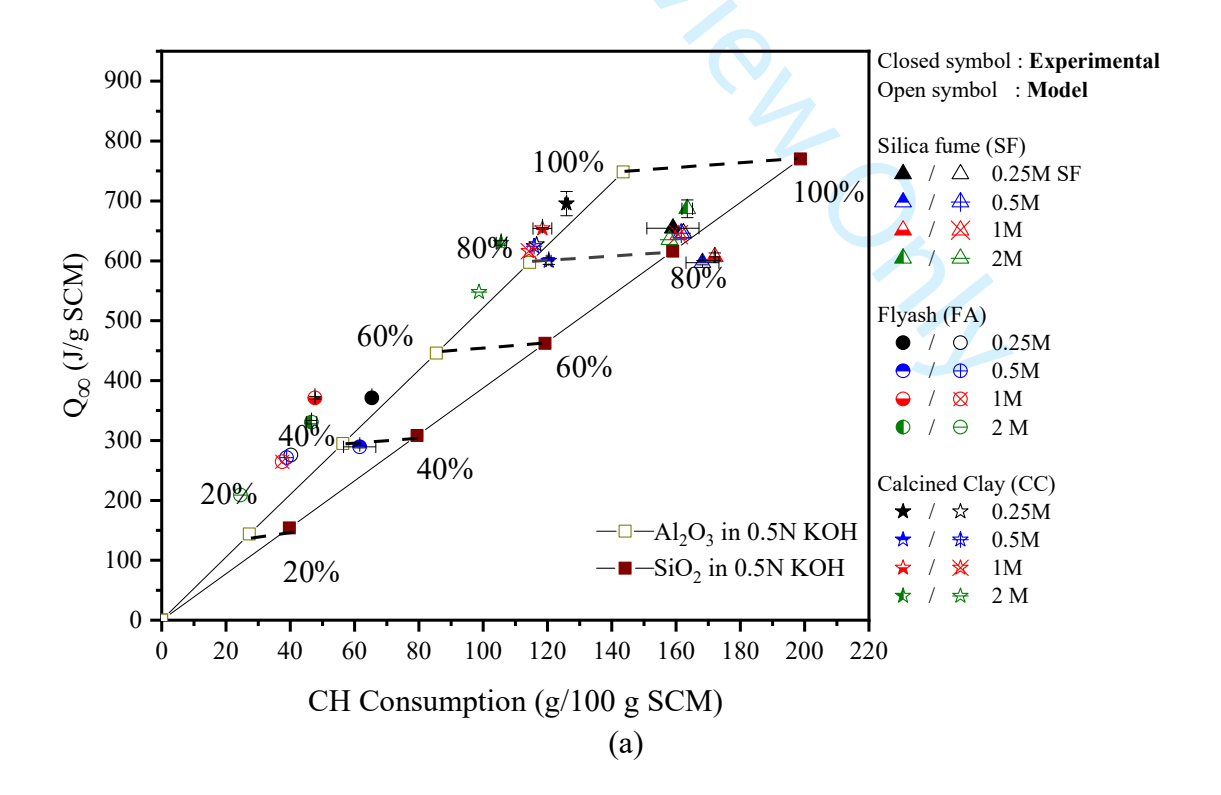


Figure 7- Plot showing (a) the influence of alkali cation on the CH consumed and Q_{∞} in the reactivity test, (b) phase assemblage and Q_{∞} when pure SiO₂ reacts and the alkali cation is varied, and (c) phase assemblage and Q_{∞} when pure Al₂O₃ reacts and the alkali cation is varied. The values of Q_{∞} and CH consumed are also noted in Table A-1 of the appendix.



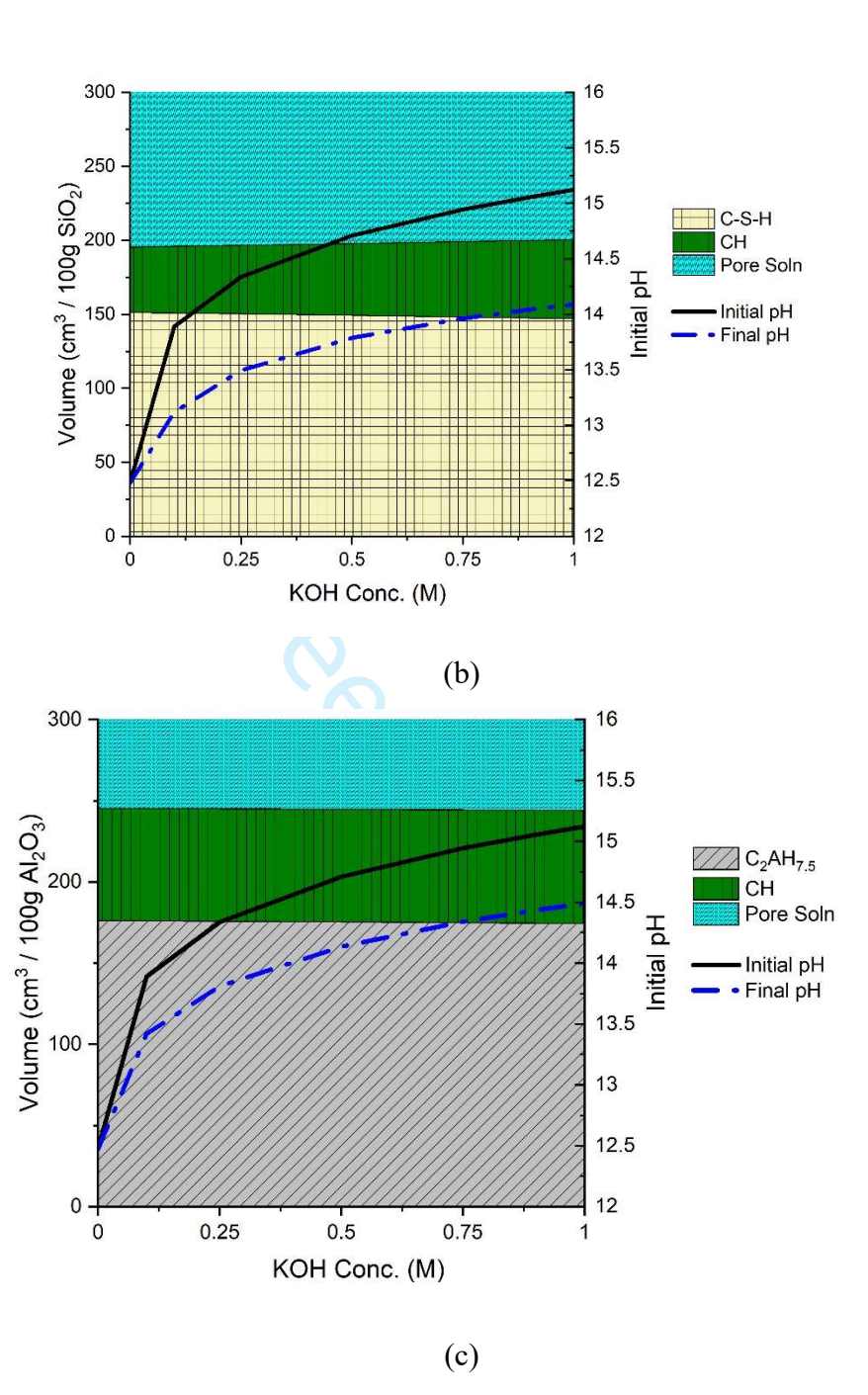


Figure 8- Plot showing (a) the influence of pH of pore solution on the CH consumed and Q_{∞} in the reactivity test, (b) the phase assemblage and Q_{∞} when pure SiO₂ reacts, and the pH is varied, and (c) the phase assemblage and Q_{∞} when pure Al₂O₃ reacts and the pH is varied. The values of Q_{∞} and CH consumed are also noted in Table A-1 of the appendix.

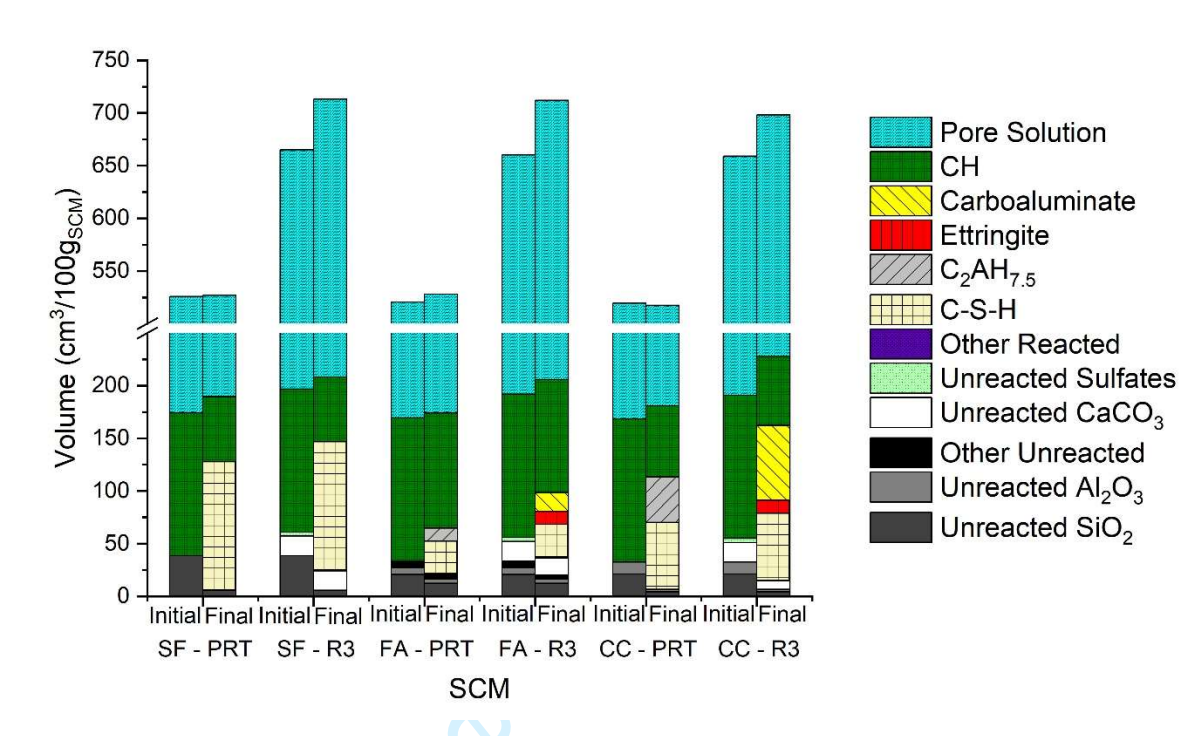


Figure 9- Volumes of initial reactants and final products for the three SCMs studied in the PRT and R3 tests.

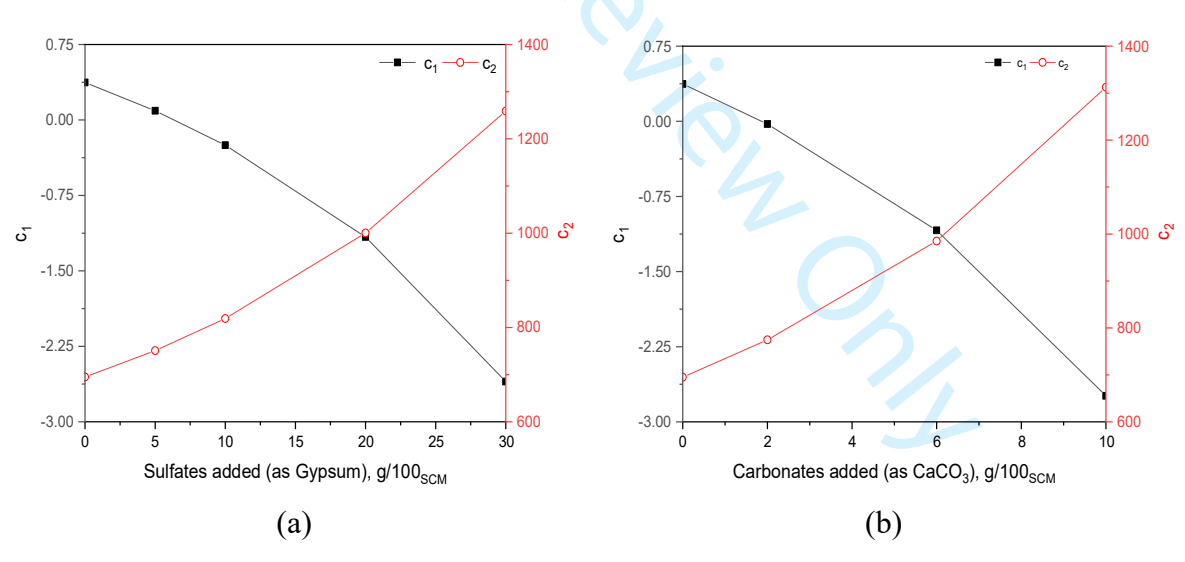


Figure 10- (a) Variation of c₁ and c₂ as a function of sulfate addition, and, (b) variation of c₁ and c₂ as a function of carbonate addition. Markers are at the locations of the sulfate/carbonate additions tested in the experiments (see Table 1).

APPENDIX A: TABULATED DATA OF RELEASED HEAT AND CONSUMED CH FOR THE EXPERIMENTAL TEST MATRIX

Table A-1: Values of Q_{∞} and CH consumed as predicted using thermodynamic modelling and as measured from experiments when the test parameters of the PRT are varied.

		1	T _		Γ_			
CH:SCM	Liquid-	Solution	Q_{∞} as	СН	Q_{∞} as	СН		
	to-	used	predicted	Consumed	measured in	Consumed		
	powder		from	as predicted	experiments	as measured		
	ratio		thermodyna	from	(J/g_{SCM})	in		
			mic	thermodyna		experiments		
			modeling (J /	mic		(g / 100g		
			g _{SCM})	modeling (g /		SCM)		
				100g SCM)				
Silica Fume								
1:1		0.5 M	438	100	493	93		
2:1	0.90	KOH KOH	646	162	547	144		
3:1			646	162	600	168		
	0.75		646	162	556	151		
	0.90	0.5 M	646	162	597	168		
3:1	1	KOH	646	162	542	147		
	1.5	KOH	646	162	600	149		
	2		646	162	606	131		
	0.90	0.25 M	1					
		КОН	647	162	654	159		
		0.5 M						
3:1		КОН	646	162	597	168		
		1M KOH	644	161	607	172		
		2 M						
		KOH	635	158	687	163		
	0.90	0.5 M						
2.1		NaOH	647	162	597	168		
3:1		0.5 M						
		KOH	646	162	635	172		
		•	Fly As	sh				
1:1		0.534	272	39	173	38		
2:1	0.90	0.5 M	272	39	221	43		
3:1		КОН	271	39	289	62		
3:1	0.75	0.534	271	39	329	60		
	0.90		271	39	289	62		
	1	0.5 M	271	39	299	60		
	1.5	KOH	271	39	287	60		
	2		271	39	300	61		
2.1		0.25 M		-				
3:1	0.90	КОН	276	40	371	65		
	1				1			

		0.5 M				
		KOH	271	39	289	62
		1M KOH	265	37	371	48
		2 M				
		KOH	209	25	331	47
3:1	0.90	0.5 M				
		NaOH	245	27	289	62
3.1		0.5 M				
		KOH	271	39	324	57
			Calcined	Clay		
1:1		0.5 M	598	100	478	72
2:1	0.90	KOH	624	116	586	110
3:1			624	116	600	120
	0.75		624	116	574	122
	0.90	0.5 M KOH	624	116	600	120
3:1	1		624	116	657	121
	1.5	KOII	624	116	643	121
	2		624	116	677	129
	0.90	0.25 M				
		KOH	627	117	696	126
		0.5 M				
3:1		KOH	624	116	600	120
		1M KOH	616	114	654	118
		2 M				
		КОН	548	99	630	106
3:1	0.90	0.5 M				
		NaOH	594	103	600	120
		0.5 M				
		KOH	624	116	603	121

Table A-2: Values of Q_{∞} and CH consumed as predicted using thermodynamic modelling and as measured from experiments when sulfates and carbonates are added in the PRT.

Sulfate	Carbonate	Q_{∞} as predicted	CH Consumed	Q_{∞} as	CH Consumed		
Added as	Added as	from	as predicted	measured in	as measured in		
Gypsum	Gypsum	thermodynamic	from	experiments (J	experiments (g		
(g gypsum	(g CaCO ₃ / modeling (J /		thermodynamic	/ g _{SCM})	/ 100g SCM)		
/ 100 g	100 g	g _{SCM})	modeling (g /				
SCM)	SCM)		100g SCM)				
Silica Fume							
0		646	162	597	168		
5		646	160	607	161		
10	0	646	157	621	169		
20		646	153	626	165		
30		647	149	597	171		

	0	646	162	597	168			
0	2	646	162	607	170			
	6	646	162	621	171			
	10	646	162	626	173			
			Fly Ash					
0		271	39	289	62			
5		285	42	315	79			
10	0	306	47	399	63			
20]	334	53	459	88			
30		335	49	516	100			
	0	271	39	289	62			
0	2	300	48	315	58			
U	6	336	57	399	58			
	10	343	55	459	48			
Calcined Clay								
0		624	116	600	120			
5		635	118	630	127			
10	0	656	123	672	130			
20		698	134	706	140			
30		741	145	764	153			
	0	624	116	600	120			
0	2	653	125	630	121			
U	6	711	143	672	123			
	10	769	162	706	132			
				600 630 672 706				

TRACKED VERSION

POZZOLANIC REACTIVITY TEST OF SUPPLEMENTARY CEMENTITIOUS MATERIALS

Antara Choudhary, Keshav Bharadwaj, Rita Maria Ghantous, O. Burkan Isgor*, and W. Jason Weiss

*Corresponding author, burkan.isgor@oregonstate.edu

ABSTRACT

The reactions of supplementary cementitious materials (SCMs) in concrete can be pozzolanic, hydraulic, or a combination of both. This paper focuses on the pozzolanic reactivity test (PRT) for SCMs that are blends of reactive aluminous and siliceous phases. The PRT quantifies reactivity by measuring heat release (Q) and calcium hydroxide (CH) consumption, which are interpreted using thermodynamic modeling. The robustness of PRT is examined by experimentally varying CH-to-SCM ratio, solution-to-solid ratio, sulfate content, alkali type (Na vs. K), and alkali content. The paper also assesses similarities and differences between the PRT and the R3 test (ASTM C1897). It is-was found that sulfates, which are used in the R3 test, did not impact the siliceous reactions; however, they lead to the preferential formation of reaction with aluminous phases to form monosulfo-aluminates and ettringite—with aluminous phases. A generalized relationship for the degree of reactivity is proposed as a function of Q and CH consumption.

Keywords: Pozzolanic reaction, reactivity, fly ash, silica fume, calcined clay, supplementary cementitious materials, thermodynamic modeling, GEMS

BIOGRAPHICAL SKETCH OF AUTHORS

ACI member **Antara Choudhary** is a Ph.D. Student at Oregon State University. Her research interests include the reaction chemistry of supplementary materials and fillers, cement **hydration** hydration, and durability of concrete.

ACI member **Keshav Bharadwaj** is a Ph.D. Student at Oregon State University. His research interests include thermodynamic modeling, reactivity and transport in cementitious systems, <u>and</u> predicting the properties of concrete using thermodynamic/kinetic modeling approaches.

ACI member **Rita Maria Ghantous**, is a Research Associate in the School of Civil and Construction Engineering at Oregon State University. She is a member of ACI Committee 130. Her research interests include carbonation, durability, and sustainability of concrete and cementitious materials.

O. Burkan Isgor, FACI, is a professor in the School of Civil and Construction Engineering at Oregon State University. He is the chair of ACI Committee 222. His research interests include corrosion of steel in concrete, service-life modeling, and thermodynamic modeling.

Jason Weiss, FACI, is the Edwards Distinguished Professor of Engineering in the School of Civil and Construction Engineering at Oregon State University. He is Editor in Chief of the ACI Materials Journal and a Member of the ACI Board.

INTRODUCTION

Supplementary cementitious materials (SCM) have been widely used to partially replace Ordinary Portland Cement (OPC) in modern concrete (1, 2). Common SCMs include coal ashes (e.g., fly ash), ground granulated blast-furnace slag, silica fume, metakaolin, pumice, ground glass, calcined clay, or rice husk ash (3-7). These SCMs typically contain a combination of reactive and nonreactive silica, alumina, and calcium, and they can undergo both pozzolanic and hydraulic reactions depending on their chemical compositions (8-14). Hydraulic reactions of calcium-rich phases in the presence of reactive silica can produce calcium silicate hydrate (C-S-H) and calcium hydroxide (CH) in addition to those produced by the reactions of OPC clinker and water. The silica and alumina phases of the SCM typically react pozzolanically with CH in the system (15-18). Pozzolanic reactions are considered secondary reactions as their occurrence depends on the availability of CH produced by the hydraulic reactions (19). SCMs like silica fume, Class F fly ash, and calcined clay mainly react pozzolanically with CH in the presence of adequate moisture to produce stable cementing compounds (20). SCMs like slag are primarily hydraulic (21-23). Pozzolanic reactions make SCMs highly beneficial in concrete through two primary mechanisms. First, the partial replacement of OPC with SCM- leads to a lower OPC clinker content in the mixture (dilution), which reduces the carbon dioxide (CO₂) footprint of the concrete (13, 14, 24, 25). Second, pozzolanic reactions produce more C-S-H, making the concrete stronger and more durable (26-28). While dilution is directly related to SCM's replacement level in the mixture, several other factors such as chemical composition and reactivity of SCMs affect pozzolanic reactions. Traditionally, the reactivity of SCMs in OPC-based mixtures is quantified through the strength activity index (SAI) as defined by ASTM C311 (29). Several specifications use SAI as a criterion for allowing SCM to be used in concrete. For example, ASTM C618 (30) specifies that fly ashes need to satisfy a minimum SAI for use in concrete. Similarly, ASTM C 989 (6) specifies SAI requirements for using slag in concrete. However, it is widely accepted that SAI is a poor indicator of pozzolanic (or chemical) reactivity because non-reactive SCMs have been shown to pass the SAI criteria of published specifications (31, 32).

To address some of the issues with strength testing, several test methods have been developed to assess the pozzolanic reactivity of SCMs. The lime reactivity test (IS 1727-1967) (33) has practical issues due to long test duration and reproducibility (32, 34). The Frattini test (EN 196-5) (35, 36), the reactive silica test (EN 196-2 (37) and EN 197-1(38)), and the modified Chapelle test (NF P18-513) (39-41) have all been proposed to address this challenge. More recently, the R3 test method is developed, initially by Snellings and Scrivener (42) and later standardized in ASTM C1897-20 (43), as a more rapid test for assessing pozzolanic reactivity of SCMs. The R3 method determines the reaction potential of an SCM by mixing it with CH in a medium that contains sulfates, carbonates, and alkali and measuring the heat of reaction (Q) or the non-evaporable water of the reacted paste. This test is accelerated by maintaining the temperature of the paste at 40°C.

In parallel with the R3 test, another test, dubbed as the Pozzolanic Reactivity Test (PRT), was developed (44). The PRT method determines the reaction potential of an SCM by mixing it with CH in an alkaline solution. The Q and CH consumption are measured at 50°C for ten days and the ultimate heat of reaction (Q_{∞}) is determined. The results of this test, Q_{∞} and CH consumption, are superimposed on plots of predetermined degrees of reaction of pure SiO₂ and Al₂O₃ systems to estimate the maximum degree of reactivity (DOR*) of the SCM (45-47). The DOR* of an SCM is the theoretical maximum mass fraction of the SCM that can react. A series of papers have demonstrated the use of the PRT (45, 48-52) with refined predictions of DOR* (53, 54), especially when calcium oxide (CaO) is present in the SCM (45, 50). The PRT provides a quantifiable DOR*,

which has been shown to be related to the glass (amorphous) content in the SCM (45, 55). The DOR* can also be used as an input in thermodynamic modeling. Recent work has used these models to make successful predictions of several parameters of OPC+SCM pastes and concrete, such as the porosity, compressive strength, formation factor, CH content, calcium oxychloride formation potential, and time to freeze-thaw damage (25, 28, 47, 48, 53, 54, 56-65).

The R3 test and PRT methods are similar conceptually; however, the two methods differ practically in a few distinct areas. First, the tests are performed at different temperatures: the R3 test is performed at 40°C and the PRT is at 50°C, and this difference is not expected to cause major differences in the way the two methods assess pozzolanic reactivity. The testing temperature used is mainly dependent on user preference. Higher temperatures (40°C or 50°C) generally result in a faster test, however, they might also lead to reactions that do not typically occur at room temperature (19). This is a distinction that can be investigated; however, it is not in the scope of the study presented in this paper. The second area in which the tests differ is in the use of sulfate or carbonate. Unlike the PRT test (where no sulfate or carbonate is added for the test), the R3 test uses added potassium sulfate (4.8 g SO₃/100 g SCM) and calcium carbonate (50 g CaCO₃/100 g SCM) in the simulated solution. This fundamental difference between the two tests on the results of the reactivity tests is investigated in this paper. The third difference is in the liquid-to-powder ratio (ratio of the mass of alkaline pore solution added to the mass of SCM+CH in the test) with the R3 method using a ratio of 1.2 and the PRT using 0.9. Finally, the pore solution pH (alkali loading) is also different between the two test methods, with the R3 test using K₂O=1.96 g / 1 L= 0.07 M (corresponding to a pH of 12.85) and the PRT using KOH=0.5 M (corresponding to a pH of 13.7).

In this paper, the differences between the R3 and PRT tests are studied experimentally and using thermodynamic calculations. The robustness of the PRT is examined by experimentally varying several test parameters: the CH-to-SCM ratio, the liquid-to-powder ratio, sulfate and carbonate contents, alkali cation type (NaOH vs. KOH), and alkalinity of the pore solution (pH of pore solution).

RESEARCH SIGNIFICANCE

This paper aims to provide insight into the robustness of the PRT, which quantifies the maximum degree of reactivity (DOR*) of an SCM. The quantification of DOR* is important because it is needed as an input for thermodynamic models. The robustness of the PRT is assessed by studying the impact of varying testing parameters such as the SCM:CH mass ratio, liquid-to-powder mass ratio, pore solution alkalinity, and the chemical composition of the test mixture. This work provides recommendations on the testing of pozzolanic reactivity and is a step toward developing performance specifications for SCMs.

EXPERIMENTAL INVESTIGATION

The PRT consists of preparing a paste by combining one-part SCM by mass, three parts CH, and 0.5 M KOH solution. The method has a solution-to-dry powder ratio of 0.9. After weighing the constituent materials, the paste is thoroughly mixed according to the procedure outlined in previous work (50). In the standard procedure, 40 g of SCM is mixed with 120 g of CH and 144 g of 0.5 M KOH solution. The heat of hydration reaction is measured from mixing up after mixing for 240-hours (10-days) at a temperature of 50°C using an isothermal calorimeter. The extent of the pozzolanic reaction is determined by measuring the amount of CH consumed by the SCM

reaction after ten days at 50°C. The CH consumed is measured using a thermogravimetric analyzer.

The details on the approach are provided in previous works (45, 5958).

Table 1 describes the experimental test matrix. The varied test parameters are shown in the first column and include the CH:SCM mass ratio, liquid-to-powder mass ratio, sulfate content (as gypsum), carbonate content (as calcium carbonate), alkali content, and alkali pore solution cation type. The sulfate levels are representative of and exceed the typical sulfate levels in concrete systems (6766). Note that the "baseline case" (listed in the last column) includes the test parameters used for the PRT test (CH:SCM=3:1, liquid-to-powder ratio—0.9, etc.). The table provides the ranges over which the test parameters are varied. These ranges cover and extend beyond the differences between the R3 test and the PRT test parameter values.

Three SCMs are tested: silica fume (SF: 95.9% siliceous), class F fly ash (FA: 51.9% siliceous and 21.7% aluminous), and calcined clay (CC: 54.2% siliceous and 37.5% aluminous). The chemical composition of these SCMs is listed in Table 2.

THERMODYNAMIC MODELING

Thermodynamic modeling is a tool that can be used to determine the reaction products of cementitious mixtures at equilibrium (6867-7069). It can be used to calculate the mass and volume fractions of solid and gaseous phases and concentrations of ionic species by minimizing the system's Gibbs free energy. In this work, GEMS3K v3.5 (7470, 7271) and the Cemdata 18 (6867) database were used to simulate reactions that take place in different examined variations of the PRT test as per Table 1. Specifically, it is used to calculate the amount of reaction products, as well as Q_{∞} and CH consumed during the reactions. Thermodynamic modeling also provides the theoretical amorphous silica and alumina lines that are used to quantify DOR* (45, 5958). These

theoretical lines for pure SiO_2 and pure Al_2O_3 , which are typically used to quantify the reactivity of fly ashes, are shown in- Figure 1. These lines indicate the Q_∞ and CH consumption pairs when pure silica and pure alumina are allowed to undergo pozzolanic reactions at different reactivities ranging from 0 to 100%. It should be noted that these theoretical lines are customized based on the composition of the SCM that is tested. In thermodynamic calculations presented in this work, some phases are blocked from forming based on evidence in the literature that they do not form in the time scales and temperature of the PRT test. The blocked phases include C_3AH_6 (7372, 7473), Gibbsite (6867), and some monosulfate phases (C_4AH_{13} , C_4AH_{19} , and C_4AsH_{12} (45)). The SiO_2 and Al_2O_3 lines are refined from previous work (45) to include the pore solution's enthalpy while calculating the heat released.

RESULTS AND DISCUSSION

Typical results from experiments and simulation

The experimental results obtained from the PRT conducted following the experimental matrix described in Table 1 are discussed in this section. Figure 2 shows the Q_{∞} and CH consumed results obtained from thermodynamic simulations of the pozzolanic reactions of SF, FA, and CC as compared to the experimental results. The values of Q_{∞} and CH consumed for all the tests performed are also provided in Table A-1 and Table A-2 of the appendix. The majority of the modeled values lie within \pm 20% of the experimental values, indicating a good agreement between the model and the experiment. The next few subsections will examine the variation of each test parameter in detail and provide a discussion of the results.

Influence of varying CH:SCM ratio on the results of the PRT

Figure 3 (a) shows experimental results of the PRT along with results from the thermodynamic calculations for cases where the CH:–SCM is varied for different SCMs. As the CH:–SCM increases, the Q_{∞} and CH consumed increase, but Q_{∞} /CH consumed decreases, suggesting a potential change in the reaction products. To better understand the changes that may be occurring, the phase assemblages are examined.

Figure 3 (b) shows a plot of phase assemblages at equilibrium for various CH:SCM mass ratio is varied for pure SiO₂. As CH is added to the pure silica system, the silica reacts with water and the CH to form C-S-H phases. At low CH:SiO₂ levels (CH:SiO₂ <0.61), a portion of the silica remains unreacted. A minimum of 61 g of CH is required for the complete reaction of 100 g SiO₂ (solid red line). As the CH:SiO₂ is increased from 0.61 to 1.98 (red dashed line), various forms of C-S-H with varying C/S form (Jennite-D, Jennite-H, Tobermorite-D, Tobermorite-H). As a result, the average C/S of the C-S-H increases from 0.7 (at a CH:SiO₂ of 0.61) to 1.7 (at a CH:SiO₂ of 1.98)). For CH:SiO₂ above 1.98, unreacted CH remains, and the total volume of C-S-H, as well as the proportions of the C-S-H variations, remain constant.

Figure 3 (c) shows a plot of the phase assemblages at equilibrium for the pure alumina system. As CH is added to the pure alumina system, the alumina reacts with water and the CH to form C-A-H phases (C₂AH_{7.5} forms in the PRT at 50°C). At low CH contents a portion of the alumina remains. A minimum of 144 g of CH is required for the complete reaction of 100 g Al₂O₃ (shown as the red dashed line). If the CH:Al₂O₃ is less than 1.44, unreacted alumina remains, and if the CH:Al₂O₃ is greater than 1.44, unreacted CH remains.

The thermodynamic calculations indicate that, for any SCM, the minimum CH:SCM required for complete hydration is 1.98:1. However, it is possible that kinetic effects and local physical

availability of CH at low CH:SCM mass ratios may dominate, and therefore, the CH:SCM of 3:1 is recommended for the PRT.

The experimental test results of FA (circles) and CC (stars) (Figure 3 (a)) indicate that CH is still present after the reactivity test (10 days at 50°C) for all CH:SCM ratios (3:1, 2:1, and 1:1). This is because the FA or CC are not comprised of pure reactive aluminate or silicate and they do not have a DOR* of 100%. On the other hand, at a CH:SCM=1:1, the tested SF (96% siliceous) appears to consume the entire available CH (all 100 g CH added is consumed), which is also predicted by thermodynamic modeling.

Influence of varying liquid-to-powder ratio on the results of the PRT

Figure 4 shows the experimental results of varying the liquid (0.5 M KOH solution) to powder (SCM+CH) mass ratio. The liquid-to-powder ratios tested are 0.75, 0.9, 1, 1.5, and 2 (shown in Table 1). Theoretically, a liquid-to-powder ratio of 0.75 provides sufficient water and CH for complete reaction of both aluminate and silicate phases in the SCM. However, achieving a workable mixture at that liquid-to-powder ratio can be challenging for highly reactive materials with a high surface area like SF. The variation in the results of CH consumed for SF and CC could be attributed to the physical dispersion and local availability of CH around the SCMs. As the liquid-to-powder ratio increases, the SCM dispersion improves, and the reaction would tend toward equilibrium. However, the slight variations in the experimental results on altering liquid-to-powder ratios, result in a relatively small variation in DOR* (DOR* varies from 71% to 79% for SF, 43% to 39% for FA, and 75% to 89% for CC).

Thermodynamic modeling predicts that a minimum of 24 g water is required for a complete reaction of 100 g SiO₂ and CH to form C-S-H (the C-S-H formed has a C/S of 0.72), and a minimum of 97 g of water required for complete reaction of 100 g Al₂O₃ to form C₂AH_{7.5}. If the

CH-to-SCM mass ratio is constant at 3:1, the minimum liquid-to-powder mass ratio required for complete hydration of either SiO₂ or Al₂O₃ is 0.24. Therefore, <u>for</u> all tested cases, the values of liquid-to-powder ratios (0.75 to 2.00) satisfy this minimum requirement.

Influence of sulfates addition on the results of the PRT

Figure 5 (a) shows the experimental results of the PRT when sulfates are present. The sulfates (added as gypsum, CaSO₄.2H₂O) in the SCM+CH+liquid mixture vary from $0_g/100_{gSCM}$ (the PRT baseline case) to $30_g/100_{gSCM}$ for the tested SCMs. The addition of sulfate has a negligible impact on the DOR* of the SF (the DOR* values are within 5% of each other). This is because the tested SF has little to no alumina which is known to react with sulfates (Table 2). For both the FA and CC systems, when the sulfate is increased, the Q_{∞} and CH consumed increased (approximately linearly proportional to the mass of gypsum added). For fly ash, Q_{∞} increased by $0.8_g/g_{gypsum}$ added, and the CH consumed increased by $0.15_g/g_{gypsum}$ added. For CC, Q_{∞} increased by $0.6_g/g_{gypsum}$ added, and the CH consumed increased by $0.1_g/g_{gypsum}$ added. Also, it can be seen in Figure 5 (a) the experimental results show a similar trend as what is predicted using thermodynamic simulations.

Figure 5 (b) shows the phase assemblage of the equilibrium reaction of pure SiO_2 as sulfates are added. The CH: SCM mass ratio is kept at 3:1 and the liquid-to-powder mass ratio at 0.90. As the gypsum content increases from 0 g/100 g_{SCM} to 30 g/100 g_{SCM} , thermodynamic modeling predicts

that the siliceous reactions are unaffected, i.e., the same amount of C-S-H forms with the same C/S ratio (C/S = 1.7). The CH consumption and Q_{∞} remain unchanged as well.

Figure 5 (c) shows the phase assemblage of the equilibrium reaction of pure Al_2O_3 system as sulfates are added. The sulfates react with the alumina, CH, and water in the mixture preferentially to form mono-sulfate phases. Any excess alumina (left over after all sulfates have been consumed) reacts with the CH and water in the mixture to form C-A-H phases ($C_2AH_{7.5}$). The reaction of alumina that produces mono-sulfate generates more Q_∞ than the reaction that produces the C-A-H phase observed (approximately 3.25 J/g_{gypsum} added more Q_∞ is produced). The reaction of alumina that produces mono-sulfate, however, does not seem to consume more CH than the reaction that produces C-A-H. Therefore, the alumina reaction is impacted by the presence of sulfates, and when sulfates are present, Q_∞ increases (due to changes in the reaction products, i.e., the formation of mono-sulfates at the expense of C-A-H phases). However, the CH consumed by the alumina-containing SCMs (FA and CC) seems to increase proportionally with the added sulfates. This is possible—possibly due to the prefrential preferential formation of AFm in these systems over $C_2AH_{7.5}$ (7574, 7675) The formation of AFm approximately consumes an additional 73.5 g_{CH}/100 g_{alumina} more than formation of $C_2AH_{7.5}$.

Influence of calcium carbonates on the results of the PRT

Figure 6 (a) shows the experimental results of the PRT when calcium carbonates are present. The calcium carbonate in the SCM+CH+liquid mixture vary varies from $0_g/100_{gSCM}$ (baseline case for the PRT) to $10_g/100_{gSCM}$ for the tested SCMs. The addition of calcium carbonate has an insignificant impact on the reactivity of SF (the DOR* values are within 5% of each other). This is because the tested SF has little to no alumina (Table 2). For both the FA and CC systems, when the mass of calcium carbonate added is was increased, Q_{∞} and the consumption of CH consumed

increased (approximately linearly proportional to the mass of calcium carbonate added). For fly ash, Q_{∞} increased by 1.6J/gC_{aCO3} added and the CH consumed decreased by 0.1g/gC_{aCO3} added for the FA. For CC, Q_{∞} increased by 1.2J/gC_{aCO3} added, and the CH consumed increased by 0.06 g/gC_{aCO3} added. The experimental results of Q_{∞} and CH consumed show a similar trend as the predictions using-from thermodynamic modeling, as shown in Figure 6 (a).

Figure 6 (b) shows the phase assemblage of the equilibrium reaction of pure SiO_2 as carbonates are added. The CH: SCM mass ratio is kept at 3:1 and liquid-to-powder mass ratio at 0.90. As the calcium carbonate content is increased from $0_g/100g_{SCM}$ to $10_g/100g_{SCM}$, thermodynamic modeling predicts that the siliceous reactions are unaffected, i.e., the same amount of C-S-H forms with the same C/S ratio (C/S=1.7). The CH consumption and Q_{∞} remain unchanged as well.

Figure 6 (c) shows the phase assemblage of the equilibrium reaction of the pure Al_2O_3 system as carbonate is added. The carbonate reacts with the alumina, CH, and water in the mixture preferentially to form hemi-/mono-carbonate phases. Any excess alumina left over after all the carbonates have reacted reacts with the CH and water in the mixture to form C-A-H phases ($C_2AH_{7.5}$). The reaction of alumina that produces hemi-/mono-carbonates generates more heat than the reaction that produces the C-A-H phase observed (an increase of approximately 10.95 J/g_{CaCO3} added more heat is produced). The reaction of alumina that produces hemi-/mono-carbonates also consumes more CH than the reaction that produces C-A-H (an increase of approximately 2.23 g/g_{CaCO3} added more CH is consumed). Therefore, the alumina reaction is impacted by the presence of carbonates, and when carbonates are present, the Q_{∞} and CH consumed increase (due to changes in the reaction products – formation of hemi-/mono-carbonates at the expense of C-A-H phases). This is also observed in the experimental results of FA and CC, which contain reactive alumina according to Table 2.

Influence of alkali cation on the results of the PRT

Figure 7 (a) shows the experimental results of PRT with two different alkali pore solutions (KOH and NaOH) for the tested SCMs. It can be seen that the alkali content and cations have almost no impact on the results. The calculated values of the DOR* for SF, FA and CC are within 7%, 8%, and 0.5% of each other, repsectively respectively.

Figure 7 (b) and Figure 7 (c) show the result of varying the alkali cation for the PRT for pure SiO₂ and pure Al₂O₃, respectively. As alkali cations in the pore solution are changed (from pure 0.5 M KOH to pure 0.5 M NaOH) for both systems, the only change observed is in the pure siliceous system (a roughly 1% decrease in C-S-H volume when NaOH is used instead of KOH), where the C-S-H may bind potassium differently than sodium. It appears that the type of cation does not impact the PRT.

Influence of pH on the results of the PRT
Figure 8(a) shows 1 Figure 8(a) shows the experimental results of the PRT with different pore solution concentrations for the tested SCMs. Figure 8 (b) and Figure 8 (c) depict the modeled phase assemblage of equilibrium reaction of pure SiO₂ and pure Al₂O₃ for different pore solution concentrations of KOH.

As seen from Figure 8 (b), as the concentration of hydroxyl ions in the pore solution are is increased from 0.25 M (pH of 12.7) to 2 M (pH of 15.2), the volume of C-S-H that forms changes slightly due to the different amount of alkali binding (approximately 2% change in volume over the pH range studied). The amount of CH that becomes soluble is affected by the amount of KOH in the solution. There is no noteworthy change in the Q_{∞} or CH consumed in the model. Similarly, from Figure 8(c), it can be seen that the change in the pore solution pH has a minimal impact on the phase assemblage (about a 1% change in volume of C-A-H that forms), and there is no noteworthy change in the Q_{∞} or CH consumed.

Comparing the PRT with other reactivity tests

This section discusses the comparison of the PRT with the R3 test procedure. Similarities and differences are shown in Table 3 and Figure 9. As previously mentioned, the most important difference appersappears to be the addition of sulfates and calcium carbonates to the reactants in the R3 test. The addition of these materials results in a substantial difference for aluminous systems. For example, when sulfates are added, the alumina in the SCM reacts to form monosulfate phases rather than C-A-H phases, which leads to a higher Q_{∞} . When carbonates and sulfates are present, the reactive alumina first forms ettringite, and the remaining reactive alumina forms carbo-aluminate phases. When sulfates are added to siliceous systems the reactions are relatively unaffected and both tests are similar. Therefore, if sulfates or/and carbonates are added, the changes to the reaction products needs to be accounted for while calculating the reactivity of the SCM.

Figure 9 shows the initial reactants and final reaction products in the PRT and R3 tests for the three SCMs tested. The first column for each system shows the volumes of initial reactants and the second column shows the volume of reacted products. First, it can be seen when looking at the SCMs in the PRT test that SF reacts pozzolanically to form C-S-H, and FA and CC react pozzolanically to form C-S-H and C-A-H (C₂AH_{7.5}). In the R3 test, the SF reacts to form C-S-H (similar to the PRT), but the FA and CC react to form ettringite and carboaluminates rather than C-A-H. For example, when 100_g of the tested CC is subjected to the PRT, 12_cm³/100_g_{SCM} of C₂AH_{7.5} forms, while in the R3 test, no C-A-H forms (12_cm³/100_g_{SCM})_of ettringite and 71 cm³/100_g_{SCM} -of carboaluminate forms instead). This change in the phase assemblage in the R3

test (formation of ettringite and carboaluminates rather than C-A-H) leads to a higher measured Q_{∞} and CH consumed (see Table 3). The relative proportions of these three reactions can also change. It can also be seen that in the R3 test, for the compositions of the SCMs tested, all the sulfate is consumed (to form ettringite) but not all the carbonate is consumed.

It should be noted that in both the R3 and PRT tests, the volumes of C-S-H that forms are within 0.2 cm³/100 gscm of each other (the reaction of 100 g SF produces 122 cm³ C-S-H, that of 100 g FA produces 31 cm³ C-S-H, and that of 100 g CC produces 64 cm³ C-S-H). This is because the formation of C-S-H only depends on the pozzolanic reaction of silica in the SCM, and is unaffected by the presence of sulfates and carbonates.

In summary, the R3 test adds sulfates and carbonates; however, even the addition of a constant amount of sulfate and carbonate can cause various phases (and various amounts of each phase) to form when SCMs of different composition (and different percentages of reactive phases) are tested. For example, if an SCM with very low alumina content is tested, ettringite + hemicarbonates + monocarbonates would form in the R3 test, while if an SCM with high alumina is tested, ettringite + monocarbonates would form (the phases that form can be determined from the carbonate-sulfate-alumina stability diagram in (7476)). This difference in the phase assemblage would result in different amounts of heat release (or non-evaporable water) measured. Therefore, SCMs of similar reactivities but different alumina contents could result in very different Q_{∞} (or non-evaporable water) measurements. The PRT on the other hand does not add sulfates and carbonates, and consistent phases form as a result of the pozzolanic reaction (C-S-H from silica, and C-A-H from alumina). This makes the PRT a more robust tool to evaluate the reactivity of alumina containing SCMs such as fly ash, metakaolin (or calcined clays), natural pozzolans, etc. Additionally, the R3 test output can only be used as a qualitative comparison tool between two

SCMs (determine which SCM is more reactive or to distinguish pozzolanic materials from inert fillers), while the PRT has been extended to allow for calculation of an absolute numerical value of reactivity (DOR*) which is described in the following section.

Relationship between CH consumed, Qo, pore solution composition and DOR*

The PRT measures the DOR* of an SCM. For experimental results that fall in between the theoretical reactivity of pure SiO₂ and pure Al₂O₃, the results can be interpolated to obtain DOR* using:

$$DOR^* = \frac{Q_{\infty} - c_1 \cdot CH_{consumed}}{c_2} \tag{1}$$

where Q_{∞} is the Q_{∞} measured using the an isothermal calorimeter (IC) (in J/g_{SCM}), $CH_{consumed}$ is the CH consumed by 100_g SCM measured using the a thermogravimetric analyzer (TGA) (in g/100_g_{SCM}), and c_1 is 0.373 and c_2 is 695 for the PRT.

For conditions other than the PRT, the c_1 and c_2 constants that can be calculated from the theoretical Q_{∞} and CH consumed at complete reaction of SiO₂ and Al₂O₃ using equation (2) and (3), shown below:

$$c_{1} = \frac{Q_{\infty}^{SiO_{2}} - Q_{\infty}^{Al_{2}O_{3}}}{CH_{consumed}^{SiO_{2}} - CH_{consumed}^{Al_{2}O_{3}}}$$
(2)

$$c_{2} = \frac{Q_{\infty}^{Al_{2}O_{3}} \cdot CH_{consumed}^{SiO_{2}} - Q_{\infty}^{SiO_{2}} \cdot CH_{consumed}^{Al_{2}O_{3}}}{CH_{consumed}^{SiO_{2}} - CH_{consumed}^{Al_{2}O_{3}}}$$

$$(3)$$

where $Q_{\infty}^{SiO_2}$ and $Q_{\infty}^{Al_2O_3}$ are the Q_{∞} when pure 100% reactive silica and alumina react with CH and water, respectively (for the PRT, these values are $Q_{\infty}^{SiO_2} = 769 \text{_J/g}_{SCM}$ and $Q_{\infty}^{Al_2O_3} = 749 \text{_J/g}_{SCM}$), and, $CH_{consumed}^{SiO_2}$ and $CH_{consumed}^{Al_2O_3}$ are the CH consumed when pure 100% reactive silica

and alumina react with CH and water, respectively (for the PRT, these values are $CH_{consumed}^{SiO_2} = 198 \text{ g}/100 \text{ g}_{SCM}$ and $CH_{consumed}^{Al_2O_3} = 144 \text{ g}/100 \text{ g}_{SCM}$).

The values of c_1 and c_2 are only dependent on the test parameters and not on the SCM chemistry. For example, for the R3 test, the values are $c_1 = 9.70$ and, $c_2 = -1151$. If sulfates are added during the test (though we do not recommended the addition of sulfates for testing pozzolanic reactivity), the values of c_1 and c_2 vary as a function of sulfate and carbonate addition as shown in the Figure 10 (note that the figure shows independent addition of sulfate or carbonate, not both together; if both are present together such as in the R3 test, thermodynamic calculations need to be performed to calculate the values of c_1 and c_2).

CONCLUSION

This paper examineds the influence of the testing parameters on the results of the PRT (pozzolanic reactivity test) for SCMs. In the PRT, the SCM is mixed with CH and alkaline pore solution and the heat released and CH consumed by the pozzolanic reactions are measured. Two ideal pozzolanic materials (amorphous SiO₂ and Al₂O₃) are thermodynamically modeled to provide the reference values of heat released and CH consumed by an SCM. Three pozzolanic materials are were measured experimentally: silica fume (primarily siliceous), class F fly ash (22% aluminous and 52% siliceous), and calcined clay (38% aluminous and 54% siliceous). The aluminous reaction has a higher ratio of Q_∞ for the same amount of CH consumed. The influence of varying several test parameters including (e.g., the CH to SCM ratio, water to CH+SCM ratio, sulfate addition, carbonate addition, alkali loading, and alkali species), wasis assessed.

A CH:SCM ratio of 3:1 is recommended <u>for determining reactivity, which is </u>-(consistent with that <u>whatwhich</u> is currently used in both <u>R3</u> test <u>and PRTs</u> (43, 44). <u>T</u>The minimum liquid-to-powder ratio for a complete reaction of any SCM is theoretically determined to be 0.25; however, experimentally, it is observed that a value above 0.9 is needed to enable the samples to be prepared for consistent results. Liquid-to-powder ratios beyond 0.9 do not impact the results.

The siliceous reactions are unaffected by the presence of sulfate or carbonate (the same volume of C-S-H forms with the same C/S); however, the aluminous reactions are affected by the addition of both sulfate and carbonate both. The impact of sulfate and carbonate is not due to a change in the pozzolanic reaction of the aluminous material but rather due to the formation of alternative reaction products. When no sulfates or carbonates are present, C-A-H phases (C₂AH_{7.5}) form due to the pozzolanic reaction of the Al₂O₃ in the SCM. In the presence of sulfates, monosulfates and ettringite are preferentially formed instead of C-A-H phases. In the presence of carbonates, Al₂O₃ preferentially reacts to form carboaluminates rather than C-A-H phases. This change to the reaction products is accompanied by an increase in heat release and CH consumption. As such, the addition of sulfates or carbonates is not recommended for the measurement of pozzolanic reactivity. However, if sulfates or carbonates present in the system, their impact on DOR* can be considered mathematically.

Variations in the hydroxide composition (cation used, K vs. Na) have a negligible impact on the reactivity for the same equivalent alkali loading (the variation in the DOR* for SF, FA, and CC is under 6%). The change alkali loading (pH/molarity) does impact the kinetics of the experiment though the equilibrium reactions (and reactivity of the SCM) remain relatively unaffected. A generalized relationship is developed between the Q_{∞} , and the CH consumed to mathematically calculate the DOR* of a pozzolan using the results of the PRT for the typical PRT and R3 testing

conditions. The PRT test is shown to be a test that primarily measures the pozzolanic reaction and quantifies the maximum reactivity for an SCM. The paper recommends using standardized PRT to measure SCM DOR* due to practical advantages.

ACKNOWLEDGMENTS

The authors gratefully acknowledge the financial support provided by ARPA-E (Advanced Research Projects Agency-Energy), CALTRANS (California Department of Transportation), and National Science Foundation (Grant No. NSF CMMI 1728358). The authors gratefully acknowledge support from the Edwards Distinguished Chair at Oregon State. The authors also acknowledge fruitful discussions with Prof. Barbara Lothenbach (EMPA, Switzerland). The authors also acknowledge Oliver Hudson Opdahl and Audrey Collins for their laboratory assistance.

REFERENCES

- 1. A Neville, "Properties of Concrete, (3rd edn.)Edition, Pitman," London, UK. 1981.
- 2. S Mindess, F Young and D Darwin, "Concrete, 2nd Edition," Technical Documents. Prentice Hall, 2003, 644 pp.
- 3. P Barnes and J Bensted, "Structure and performance of cements," CRC Press, 2002.
- 4. GS Barger, ER Hansen, MR Wood, T Neary, DJ Beech and D Jaquier, "Production and use of calcined natural pozzolans in concrete," Cement, concrete and aggregates, V. 23, No. 27, 2001, pp. 73-80.
- 5. B Uzal, L Turanli and PK Mehta, "High-volume natural pozzolan concrete for structural applications," ACI Materials Journal, V. 104, No. 5., 2007, pp. 535-538.

- 6. ASTM C989-18, "Standard Specification for Slag Cement for Use in Concrete and Mortars," Book Standard Specification for Slag Cement for Use in Concrete and Mortars, Editor, ed.^eds., ASTM International, CityWest Conshohocken, 2018, pp.
- 7. JM Aldred, TC Holland, DR Morgan, DM Roy, MA Bury, RD Hooton, J Olek, MJ Scali, RJ Detwiler and TM Jaberet al., "Guide for the use of silica fume in concrete," ACI—American Concrete Institute—Committee 234,: Farmington Hills, MI, USA, V. 234—2006.
- 8. B Lothenbach, K Scrivener and R Hooton, "Supplementary cementitious materials," Cement and concrete research, V. 41, No. 12-, 2011, pp. 1244-1256.
- 9. MC Juenger and R Siddique, "Recent advances in understanding the role of supplementary cementitious materials in concrete," Cement and Concrete Research, V. 78-, 2015, pp. 71-80.
- 10. R Khatri, V Sirivivatnanon and W Gross, "Effect of different supplementary cementitious materials on mechanical properties of high performance concrete," Cement and Concrete research, V. 25, No. 1-, 1995, pp. 209-220.
- 11. MC Juenger, R Snellings and SA Bernal, "Supplementary cementitious materials: New sources, characterization, and performance insights," Cement and Concrete Research, V. 122. 2019, pp. 257-273.
- 12. JM Justice, "Evaluation of metakaolins for use as supplementary cementitious materials,"

 Book Evaluation of metakaolins for use as supplementary cementitious materials, Editor, ed.^eds.,

 M. Sc. Thesis, Georgia Institute of Technology, CityAtlanta, GA, 2005, pp. 134.
- 13. V Papadakis and S Tsimas, "Supplementary cementing materials in concrete: Part I: efficiency and design," Cement and concrete research, V. 32, No. 10-, 2002, pp. 1525-1532.

- 14. V Papadakis, S Antiohos and S Tsimas, "Supplementary cementing materials in concrete: Part II: A fundamental estimation of the efficiency factor," Cement and Concrete research, V. 32, No. 10-, 2002, pp. 1533-1538.
- 15. M Ghrici, S Kenai and M Said-Mansour, "Mechanical properties and durability of mortar and concrete containing natural pozzolana and limestone blended cements," Cement and Concrete Composites, V. 29, No. 7-, 2007, pp. 542-549.
- 16. HJKOKES Klaartje De Weerdt, H Justness, KO Kjellsen amd E Sellevold, "Fly ashlimestone ternary composite cements: synergetic effect at 28 days," NCRNordic Concrete Research, V. 42, No. 4, 12/15/2010, pp. 51-70.
- 17. M Ahmaruzzaman, "A review on the utilization of fly ash," Progress in energy and combustion science, V. 36, No. 3-, 2010, pp. 327-363.
- 18. R Siddique, "Utilization of silica fume in concrete: Review of hardened properties," Resources, Conservation and Recycling, V. 55, No. 11-, 2011, pp. 923-932.
- 19. F Deschner, B Lothenbach, F Winnefeld and J Neubauer, "Effect of temperature on the hydration of Portland cement blended with siliceous fly ash," Cement Concrete Res<u>earch</u>, V. 52, Oct. 2013, pp. 169-<u>1</u>81.
- 20. K Vessalas, P Thomas, A Ray, J-P Guerbois, P Joyce and J Haggman, "Pozzolanic reactivity of the supplementary cementitious material pitchstone fines by thermogravimetric analysis," Journal of Thermal Analysis and Calorimetry, V. 97, No. 1-, 2009, pp. 71-76.
- 21. M House, CD Bella, H Sun, G Zima, L Barcelo and W Weiss, "Influence of Slag Aggregate Production on Its Potential for Use in Internal Curing," Transportation Research Record: Journal of the Transportation Research Board, V. 2441-, 2014, pp. 105-111.

- 22. G Menéndez, V Bonavetti and E Irassar, "Strength development of ternary blended cement with limestone filler and blast-furnace slag," Cement and Concrete Composites, V. 25, No. 1–2 2003, pp. 61-67.
- 23. C Shi, "Steel slag—its production, processing, characteristics, and cementitious properties," Journal of materials in civil engineering, V. 16, No. 3-, 2004, pp. 230-236.
- 24. PK Mehta and PJ Monteiro, "Concrete: microstructure, properties, and materials." McGraw-Hill Education; 2014, 684 pp.
- 25. I De la Varga, J Castro, D Bentz, F Zunino and J Weiss, "Evaluating the hydration of high volume fly ash mixtures using chemically inert fillers," Construction and Building Materials, V. 161, 10 February 2018. 2018, pp. 221-228.
- 26. M Thomas, "Optimizing the use of fly ash in concrete." Portland Cement Association Skokie, IL; 2007, 24 pp.
- 27. ASTM_C1709; "C 1709: Standard Guide for Evaluation of Alternative Supplementary Cementitious Materials (ASCM) for Use in Concrete," <u>ASTM International, West Conshohocken,</u>

 2018Book C 1709: Standard Guide for Evaluation of Alternative Supplementary Cementitious

 Materials (ASCM) for Use in Concrete, Editor, ed.^eds., City, 2018, pp.
- 28. P Suraneni, V Azad, O Isgor and W Weiss, "Concrete paving mixture compositions that minimize deicing salt damage," Transp.-ortation Research. Record, V. 2629-, 2017, pp. 24-32.
- 29. ASTM,—"_C311 :- "Standard Test Methods for Sampling and Testing Fly Ash or Natural Pozzolans for Use in Portland-Cement Concrete," <u>ASTM International</u>, <u>West Conshohocken</u>, <u>2018Book C311</u>: Standard Test Methods for Sampling and Testing Fly Ash or Natural Pozzolans for Use in Portland-Cement Concrete, Editor, ed. ^eds., City, 2018, pp.

- 30. ASTM_C618, "Standard Specification for Coal Fly Ash and Raw or Calcined Natural Pozzolan for Use in Concrete," <u>ASTM International, West Conshohocken, 2019Book Standard Specification for Coal Fly Ash and Raw or Calcined Natural Pozzolan for Use in Concrete, Editor, ed.^eds., ASTM, City, 2019, pp. 5.</u>
- 31. RT Thorstensen and P Fidjestol, "Inconsistencies in the pozzolanic strength activity index (SAI) for silica fume according to EN and ASTM," Materials and Structures, V. 48, No. 12-, 2015, pp. 3979-3990.
- 32. DP Bentz, A Durán-Herrera and D Galvez-Moreno, "Comparison of ASTM C311 strength activity index testing versus testing based on constant volumetric proportions," Journal of ASTM International, V. 9, No. 1-, 2011, pp. 1-7.
- 33. IS, "1727: Methods of test for pozzolanic materials," Book 1727: Methods of test for pozzolanic materials, Editor, ed.^eds., Bureau of Indian Standards New Delhi, City, 1967, pp.
- 34. W Butler, "A critical look at ASTM C 618 and C 311," Cement, Concrete and Aggregates, V. 4, No. 2-, 1982, pp. 68-72.
- 35. N Frattini, "Richerche sulla calce di idrolisi nelle paste di cimento," Ann di Chim Appl, V. 39-, 1949, pp. 616-620.
- 36. R Snellings and KL Scrivener, "Rapid screening tests for supplementary cementitious materials: past and future," Materials and Structures, V. 49, No. 8-, 2016, pp. 3265-3279.
- 37. BS EN,-196-2 "Methods of testing cement-Part 2: Chemical analysis of cement," British Standards Institution. 2005.
- 38. BS EN, "_197-1, "Cement-Part 1: Composition, specifications and conformity criteria for common cements," British Standards Institution. 2000.

- 39. E Ferraz, S Andrejkovičová, W Hajjaji, AL Velosa, AS Silva and F Rocha, "Pozzolanic activity of metakaolins by the French Standard of the modified Chapelle Test: A direct methodology," Acta Geodyn. Geomater, V. 12, No. 3-, 2015, pp. 289-298.
- 40. M Raverdy, F Brivot, A Paillere and R Dron, "Appréciation de l'activité pouzzolanique de constituents secondaires," <u>Proceedings of the 7th International Congress on the Chemistry of CementBook Appréciation de l'activité pouzzolanique de constituents secondaires, 3, Editor, ed.^eds., Vol. 3City, 1980, pp. 36-41.</u>
- 41. J Chapelle, "Attaque sulfo-calcique des laitiers et des pouzzolanes." Imprimerie Centrale de l'Ortois-Orras;, 1958.
- 42. F Avet, R Snellings, AA Diaz, MB Haha and K Scrivener, "Development of a new rapid, relevant and reliable (R3) test method to evaluate the pozzolanic reactivity of calcined kaolinitic clays," Cement and Concrete Research, V. 85-, 2016, pp. 1-11.
- 43. ASTM, "_C1897 : "Standard Test Methods for Measuring the Reactivity of Supplementary Cementitious Materials by Isothermal Calorimetry and Bound Water Measurements," <u>ASTM International</u>, West Conshohocken, 2020Book C1897 : Standard Test Methods for Measuring the Reactivity of Supplementary Cementitious Materials by Isothermal Calorimetry and Bound Water Measurements, Editor, ed.^eds., City, 2020, pp.
- 44. P Suraneni and J Weiss, "Examining the pozzolanicity of supplementary cementitious materials using isothermal calorimetry and thermogravimetric analysis," Cement and Concrete Composites, V. 83, No. Supplement C, 2017/10/01/. 2017, pp. 273-278.
- 45. D Glosser, A Choudhary, OB Isgor and J Weiss, "Investigation of the Reactivity of Fly Ash and its Effect on Mixture Properties," ACI Materials Journal, V. In Press 116, No. 4,- 2019, pp. 193-200.

- 46. VJ Azad, P Suraneni, O Isgor and W Weiss, "Interpreting the pore structure of hydrating cement phases through a synergistic use of the Powers-Brownyard model, hydration kinetics, and thermodynamic calculations," Advances in Civil Engineering Materials, V. 6, No. 1-, 2017, pp. 1-16.
- 47. OB Isgor and J Weiss, "A nearly self-sufficient framework for modelling reactive-transport processes in concrete," Materials and Structures, V. 52, No. 1, Feb. 2019, pp. 1-17.
- 48. DB Glosser, "Equilibrium and Non-equilibrium Thermodynamic Modeling of Cement Pastes Containing Supplementary Cementitious Materials," Book Equilibrium and Non-equilibrium Thermodynamic Modeling of Cement Pastes Containing Supplementary Cementitious Materials, Ph. D. Thesis, Editor, ed.^eds., Oregon State University, CityCorvallis, OR, 2020, 206 pp.
- 49. S Ramanathan, M Kasaniya, M Tuen, MD Thomas and P Suraneni, "Linking reactivity test outputs to properties of cementitious pastes made with supplementary cementitious materials," Cement and Concrete Composites, V. 114-, 2020, pp. 103742.
- 50. P Suraneni, A Hajibabaee, S Ramanathan, Y Wang and J Weiss, "New insights from reactivity testing of supplementary cementitious materials," Cement and Concrete Composites, V. 103-, 2019, pp. 331-338.
- 51. P Suraneni and J Weiss, "Examining the pozzolanicity of supplementary cementitious materials using isothermal calorimetry and thermogravimetric analysis," Cement and Concrete Composites, V. 83. , 2017, pp. 273-278.
- 5251. P Suraneni, T Fu, V Jafari Azad, OB Isgor and J Weiss, "Pozzolanicity of finely ground lightweight aggregates," Cement and Concrete Composites, V. 88, 2018/04/01/. 2018, pp. 115-120.

- 5352. P Suraneni, VJ Azad, OB Isgor and J Weiss, "Role of supplementary cementitious material type in the mitigation of calcium oxychloride formation in cementitious pastes," Journal of Materials in Civil Engineering, V. 30, No. 10-, 2018, pp. 04018248.
- 54<u>53</u>. K Bharadwaj, D Glosser, MK Moradllo, OB Isgor and J Weiss, "Toward the Prediction of Pore Volumes and Freeze-Thaw Performance of Concrete Using Thermodynamic Modelling," Cement Concrete Research, V. 124-, 2019, pp. 105820.
- 5554. D Glosser, VJ Azad, P Suraneni, B Isgor and J Weiss, "An extension of the Powers-Brownyard model to pastes containing SCM," ACI Materials Journal, V. in Press 116, No. 5, 2019, pp. 205-216.
- 5655. MK Moradllo, C-W Chung, MH Keys, A Choudhary, SR Reese and WJ Weiss, "Use of borosilicate glass powder in cementitious materials: Pozzolanic reactivity and neutron shielding properties," Cement and Concrete Composites, V. 112-, 2020, pp. 103640.
- 57<u>56</u>. K Bharadwaj, RM Ghantous, FN Sahan, BO Isgor and J Weiss, "Predicting Pore Volume, Compressive Strength, Pore Connectivity, and Formation Factor in Cementitious Pastes Containing Fly Ash," Cement and Concrete Composites, V. In Review122, 2021, pp. 104113.
- 5859. K Bharadwaj, BO Isgor, JW Weiss, KST Chopperla, A Choudhary, G Vasudevan, et alD Glosser, JH Ideker, D Trejo., "A mixture proportioning approach for concrete with SCM based on performance constraints," In Preparation ACI Materials Journal, Accepted, 2021.
- 5958. B Isgor, J Ideker, D Trejo, J Weiss, K Bharadwaj, A Choudhary, et al. KST Chopperla, D Glosser, G Vasudevan, "Development of a performance-based mixture proportioning procedure for concrete incorporating off-spec fly ash," Book Development of a performance-based mixture proportioning procedure for concrete incorporating off-spec fly ash, Editor, ed. eds. Technical Report, Energy Power Research Institute (EPRI), Oregon State University, City, 2020, 78 pp.

- 6059. P Suraneni, VJ Azad, BO Isgor and WJ Weiss, "Calcium oxychloride formation in pastes containing supplementary cementitious materials: Thoughts on the role of cement and supplementary cementitious materials reactivity," RILEM Technical Letters, V. 1-, 2016, pp. 24-30.
- 6160. P Suraneni, VJ Azad, OB Isgor and WJ Weiss, "Use of fly ash to minimize deicing salt damage in concrete pavements," Transportation Research Record, V. 2629, No. 1-, 2017, pp. 24-32.
- 6261. D Glosser, A Choudhary, J Ideker, D Trejo, WJ Weiss and OB Isgor, "Thermodynamic Investigation of Cementitious Mixtures Incorporating Off-Spec Fly Ashes." 2019.
- 6362. P Suraneni, VJ Azad, OB Isgor and WJ Weiss, "Deicing salts and durability of concrete pavements and joints," Concrete International, V. 38, No. 4-, 2016, pp. 48-54.
- 64<u>63</u>. HS Esmaeeli, Y Farnam, DP Bentz, PD Zavattieri and WJ Weiss, "Numerical simulation of the freeze–thaw behavior of mortar containing deicing salt solution," Materials and Structures, V. 50, No. 1, November 04. 20162017, pp. 961-20.
- 6564. P Suraneni, J Monical, E Unal, Y Farnam and W Weiss, "Calcium oxychloride formation potential in cementitious pastes exposed to blends of deicing salt," ACI Mater.—<u>ials Journal</u>, V. 114, No. 4., 2017, pp. 631-641.
- 6665. SN Whatley, P Suraneni, VJ Azad, OB Isgor and J Weiss, "Mitigation of Calcium Oxychloride Formation in Cement Pastes Using Undensified Silica Fume," Journal of Materials in Civil Engineering, V. 29, No. 10-, 2017, pp. 04017198.
- 6766. B-BS 8110-1; "Structural use of concrete, part 1: Code of practice for design and construction;" British Standards Institution, UK. 19972007.

- 6867. B Lothenbach, DA Kulik, T Matschei, M Balonis, L Baquerizo, B Dilnesa, GD Miron, and RJ Myerset al., "Cemdata 18: A chemical thermodynamic database for hydrated Portland cements and alkali-activated materials," Cement Concrete Research, V. 115, Jan. 2019, pp. 472-506.
- 6968. B Lothenbach, T Matschei, G Möschner and FP Glasser, "Thermodynamic modelling of the effect of temperature on the hydration and porosity of Portland cement," Cement Concrete Research, V. 38, No. 1–2008, pp. 1-18.
- 7069. B Lothenbach and F Winnefeld, "Thermodynamic modelling of the hydration of Portland cement," Cement Concrete Research, V. 36, No. 2, Feb. 2006, pp. 209-226.
- 71<u>70</u>. DA Kulik, "Improving the structural consistency of CSH solid solution thermodynamic models," Cement Concrete Res<u>earch</u>, V. 41, No. 5-, 2011, pp. 477-<u>4</u>95.
- 7271. DA Kulik, T Wagner, SV Dmytrieva, G Kosakowski, FF Hingerl, KV Chudnenko, and UR Berneret al., "GEM-Selektor geochemical modeling package: revised algorithm and GEMS3K numerical kernel for coupled simulation codes," Computational Geosciences, V. 17, No. 1-, 2013, pp. 1-24.
- 7372. V Antonovič, J Kerienė, R Boris and M Aleknevičius, "The effect of temperature on the formation of the hydrated calcium aluminate cement structure," Procedia engineering, V. 57-, 2013, pp. 99-106.
- 7473. HF Taylor, "Cement chemistry, 2nd Edition,." Thomas Telford, London; 1997, 459 pp.
- 7574. P Garcés, EG Alcocel, S Chinchón, CG Andreu and J Alcaide, "Effect of curing temperature in some hydration characteristics of calcium aluminate cement compared with those of Portland cement," Cement Concrete Research, V. 27, No. 9-, 1997, pp. 1343-1355.
- 7675. C Gosselin, "Microstructural development of calcium aluminate cement based systems with and without supplementary cementitious materials," Book Microstructural development of

calcium aluminate cement based systems with and without supplementary cementitious materials, Editor, ed. eds. Ph. D. Thesis, EPFL, Lausanne, Switzerland City, 2009, pp.

77.6. T Matschei, B Lothenbach and F Glasser, "The AFm phase in Portland cement," Cement Concrete Res<u>earch</u>, V. 37, No. 2-, 2007, pp. 118-<u>1</u>30.



TABLES AND FIGURES

List of Tables:

Table 1: Experimental test matrix

Table 2: Chemical characterization of SCMs used

Table 3: Comparison of the PRT and R3 test methods

Table A-1: Values of Q∞ and CH consumed as predicted using thermodynamic modelling and as measured from experiments when the test parameters of the PRT are varied

Table A-2: Values of $Q\infty$ and CH consumed as predicted using thermodynamic modelling and as measured from experiments when sulfates and carbonates are added in the PRT.

List of Figures:

Figure 1- Thermodynamically simulated lines of pozzolanic reactions of <u>amourphous</u> amorphous silica (SiO₂) and alumina (Al₂O₃)

Figure 2- Plot of experimentally measured and model-predicted values of (a) CH Consumed and (b) Q_{∞} for the PRT test.

Figure 3- Plot showing (a) the influence of CH to SCM ratio on the CH consumed and Q_{∞} in the reactivity test, (b) the phase assemblage when pure SiO₂ reacts with CH, and (c) the phase assemblage when pure Al₂O₃ reacts with CH. The values of Q_{∞} and CH consumed are also noted in Table A-1 of the appendix3.

Figure 4- The influence of liquid to SCM+CH ratio on the CH consumed and Q_{∞} in the reactivity test. The values of Q_{∞} and CH consumed are also noted in Table A-1 of the appendix3.

Figure 5- Plots showing (a) the influence of $[SO_4]^{2-}$ on the CH consumed and Q_∞ in the reactivity test, (b) the phase assemblage and Q_∞ when pure SiO_2 reacts with CH and sulfates are added, (c) the phase assemblage and Q_∞ when pure Al_2O_3 reacts with CH and sulfate is added. The values of Q_∞ and CH consumed are also noted in Table A-2 of the appendix4.

Figure 6- Plots showing (a) the influence of CaCO3 on the CH consumed and Q_{∞} in the reactivity test, (b) the phase assemblage and Q_{∞} when pure SiO₂ reacts with CH and carbonates are added, and (c) the phase assemblage and Q_{∞} when pure Al₂O₃ reacts with CH and carbonates are added. The values of Q_{∞} and CH consumed are also noted in Table A-2 of the appendix4.

Figure 7- Plot showing (a) the influence of alkali cation on the CH consumed and Q_{∞} in the reactivity test, (b) phase assemblage and Q_{∞} when pure SiO₂ reacts and the alkali cation is varied, and (c) phase assemblage and Q_{∞} when pure Al₂O₃ reacts and the alkali cation is varied. The values of Q_{∞} and CH consumed are also noted in Table A-1 of the appendix 3.

Figure 8- Plot showing (a) the influence of pH of pore solution on the CH consumed and Q_{∞} in the reactivity test, (b) the phase assemblage and Q_{∞} -when pure SiO₂ reacts, and the pH is varied, and (c) the phase assemblage and Q_{∞} when pure Al₂O₃ reacts and the pH is varied. The values of Q_{∞} and CH consumed are also noted in Table A-1 of the appendix3.

Figure 9- Volumes of initial reactants and final products for the three SCMs studied in the PRT and R3 tests.

Figure 10- (a) Variation of c₁ and c₂ as a function of sulfate addition, and, (b) variation of c₁ and c₂ as a function of carbonate addition. Markers are at the locations of the sulfate/carbonate additions tested in the experiments (see Table 1).

Table 1: Experimental test matrix

Table 1: Experimental test matrix								
Varied test parameter	CH:SCM	Liquid: SCM	Sulfate (g/100_g SCM)	Calcium Carbonate (g/100_g SCM)	NaOH (M)	КОН (<i>M</i>)	Baseline	
	3:1	0.90	0	0	0.00	0.50	٧	
СН	2:1	0.90	0	0	0.00	0.50		
	1:1	0.90	0	0	0.00	0.50		
	3:1	0.75	0	0	0.00	0.50		
I : 11 COM	3:1	0.90	0	0	0.00	0.50	٧	
Liquid-to-SCM ratio	3:1	1.00	0	0	0.00	0.50		
Tauo	3:1	1.50	0	0	0.00	0.50		
	3:1	2.00	0	0	0.00	0.50		
	3:1	0.90	0	0	0.00	0.50	٧	
	3:1	0.90	5	0	0.00	0.50		
Sulfate	3:1	0.90	10	0	0.00	0.50		
	3:1	0.90	20	0	0.00	0.50		
	3:1	0.90	3 0	0	0.00	0.50		
	3:1	0.90	0	0	0.00	0.50	٧	
Calcium	3:1	0.90	0	2	0.00	1.00		
Carbonate	3:1	0.90	0	6	0.50	0.00		
	3:1	0.90	0	10	0.50	0.00		
Alkali/Molarity	3:1	0.90	0	0	0.00	0.25		
	3:1	0.90	0	0	0.00	0.50	٧	
	3:1	0.90	0	0	0.00	1.00		
	3:1	0.90	0	0	0.00	2.00		
	3:1	0.90	0	0	0.50	0.00		

Table 2: Chemical characterization of SCMs used

%	Silica Fume (SF)	Fly Ash (FA)	Calcined Clay (CC)
SiO ₂	95.88	51.86	53.22
Al ₂ O ₃	0.69	21.70	36.90
Fe ₂ O ₃	0.12	5.04	1.21
CaO	0.70	8.61	0.57
MgO	0.26	2.58	0.36
SO ₃	0.15	0.78	0.06
LOI	4.30	1.42	2.21
Na ₂ O	0.16	2.58	0.15
K ₂ O	0.49	1.45	0.68
TiO ₂	0.01	1.19	1.87
P ₂ O ₅	0.05	0.23	0.11
ZnO	0.06	0.02	0.01
Mn ₂ O ₃	0.04	0.03	0.01
Cl	0.01	0.01	0.01

Table 3: Comparison of the PRT and R3 test methods

Test Parameter		PRT	R3	
CH:SCM		3:1	3:1	
Liquid-to-powder	· ratio	0.9	1.2	
Pore Solution alka	alinity	0.5M KOH	0.07M KOH	
CaCO3 adde	d	None	50g/100gscm	
Sulfates adde	d	None	10.547g K ₂ SO ₄ /100g _{SCM}	
T		Value of ultimate pozzolanic	Bound Water,	
Test Output	•	reactivity (DOR*)	Heat of Reaction	
Theoretical O	SF	646	648	
Theoretical Q∞	FA	277	378	
(J/g_{SCM}) CC		519	778	
Theoretical CH SF		162	162	
Consumed (g/100 FA		55	59	
g _{SCM}) CC		148	153	

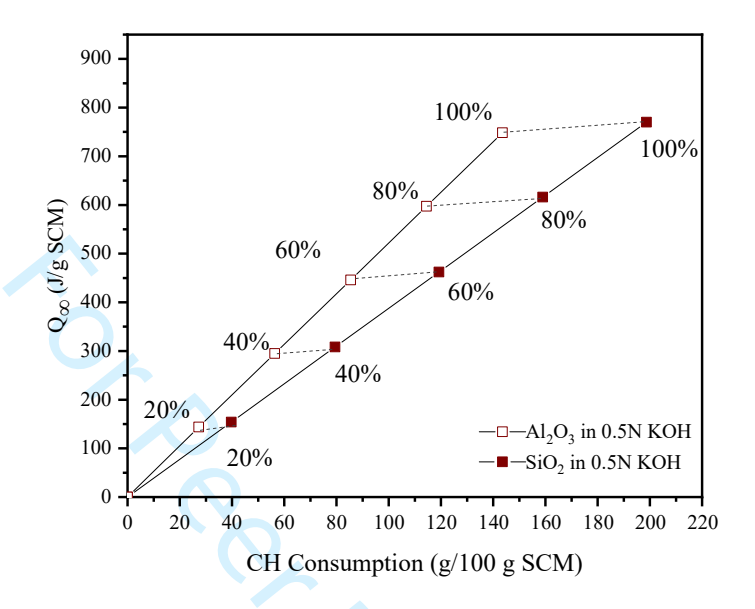


Figure 1- Thermodynamically simulated lines of pozzolanic reactions of amourphous amorphous silica (SiO₂) and alumina (Al₂O₃) at various degrees of reaction

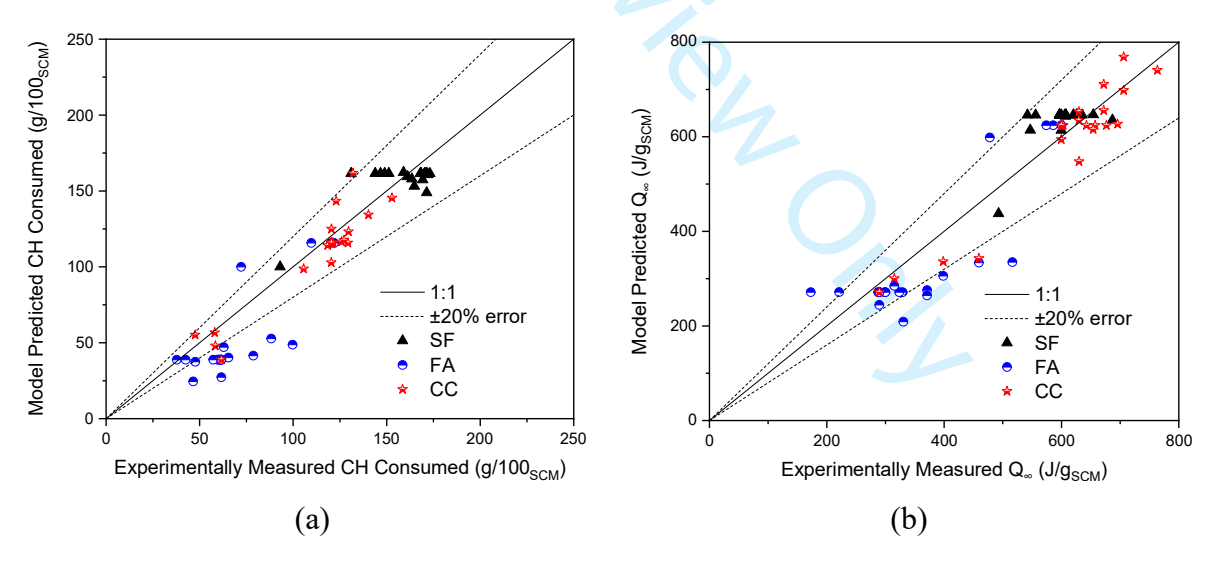
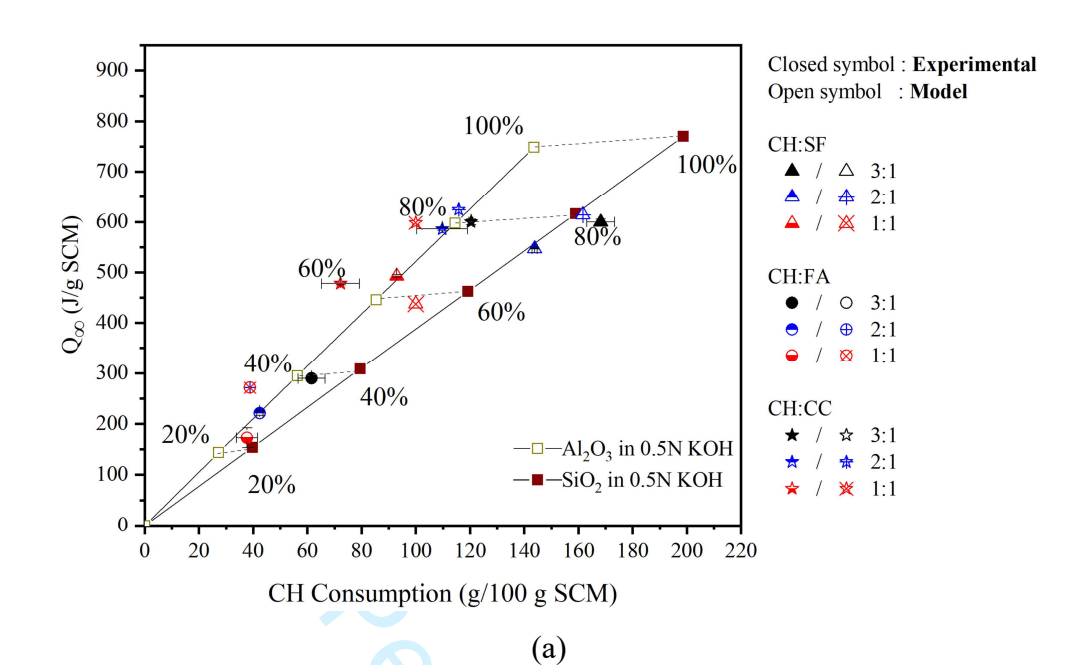
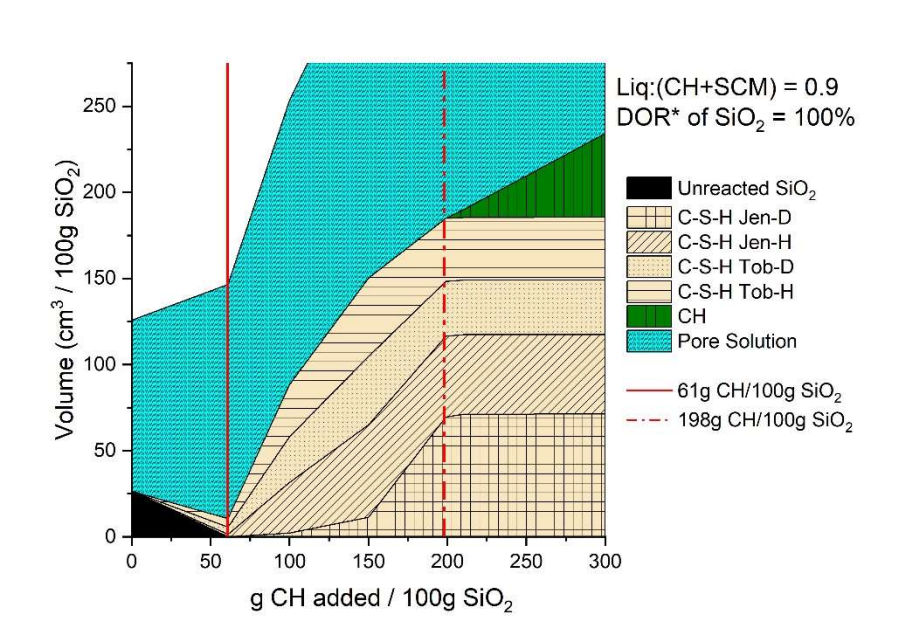


Figure 2- Plot of experimentally measured and model-predicted values of (a) CH Consumed and (b) Q_{∞} for the PRT test. The values of Q_{∞} and CH consumed are also noted in Table A-13 and Table A-2 of the appendix4.





(b)

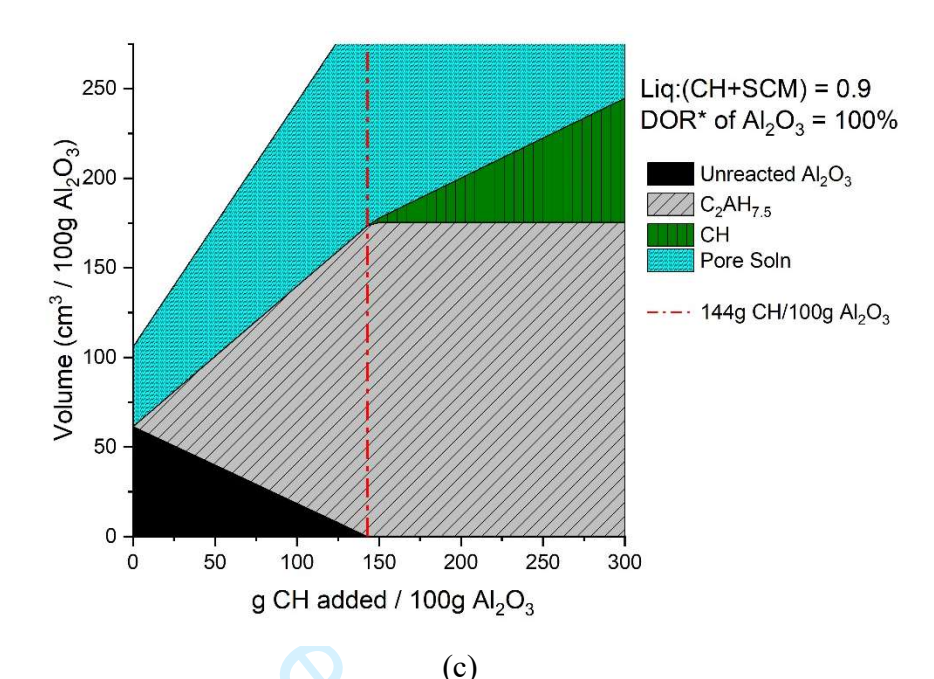


Figure 3- Plot showing (a) the influence of CH to SCM ratio on the CH consumed and Q_{∞} in the reactivity test, (b) the phase assemblage when pure SiO_2 reacts with CH, and (c) the phase assemblage when pure Al_2O_3 reacts with CH. Vertical lines represent the critical CH:SCM as described in the test. The values of Q_{∞} and CH consumed are also noted in Table A-1 of the appendix3.

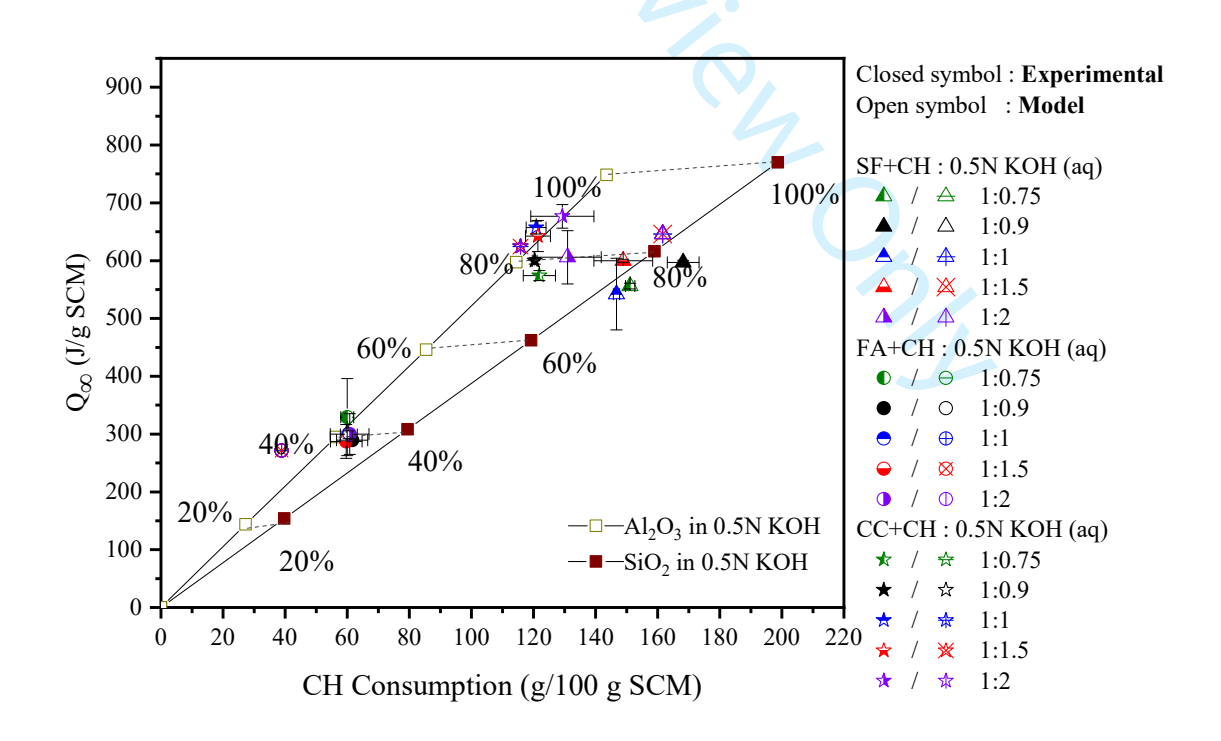
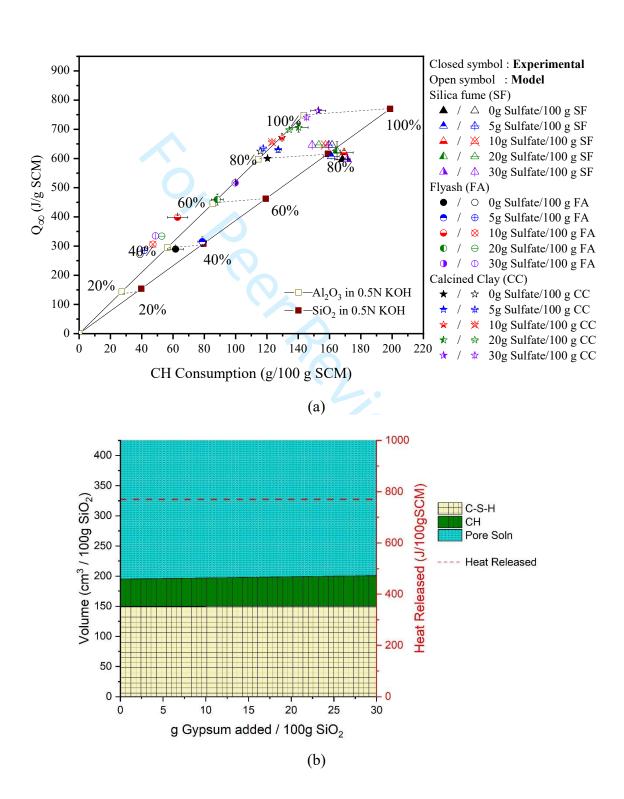


Figure 4- The influence of liquid to SCM+CH ratio on the CH consumed and Q_{∞} in the reactivity test. The values of Q_{∞} and CH consumed are also noted in Table A-1 of the appendix3.



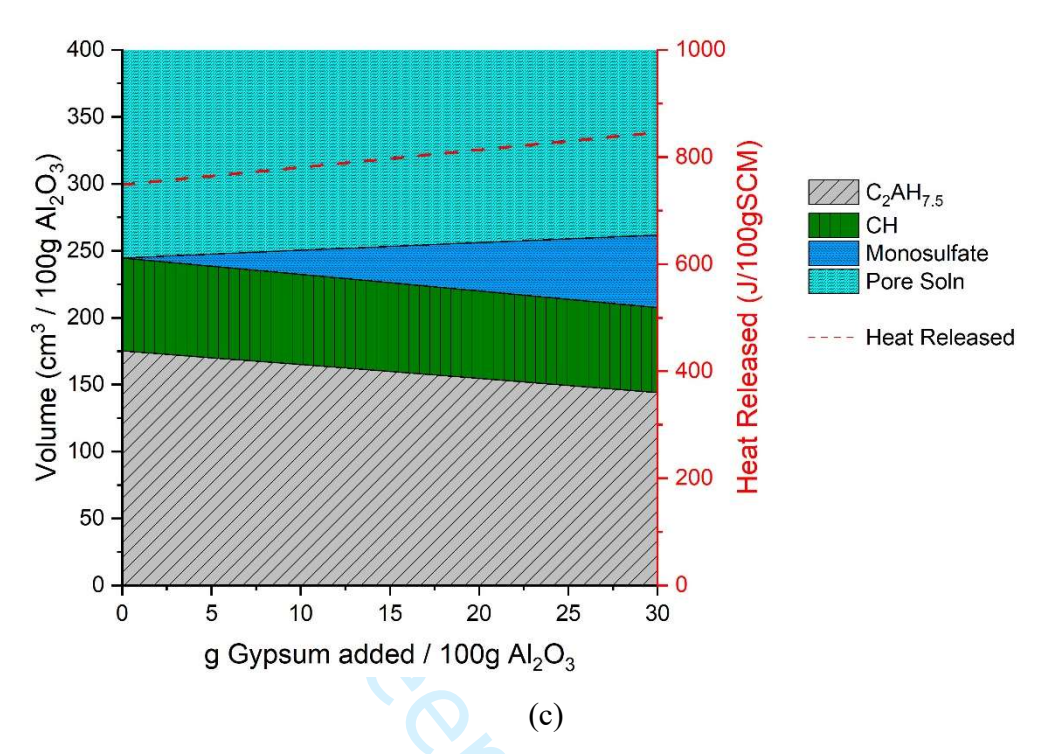
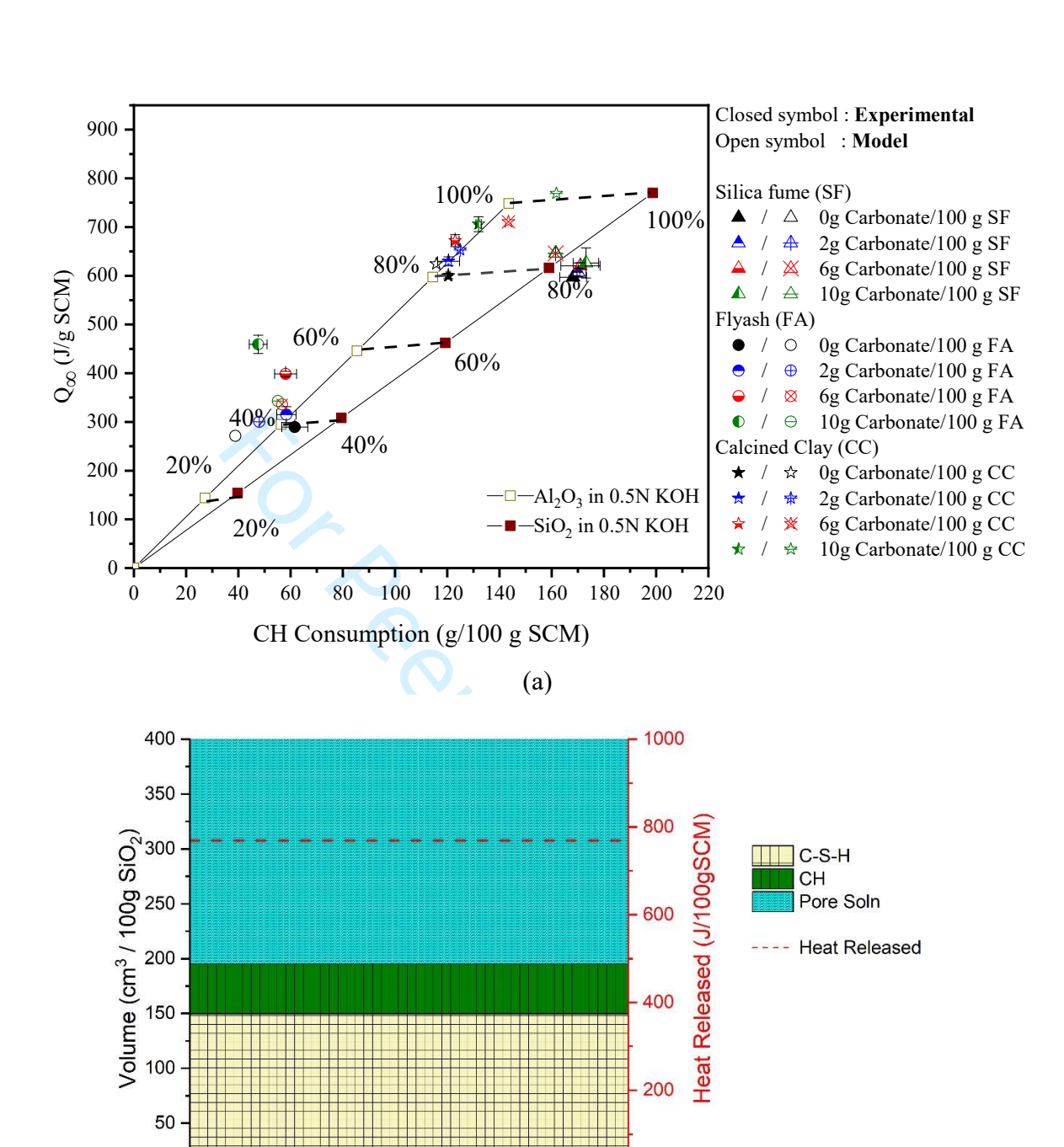


Figure 5- Plots showing (a) the influence of $[SO_4]^{2-}$ on the CH consumed and Q_∞ in the reactivity test, (b) the phase assemblage and Q_∞ when pure SiO_2 reacts with CH and sulfates are added, (c) the phase assemblage and Q_∞ when pure Al_2O_3 reacts with CH and sulfate is added. The values of Q_∞ and CH consumed are also noted in Table A-2 of the appendix4.



(b)

g CaCO₃ added / 100g SiO₂

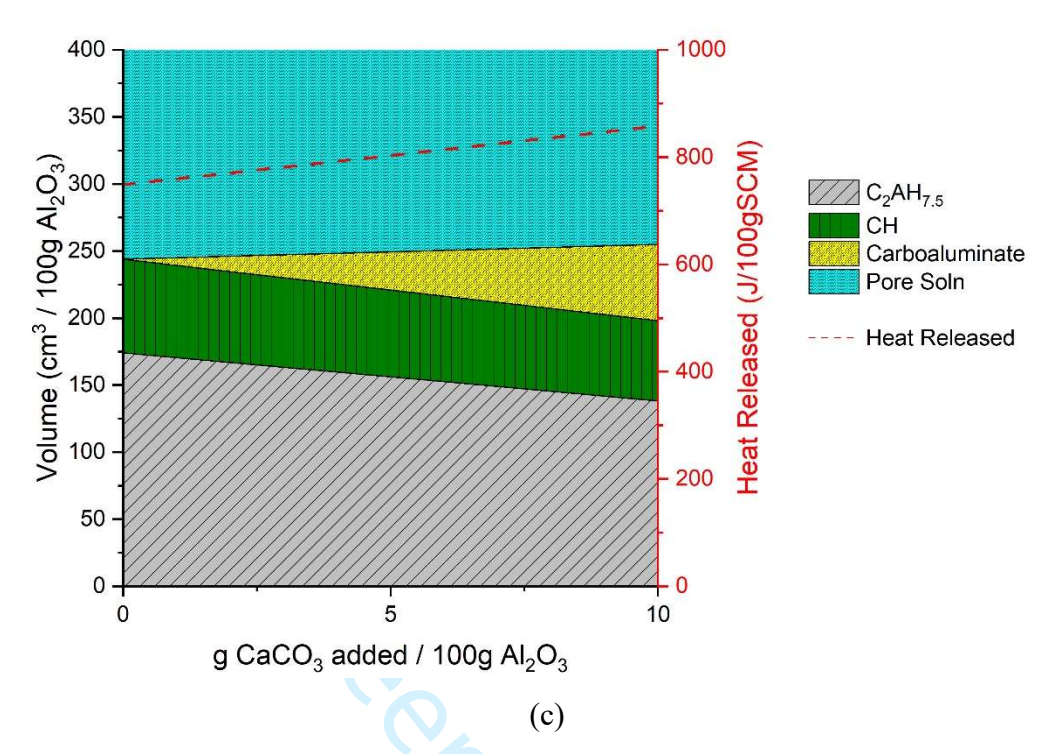
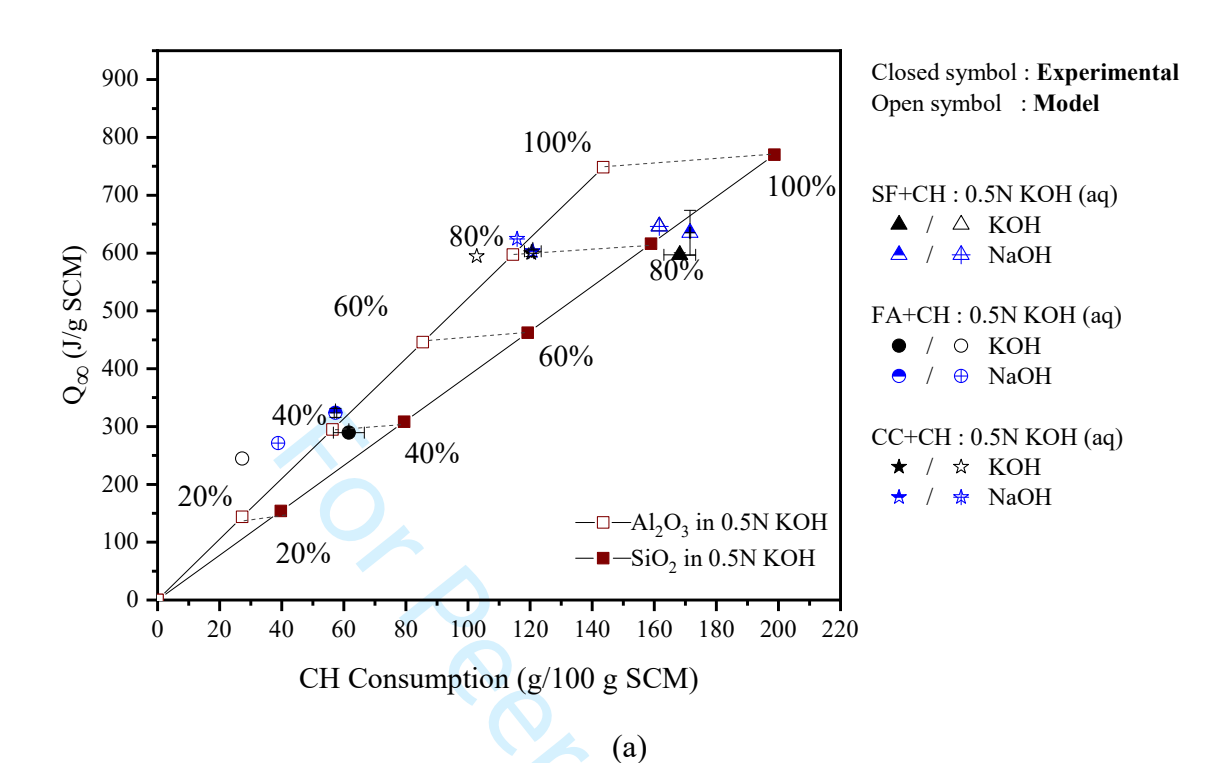
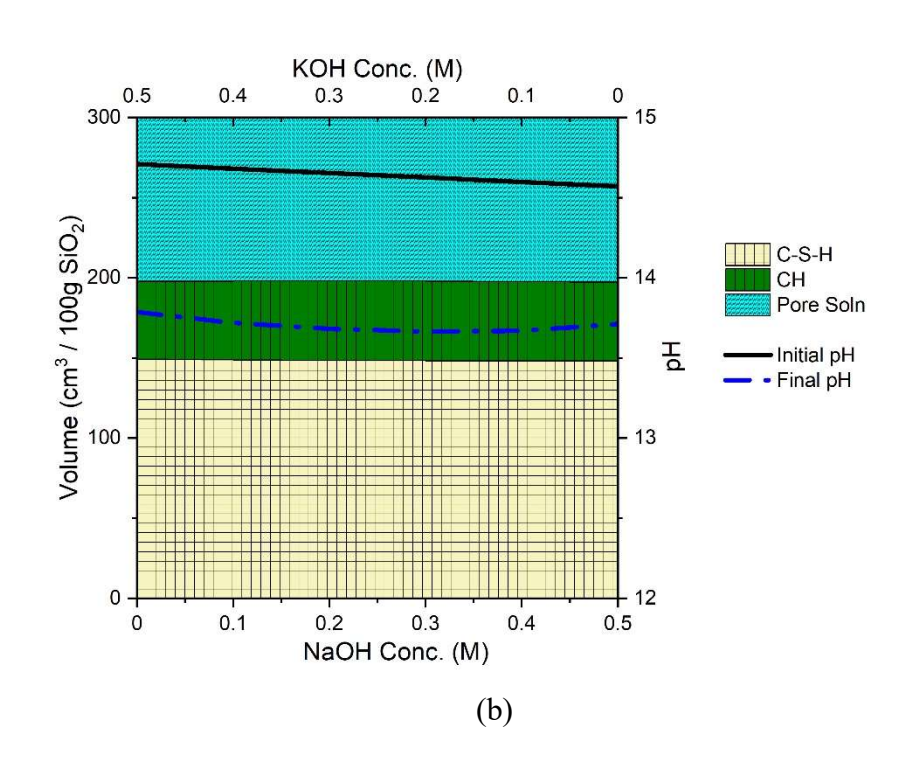


Figure 6- Plots showing (a) the influence of CaCO₃ on the CH consumed and Q_{∞} in the reactivity test, (b) the phase assemblage and Q_{∞} when pure SiO₂ reacts with CH and carbonates are added, and (c) the phase assemblage and Q_{∞} when pure Al₂O₃ reacts with CH and carbonates are added. The values of Q_{∞} and CH consumed are also noted in Table 4A-2 of the appendix.





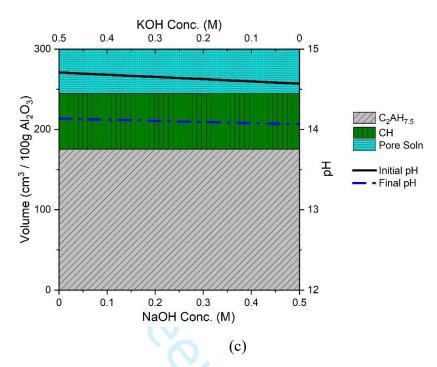
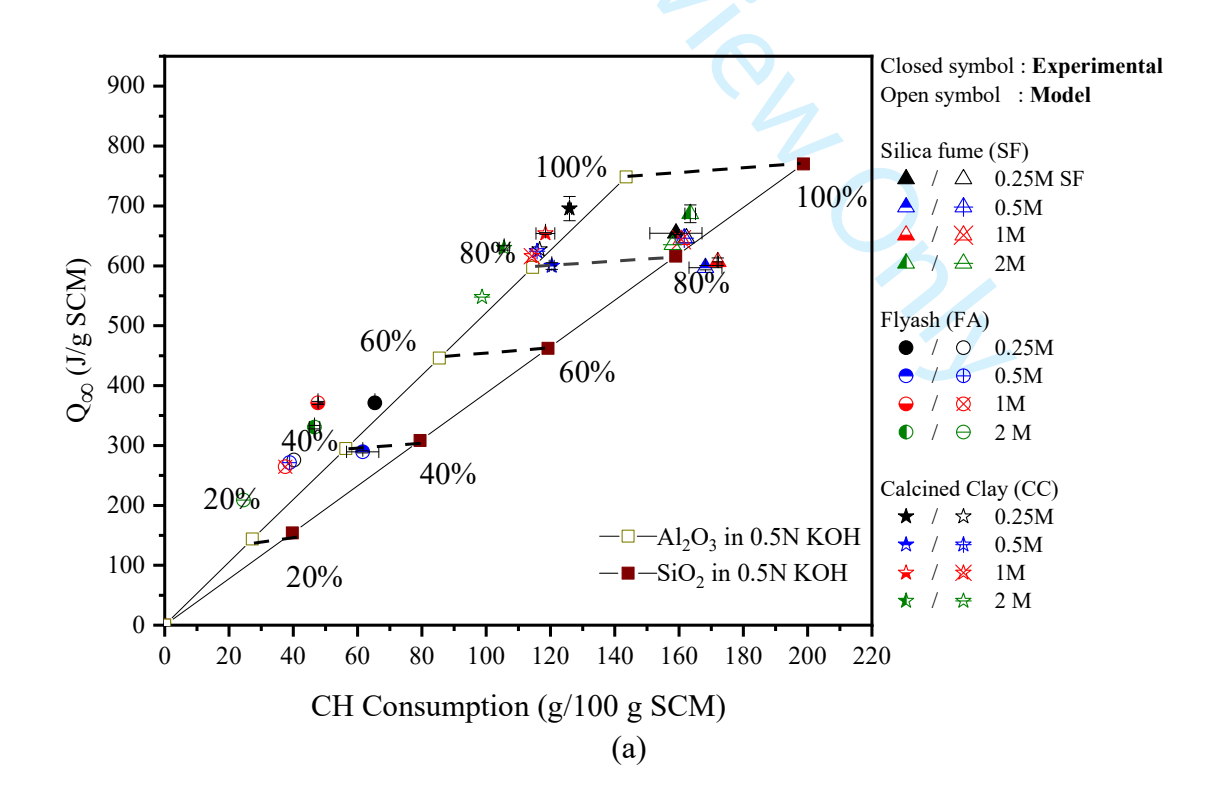


Figure 7- Plot showing (a) the influence of alkali cation on the CH consumed and Q_{∞} in the reactivity test, (b) phase assemblage and Q_{∞} when pure SiO₂ reacts and the alkali cation is varied, and (c) phase assemblage and Q_{∞} when pure Al₂O₃ reacts and the alkali cation is varied. The values of Q_{∞} and CH consumed are also noted in Table A-1 of the appendix3.



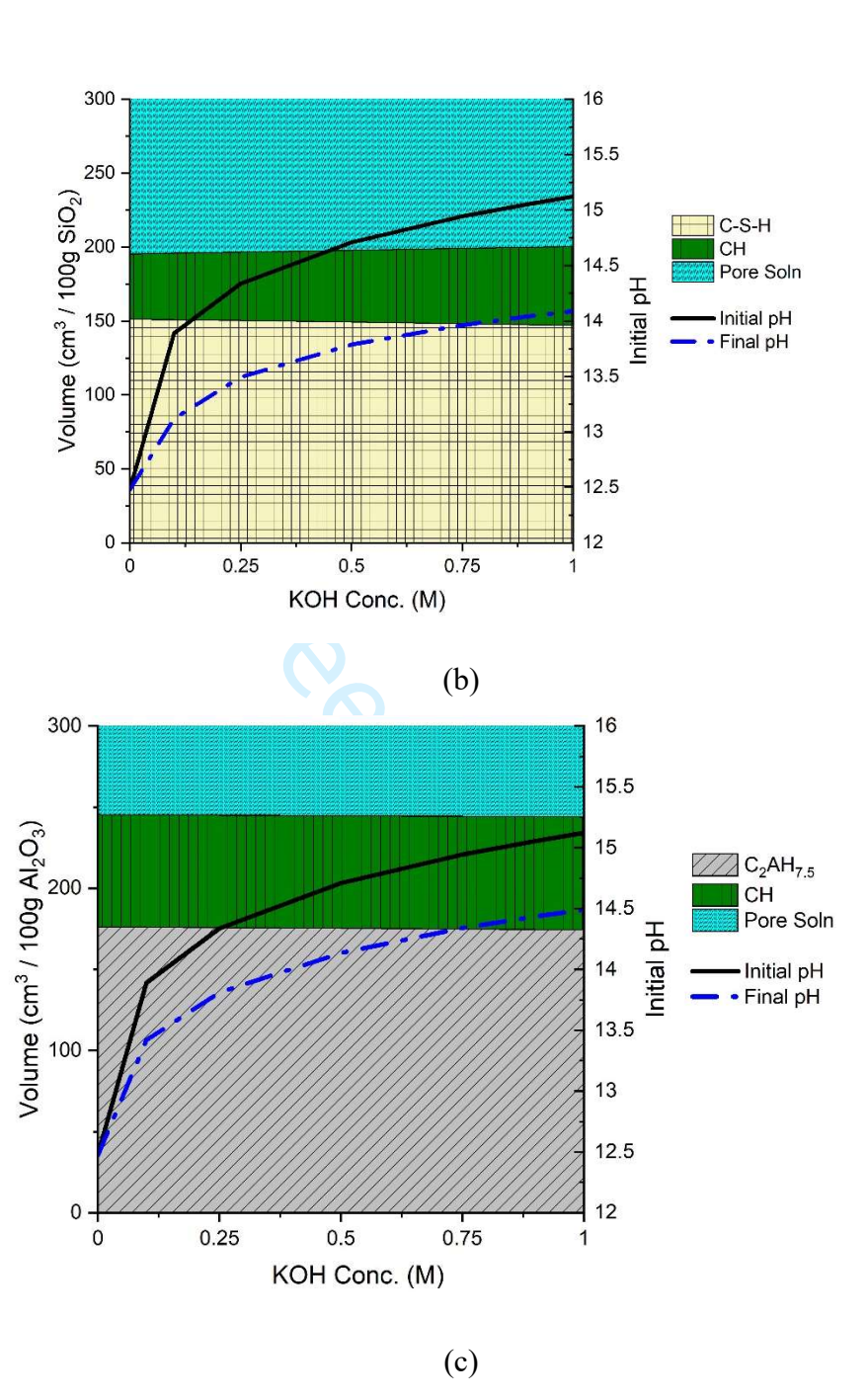


Figure 8- Plot showing (a) the influence of pH of pore solution on the CH consumed and Q_{∞} in the reactivity test, (b) the phase assemblage and Q_{∞} when pure SiO₂ reacts, and the pH is varied, and (c) the phase assemblage and Q_{∞} when pure Al₂O₃ reacts and the pH is varied. The values of Q_{∞} and CH consumed are also noted in Table A-1 of the appendix3.

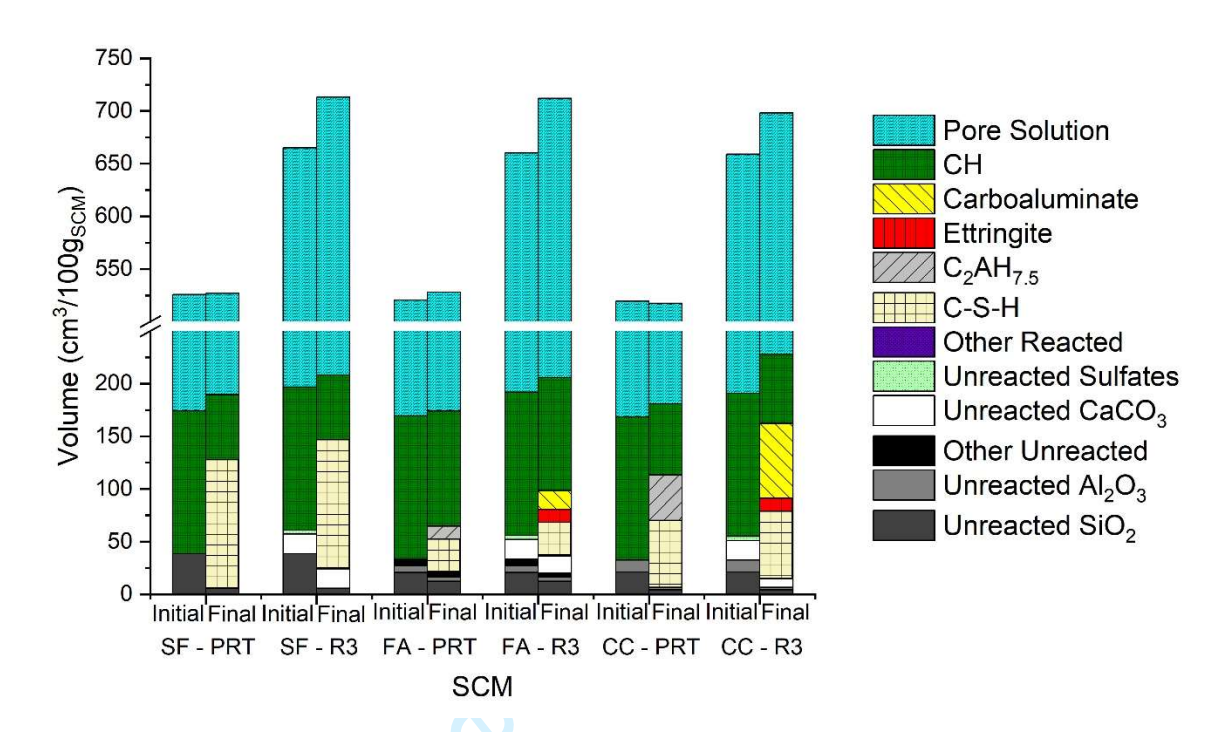


Figure 9- Volumes of initial reactants and final products for the three SCMs studied in the PRT and R3 tests.

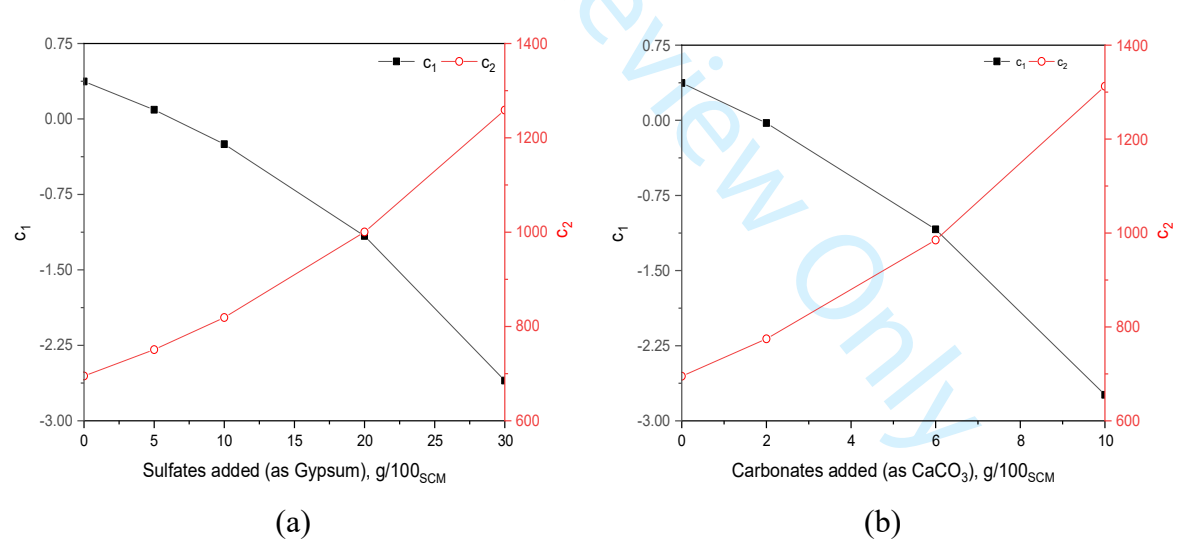


Figure 10- (a) Variation of c₁ and c₂ as a function of sulfate addition, and, (b) variation of c₁ and c₂ as a function of carbonate addition. Markers are at the locations of the sulfate/carbonate additions tested in the experiments (see Table 1).

APPENDIX A: TABULATED DATA OF RELEASED HEAT AND CONSUMED CH FOR THE EXPERIMENTAL TEST MATRIX

Table A-1: Values of Q_{∞} and CH consumed as predicted using thermodynamic modelling and as measured from experiments when the test parameters of the PRT are varied.

CH:SCM	Liquid-	Solution	Q_{∞} as	СН	Q_{∞} as	СН
	to-	used	predicted	Consumed	measured in	Consumed
	powder		from	as predicted	experiments	as measured
	ratio		thermodyna	from	(J/g_{SCM})	in
			mic	thermodyna		<u>experiments</u>
			modeling (J /	mic		$\frac{100}{(g^{-})}$
			g _{SCM})	modeling (g/		SCM)
	,			100g SCM)		
	•		Silica Fu	<u>ime</u>		
<u>1:1</u>		0.5 M	<u>438</u>	<u>100</u>	<u>493</u>	<u>93</u>
<u>2:1</u>	0.90	0.5 M KOH	<u>646</u>	<u>162</u>	<u>547</u>	<u>144</u>
<u>3:1</u>		KOH	646	<u>162</u>	<u>600</u>	<u>168</u>
	<u>0.75</u>		<u>646</u>	<u>162</u>	<u>556</u>	<u>151</u>
	0.90	0.5 M	<u>646</u>	<u>162</u>	<u>597</u>	<u>168</u>
<u>3:1</u>	1	0.5 M	646	<u>162</u>	<u>542</u>	147
	1.5	<u>KOH</u>	646	<u>162</u>	<u>600</u>	<u>149</u>
	<u>2</u>		646	162	606	131
		0.25 M				
		KOH	647	<u>162</u>	<u>654</u>	<u>159</u>
		<u>0.5 M</u>				
<u>3:1</u>	0.90		<u>646</u>	<u>162</u>	<u>597</u>	<u>168</u>
			644	161	607	172
		2 M				
		KOH	<u>635</u>	<u>158</u>	<u>687</u>	<u>163</u>
		0.5 M			4	
2.1	0.00	NaOH	<u>647</u>	<u>162</u>	<u>597</u>	<u>168</u>
<u>3:1</u>	<u>0.90</u>	<u>0.5 M</u>				
		<u>KOH</u>	<u>646</u>	<u>162</u>	635	<u>172</u>
			Fly As	<u>sh</u>		
<u>1:1</u>		0.5 M	<u>272</u>	<u>39</u>	<u>173</u>	<u>38</u>
<u>2:1</u>	<u>0.90</u>	0.5 M	<u>272</u>	<u>39</u>	<u>221</u>	<u>43</u>
<u>3:1</u>		<u>KOH</u>	<u>271</u>	<u>39</u>	<u>289</u>	<u>62</u>
	0.75		271	39	329	<u>60</u>
	0.90	0.534	<u>271</u>	39	289	<u>62</u>
<u>3:1</u>	<u>1</u>	0.5 M	<u>271</u>	39	299	<u>60</u>
	1.5	<u>KOH</u>	<u>271</u>	39	<u>287</u>	<u>60</u>
	2	1	271	39	300	<u>61</u>
2.1		0.25 M				
<u>3:1</u>	<u>0.90</u>	KOH	<u>276</u>	<u>40</u>	<u>371</u>	<u>65</u>

	1	1				ı
		<u>0.5 M</u>				
		<u>KOH</u>	<u>271</u>	<u>39</u>	<u>289</u>	<u>62</u>
		<u>1M KOH</u>	<u>265</u>	<u>37</u>	<u>371</u>	<u>48</u>
		<u>2 M</u>				
		<u>KOH</u>	<u>209</u>	<u>25</u>	<u>331</u>	<u>47</u>
		<u>0.5 M</u>				
2.1	0.90	<u>NaOH</u>	<u>245</u>	<u>27</u>	<u>289</u>	<u>62</u>
<u>3:1</u>	0.90	<u>0.5 M</u>				
		<u>KOH</u>	<u>271</u>	<u>39</u>	<u>324</u>	<u>57</u>
			Calcined	Clay		
1:1		0.5.14	<u>598</u>	<u>100</u>	<u>478</u>	<u>72</u>
2:1	0.90	<u>0.5 M</u>	<u>624</u>	<u>116</u>	<u>586</u>	<u>110</u>
3:1		<u>KOH</u>	<u>624</u>	<u>116</u>	<u>600</u>	<u>120</u>
	0.75		<u>624</u>	<u>116</u>	<u>574</u>	<u>122</u>
	0.90	0.5 M	<u>624</u>	<u>116</u>	<u>600</u>	<u>120</u>
<u>3:1</u>	1 1.5		<u>624</u>	<u>116</u>	<u>657</u>	<u>121</u>
		<u>KOH</u>	<u>624</u>	<u>116</u>	<u>643</u>	<u>121</u>
	<u>2</u>		<u>624</u>	<u>116</u>	<u>677</u>	<u>129</u>
		<u>0.25 M</u>				
	<u>0.90</u>	<u>KOH</u>	<u>627</u>	<u>117</u>	<u>696</u>	<u>126</u>
		<u>0.5 M</u>				
<u>3:1</u>		<u>KOH</u>	<u>624</u>	<u>116</u>	<u>600</u>	<u>120</u>
		1M KOH	<u>616</u>	<u>114</u>	<u>654</u>	<u>118</u>
		<u>2 M</u>				
		<u>KOH</u>	<u>548</u>	<u>99</u>	<u>630</u>	<u>106</u>
		<u>0.5 M</u>				
2.1	0.00	<u>NaOH</u>	<u>594</u>	<u>103</u>	<u>600</u>	<u>120</u>
<u>3:1</u>	0.90	<u>0.5 M</u>				
		<u>KOH</u>	<u>624</u>	<u>116</u>	603	<u>121</u>

Table A-2: Values of Q_{∞} and CH consumed as predicted using thermodynamic modelling and as measured from experiments when sulfates and carbonates are added in the PRT.

Sulfate	Carbonate	Q_{∞} as predicted	CH Consumed	Q_{∞} as	CH Consumed	
Added as	Added as	<u>from</u>	as predicted	measured in	as measured in	
<u>Gypsum</u>	<u>Gypsum</u>	thermodynamic	<u>from</u>	experiments (J	experiments (g	
(g gypsum	(g CaCO ₃ /	modeling (J /	thermodynamic	<u>/ g_{SCM})</u>	/ 100g SCM)	
<u>/ 100 g</u>	<u>100</u> g	g _{SCM})	modeling (g /			
SCM)	SCM)		<u>100g SCM)</u>			
	Silica Fume					
<u>0</u>		<u>646</u>	<u>162</u>	<u>597</u>	<u>168</u>	
<u>5</u>		<u>646</u>	<u>160</u>	<u>607</u>	<u>161</u>	
<u>10</u>	<u>0</u>	<u>646</u>	<u>157</u>	<u>621</u>	<u>169</u>	
<u>20</u>		<u>646</u>	<u>153</u>	<u>626</u>	<u>165</u>	
<u>30</u>		<u>647</u>	<u>149</u>	<u>597</u>	<u>171</u>	

	<u>0</u>	<u>646</u>	<u>162</u>	<u>597</u>	<u>168</u>
<u>0</u>	<u>2</u>	<u>646</u>	<u>162</u>	<u>607</u>	<u>170</u>
	<u>6</u>	<u>646</u>	<u>162</u>	<u>621</u>	<u>171</u>
	<u>10</u>	<u>646</u>	<u>162</u>	<u>626</u>	<u>173</u>
			Fly Ash		
<u>0</u>		<u>271</u>	<u>39</u>	<u>289</u>	<u>62</u>
<u>5</u>		<u>285</u>	<u>42</u>	<u>315</u>	<u>79</u>
<u>10</u>	<u>0</u>	<u>306</u>	<u>47</u>	<u>399</u>	<u>63</u>
<u>20</u>		<u>334</u>	<u>53</u>	<u>459</u>	<u>88</u>
<u>30</u>		<u>335</u>	<u>49</u>	<u>516</u>	<u>100</u>
	0	<u>271</u>	<u>39</u>	<u>289</u>	<u>62</u>
0	<u>2</u>	<u>300</u>	<u>48</u>	<u>315</u>	<u>58</u>
0	<u>6</u>	336	<u>57</u>	<u>399</u>	<u>58</u>
	<u>10</u>	343	<u>55</u>	<u>459</u>	<u>48</u>
		<u>Ca</u>	lcined Clay		
<u>0</u>		<u>624</u>	<u>116</u>	<u>600</u>	<u>120</u>
<u>5</u>		635	<u>118</u>	<u>630</u>	<u>127</u>
<u>10</u>	<u>0</u>	656	<u>123</u>	<u>672</u>	<u>130</u>
<u>20</u>		<u>698</u>	<u>134</u>	<u>706</u>	<u>140</u>
<u>30</u>		<u>741</u>	145	<u>764</u>	<u>153</u>
	<u>0</u>	<u>624</u>	<u>116</u>	<u>600</u>	<u>120</u>
0	<u>2</u>	<u>653</u>	<u>125</u>	<u>630</u>	<u>121</u>
0	<u>6</u>	<u>711</u>	<u>143</u>	<u>672</u>	<u>123</u>
	10	769	162	706	132